Biochimica et Biophysica Acta, 314 (1973) 267–275

BBA 46599

ESSENTIAL ROLE OF MEMBRANE ATPase OR COUPLING FACTOR FOR ANAEROBIC GROWTH AND ANAEROBIC ACTIVE TRANSPORT IN *ESCHERICHIA COLI*

T. H. YAMAMOTO, M. MÉVEL-NINIO and R. C. VALENTINE

Department of Chemistry, University of California, San Diego, La Jolla, Calif. 92037 (U.S.A.)

(Received April 2nd, 1973)

SUMMARY

Mutants of *Escherichia coli* defective in coupling electron transport to synthesis of ATP (*unc*$^-$) were isolated and screened for Mg^{2+}-ATPase activity using a rapid and sensitive Millipore filtration assay. An episome (F'16) carrying ATPase genes was used to map the *unc*$^-$ mutations near the *ilv* (isoleucine–valine) operon. Mutants missing membrane ATPase activity do not multiply anaerobically on glucose as energy source unless supplied with exogenous electron acceptors such as NO_3^-. Likewise, in the absence of exogenous electron acceptors anaerobic active transport of proline is blocked. These observations suggest that membrane ATPase has an essential role in membrane functions linked to glycolysis and thus may play an important role in energy conversion in the anaerobic membrane.

INTRODUCTION

Bacterial membranes in general are now recognized as sites for essential cellular processes such as respiration coupled to oxidative phosphorylation, photophosphorylation, and active transport[1]. In recent years the biochemistry of bacterial membrane function has been studied in considerable detail. However, relatively little is known regarding the genetic basis of membrane functions such as oxidative phosphorylation in bacteria. Butlin *et al.*[2] have recently started a biochemical–genetical study of a class of mutants defective in oxidative phosphorylation for which they suggest the term *unc*$^-$ (uncoupled). The genetic lesion was mapped on the *Escherichia coli* chromosome near the *ilv* operon. These mutants produce little if any membrane bound coupling factor activity (Mg^{2+}-ATPase). Butlin *et al.*[2] conclude that coupling factor activity is essential for oxidative phosphorylation. Respiratory linked active transport of amino acids was found to occur at normal levels[3] in the *unc*$^-$ mutant of Butlin *et al.*[2], but in reduced levels in the case of an *unc*$^-$ mutant isolated by Simoni and Shallenberger[4]. Schairer and Haddock[5] have shown that β-galactoside accumulation in whole cells of *unc*$^-$ strains is abolished by respiratory poisons, leading to their conclusion that ATPase activity is necessary for nonrespiratory driven β-galactoside accumulation. Our studies with ATPase defective mutants show that membrane-associated ATPase activity is also essential for anaerobic growth on glucose and

that ATPase negative mutants are blocked in active transport of proline under anaerobic conditions.

MATERIALS AND METHODS

Unc⁻ mutants

Spontaneous *unc*⁻ mutants of *E. coli* K12 (W3110), F⁻, were isolated using the neomycin selection procedure of Kanner and Gutnick[6]. Several mutants were also isolated using streptomycin (SM) sulfate (20 μg/ml) in place of neomycin sulfate. The SM^r strains were resistant to neomycin and had other properties similar to the neomycin resistant strains. Mutants were maintained aerobically on L-broth agar plates[7] or L-broth supplemented with 0.5% glucose. Starter liquid cultures were inoculated with colonies from L-broth plates and were grown in flasks of L-broth or minimal medium using a shaker bath at 37 °C. No more than one serial transfer was made from these starter flasks because of accumulation of spontaneous wild type revertants as described below.

Anaerobic growth experiments

Fresh L-broth cultures were started each day using as inoculum colonies from L-broth plates. Exponentially growing cells (0.5 ml) were used to inoculate screw cap tubes which were completely filled with L-broth supplemented with 0.5% glucose; no attempt was made to remove dissolved oxygen prior to inoculation. This may account for the small amount of growth observed with ATPase⁻ mutants (see below). Incubation was at 37 °C. Growth was measured using a Klett colorimeter. Spontaneous revertants (*unc*⁻→*unc*⁺) present at the end of the experiment were tested by streaking a sample of cells on succinate plates. If reversion of the culture were suspected, samples were assayed for ATPase activity using the Millipore filter assay as described below.

Episomes carrying ATPase genes

A series of strains harboring various F′-*ilv* episomes, kindly supplied by Dr B. J. Bachmann of Yale University, were used as presumptive F′ donors of ATPase genes. An *unc*⁻ recipient strain, unable to utilize succinate as energy source, was cross-streaked on minimal-succinate plates against the series of presumptive F′ donors of ATPase, which are multiple auxotrophs unable to multiply on the succinate plates. Confluent colonies appearing at the point of the cross-streak of donor and recipient were scored as presumptive evidence of F′-mediated transfer of ATPase genes. The presence of the F-factor in newly sired *unc*⁺ males, an indication of F′ rather than Hfr transfer of ATPase, was monitored by testing *unc*⁺ recombinants for sensitivity to the male phages f2 and Qβ or for donor ability of the F′-*ilv* episome. Quantitative mating of liquid cultures for transfer of ATPase was by standard procedures[7].

Assay of membrane-bound ATPase activity

A modification of the ATPase assay procedure of Evans[8] was used. ATPase reaction mixtures contained, in a final volume of 0.2 ml, 3 μmoles ATP adjusted to pH 7.0 with dilute NaOH, 20 μmoles Tris–HCl buffer at pH 9.5, and 1.0 μmole $MgCl_2$. The ATPase reaction was initiated by addition of enzyme and terminated,

after 30 min incubation at 37 °C in a water bath, by addition of 0.05 ml of 24% trichloroacetic acid and 1.75 ml $FeSO_4$ reagent. If necessary, denatured protein was removed at this stage by centrifugation for 5 min at $12000 \times g$ in a Sorvall centrifuge. Inorganic phosphate was determined by a modification of the Fiske and SubbaRow[9] procedure as described by Shapiro and Stadtman[10] using a Gilford 3000 spectrophotometer for color analysis. Protein was determined by the procedure of Lowry *et al.*[11] with bovine albumin as standard.

For screening large numbers of presumptive ATPase$^-$ mutants a rapid Millipore membrane filtration assay was developed. Suitable amounts of cells (*e.g.* approx. $5 \cdot 10^7$ cells) were transferred to a bank of Millipore filters with each Millipore funnel containing approx. 10 ml of lysozyme solution composed of 20 μg/ml lysozyme, 0.15 M Tris–HCl buffer at pH 6.5, 0.6 M sucrose, 1.0 mM EDTA[8]. After 10 min of incubation at 25 °C for partial cell wall digestion the cells were collected on cellulose nitrate membrane filters (approx. 4500 Å pore size) and washed using about 10 ml of Mg^{2+}–Tris solution containing 0.02 M Tris buffer at pH 7.5, 1.0 mM $MgCl_2$ (ref. 8); reagents contained in plastic squeeze bottles are convenient for these steps. The filter pads were removed to 5-ml test tubes containing the assay reagents; a small glass rod was used to immerse the disks in assay reagent. Release of inorganic phosphate was analyzed as above.

Uptake of proline by whole cells

The cells were grown on Davis' glucose salts medium[7]. L-broth (0.2 ml/10 ml) was routinely added to culture media to increase the growth of *E. coli* 3110. Nitrate-grown cells were cultured anaerobically (filled stationary flasks) in similar medium supplemented with 0.2% KNO_3. For uptake experiments cells were suspended in buffer solution (50 mM potassium phosphate at pH 7.5, 0.2% $(NH_4)_2SO_4$ and 0.01% $MgSO_4$) to a density equivalent to a Klett reading (540 mm filter) of 800 (about 5 mg dry weight/ml). Each transport incubation mixture contained 0.5 ml cells, 5 ml buffer solution, and glucose to a final concentration of 0.1%. The cells were preincubated for 15 min at 25 °C; radioactive [^{14}C]proline (251 Ci/mole, New England Nuclear) was diluted in unlabeled proline and added to a final concentration of 50 μM. Samples of 0.5 ml (about 0.1 mg dry weight) were removed at each time point, filtered on Millipore filters (0.45 μm) and washed three times with 1 ml of salts solution, all at 25 °C. The filters were dried and counted in toluene liquid scintillation fluid. For anaerobic active transport experiments cell samples were placed in 10-ml flasks fitted with rubber serum stoppers, flushed and evacuated *via* syringe needles through the stopper several times with nitrogen to remove oxygen. Reagents and samples were added and removed anaerobically through the serum stopper using small syringes and needles.

RESULTS

Rapid Millipore filtration assay for ATPase

In initiating this work it was necessary to isolate and screen large numbers of presumptive ATPase defective mutants. We have devised a Millipore filtration procedure suitable for assaying large numbers of strains for ATPase activity, a procedure described in Materials and Methods. The Millipore filtration assay saves several

hours in the time needed to assay ATPase activity of whole cells[8] mainly because of the replacement of several long centrifugation steps by rapid washing of the cells on the filter. In essence treatment of small quantities of whole cells with lysozyme–EDTA for short-time periods followed by trapping of the cells on Millipore filters exposes the ATPase activity on the filter. This is illustrated in Fig. 1A. Incubation of cells with lysozyme for periods longer than 10 min did not appreciably increase ATPase activity. Mg^{2+}-ATPase activity is exposed on the filter (approx. 40% of the lysozyme–EDTA treated level) simply by collecting the cells directly on the filter without prior lysozyme treatment (Fig. 1A). Presumably the cells somehow are "shocked" on the filter, thus exposing ATPase activity; in this regard ATPase activity was not found to be exposed by centrifugation of the cells at $10000 \times g$ for 5 min followed by resuspension in a Tris–HCl buffer. ATPase activity of membrane ghosts, membrane vesicles, as well as solubilized ATPase stick tightly to the cellulose nitrate filter and may be assayed accordingly (Fig. 1B). Overloading the filter leads to the plateau observed in Fig. 1B, an effect not observed with the conventional assay of Evans[8].

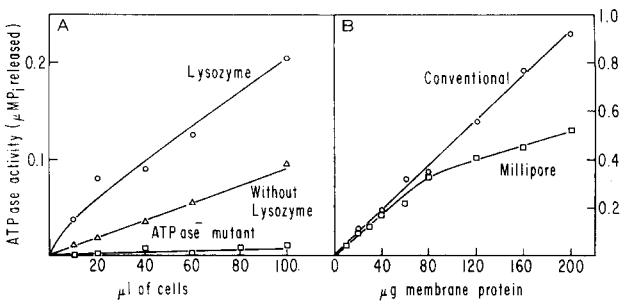

Fig. 1. (A) Millipore assay of ATPase activity of whole cells of *E. coli*. Exponentially multiplying cells at $A_{550\,nm}$ of 0.75 were used. Assay conditions for lysozyme-treated culture as described in Materials and Methods. Lysozyme and EDTA were omitted from lysing solution for cells "without lysozyme". (B) Comparison of Millipore filter assay of cell-free membrane ATPase activity *versus* "conventional" procedure. Assay conditions as described in Materials and Methods. Cell-free membrane "ghosts" with ATPase activity were prepared and stored in the frozen state using the method described by Evans[8].

We have compared the specific activities of ATPase of cells ruptured in different ways, mainly by treatment on Millipore filters, Evans' treatment[8], and sonication. Highest ATPase levels were observed after sonication. The filtration procedure gives 80% of the ATPase activity compared to sonication, an indication that not all ATPase activity is exposed on the filter. Lower values (47% compared to sonication) were obtained with the lysozyme procedure of Evans[8], perhaps due to partial solubilization of ATPase during washing of the membranes.

Unc$^-$ mutants show little if any ATPase activity, regardless of the cell breakage method we used. However, the presence of an active membrane Mg^{2+}-activated ADP hydrolyzing[8] activity capable of releasing additional P_i from ADP, the product of ATPase action, represents a potential source of error when crude preparations are being assayed. This activity is absent from purified ATPase preparations[12]. ATPase activity exposed by the filter using whole cells is a Mg^{2+}-> Mn^{2+}-> Ca^{2+}-ATPase

at pH 9. A number of enteric bacteria including *E. coli*, *Salmonella* and *Klebsiella* display ATPase activity using the Millipore method.

Mapping of coupling factor ATPase

P1 cotransduction as well as interrupted mating experiments were used by Butlin *et al.*[2] to map ATPase near *ilv* on the *E. coli* genetic linkage map. We have devised a simple technique for mapping our mutants using the F'16 (F'-*ilv*) episome which we have found carries genetic information for ATPase activity. Strains carrying the small episome, F'-*ilv* (F'16), readily donate this extrachromosomal DNA element to F^-, unc^- recipients genetically converting them to the unc^+ phenotype capable of growth on succinate and other Krebs cycle intermediates as sole source of energy. Newly sired unc^+ males are sensitive to male-specific phages and are themselves donors of F'-*ilv* suggesting F' transfer of coupling factor ATPase genes. The simplest explanation of these results is that during the original excision events of the sex factor from its Hfr integration site some coupling factor ATPase genes were carried along with *ilv* genes on the episome. The cross-streak procedure described in Materials and Methods provides a simple device for mapping new unc^- isolates; so far all six of our coupling factor mutations are covered by this episome.

Defective anaerobic growth of ATPase$^-$ mutants

In our initial experiments concerned with the anaerobic growth rates of the ATPase$^-$ mutants we have observed that mutants are capable of actively fermenting glucose broth in filled screw capped tubes after overnight incubation at 37 °C suggesting that ATPase activity was not essential for anaerobic growth. However, shorter term growth studies reveal, as shown in Fig. 2, that little growth occurs in anaerobic cultures of the unc^- strain during a time period sufficient for the completion of the entire growth cycle of wild type or the mutant growing aerobically. As seen in Fig. 2, following inoculation the anaerobic unc^- culture first develops a slight turbidity perhaps due to traces of oxygen dissolved in the medium; little further growth is observed during this experiment. Similar results have been obtained with four different mutants examined. However, after incubation for longer than 5-h revertants are

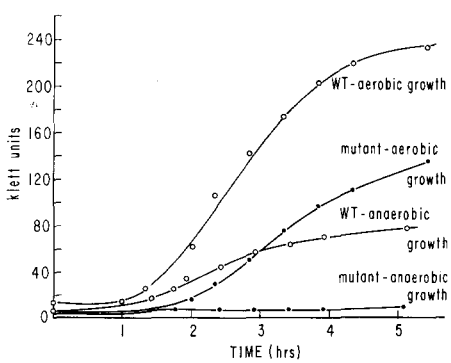

Fig. 2. Growth curves of wild type (WT) and ATPase defective strains (mutant) in glucose broth under aerobic *versus* anaerobic conditions. Anaerobic growth was carried out in completely filled screw-cap tubes adapted to fit the Klett colorimeter (540 filter). See Materials and Methods for further details.

commonly encountered. It is of some interest that addition of NO_3^- (0.2%) as terminal electron acceptor (data not shown) restores active growth to the *unc*$^-$, anaerobic culture after a short period of adaptation (approx. 60 min). Note also that the doubling time of the mutant is roughly twice that of the parent, a finding we have observed with all of our mutants.

Our major conclusion from growth studies is that *unc*$^-$ mutants defective in ATPase activity are unable to multiply anaerobically. The physiological defect(s) of the *unc*$^-$ strains was next investigated.

A lesion in active transport

Experiments in this section are concerned with anaerobic active transport or uptake of [^{14}C]proline by whole cells. This amino acid was chosen as representative of a series of 16 amino acids known to be taken up by *E. coli*[13]. As shown in Fig. 3, intact cells of *unc*$^-$ mutants defective in ATPase are completely blocked in their ability to perform active transport of radioactive proline under strictly anaerobic conditions. It should be emphasized that the defect in active transport by *unc*$^-$ strains is "conditional" with transport taking place under aerobic conditions, though at somewhat reduced levels in comparison to the wild type strain under similar conditions. In four different experiments the average values after 10 min of incubation for aerobic uptake of [^{14}C]proline for *unc*$^-$ mutant cells was 39% that of the wild type strain (100%). In these same four experiments anaerobic uptake by wild type cells was 68% that of aerobic uptake by wild type cells (100%). In comparison anaerobic uptake by *unc*$^-$ cells was only about 5% that of aerobic uptake by *unc*$^-$ cells (100%). In other words, the *unc*$^-$ strain anaerobically transports [^{14}C]proline at a rate approximately one-

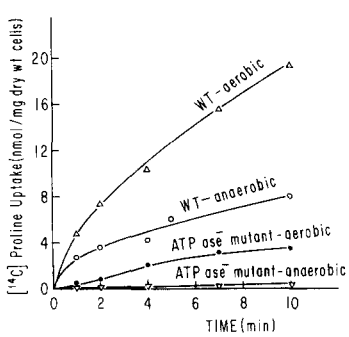

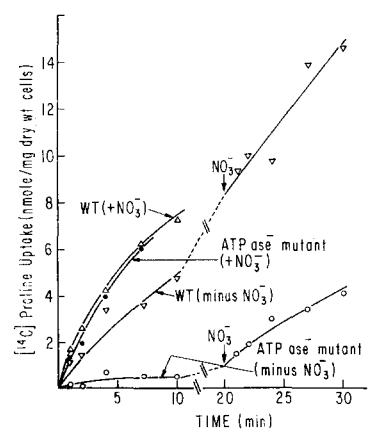

Fig. 3. Block of [^{14}C]proline uptake by whole cells of an ATPase defective mutant under strictly anaerobic conditions. The experimental conditions of Simoni and Shallenberger[4] were followed. Also see text for further details. Cellular dry weights were calculated using the expression of Simoni and Shallenberger[4].

Fig. 4. Coupling of nitrate respiration to anaerobic [^{14}C]proline uptake in an ATPase defective mutant. Conditions similar to Fig. 3, except at the times indicated by arrows 0.2% NO_3^- was added by syringe through the serum stopper.

twelfth as fast as wild type under similar conditions, a finding we have repeated with four different *unc*$^-$ strains.

The last experiment is concerned with the role of NO_3^- as terminal electron acceptor coupled to anaerobic transport. We observed that addition of NO_3^- to anaerobic glucose-broth cultures of ATPase$^-$ mutants promotes growth while control cultures without NO_3^- fail to grow. The wild type of course does not require NO_3^- for anaerobic growth on glucose. As illustrated in Fig. 4, NO_3^- is able to effectively replace O_2 as exogenous electron acceptor in NO_3^--adapted cells for anaerobic respiratory coupled transport of proline. Note that the mutant cells in the absence of acceptor (ATPase$^-$ mutant, *minus* NO_3^-) display little capacity to take up proline, a function that is restored by addition of NO_3^- (arrow). On the other hand, the wild type cells are able to transport proline anaerobically without the need of NO_3^- (wild type, *minus* NO_3^-); some stimulation is observed on addition of NO_3^- (arrow). In the two curves labelled "WT, ($+NO_3^-$)" and "ATPase mutant ($+NO_3^-$)", NO_3^- was added to the cultures at the start of the experiment.

Again this experiment shows that ATPase$^-$ mutants have a defective transport system under anaerobic conditions with anaerobic respiration of NO_3^--providing energy for anaerobic transport.

CONCLUSIONS

Our studies have been concerned with the mechanism of energy interconversion coupled to active transport in the anaerobic membrane. The elegant studies of Kaback and his associates[3,13] with membrane vesicles of *E. coli* have shed new light on the mechanism of respiratory-linked active transport of amino acids and other nutrients in *E. coli*. It should be emphasized that vesicle preparations catalyze the active concentration of amino acids and certain sugars only in the presence of a respiratory substrate such as D-lactate or succinate as electron donor and oxygen as terminal electron acceptor[13]. In other words, vesicle preparations are inactive under anaerobic conditions, in contrast to whole cells which are active under strictly anaerobic conditions (see Figs 3 and 4). Indeed *E. coli* grows at the expense of energy derived from fermentation of a variety of sugars under strictly anaerobic conditions as do many other facultative and strictly anaerobic bacteria, many of which do not synthesize cytochromes or a respiratory electron transport chain. This has led Harold[1], in a lucid survey of the recent literature in this field, to question the universality of respiratory-coupled active transport in bacteria. In simplest terms anaerobic bacteria must have an alternate mechanism(s) of energy supply for membrane work. Unfortunately little is yet known about the mechanism of energy conversion in the anaerobic membrane. Harold[1] speculates that ATP derived from substrate level phosphorylation may serve as energy source for membrane activity in anaerobic bacteria. It should be recalled that Kaback and associates[3,13] have presented clear-cut experimental evidence against phosphorylated intermediates in the respiratory-linkeed vesicle uptake system of *E. coli* (see discussion by Lombardi and Kaback[13]). However, these findings do not rule out the possibility of phosphorylated intermediates in fermentation (nonrespiratory)-coupled uptake systems. Our findings support Harold's viewpoint, mainly that the anaerobic- and respiratory-linked systems should be considered as unrelated processes.

The availability of membrane ATPase or coupling factor mutants (*unc*$^-$) of *E. coli*[2] has permitted study of the role of this enzyme in anaerobic membrane metabolism. Growth studies reveal that *unc*$^-$ mutants missing membrane ATPase activity are unable to grow anaerobically on glucose. We conclude from these experiments that anaerobic growth and anaerobic active transport somehow require membrane ATPase or coupling factor activity. This need is overcome by respiration. The simplest explanation (working hypothesis) is that *unc*$^-$ cells are totally dependent on respiration-linked energy supply for their membrane function. This is in contrast to the normal wild type *E. coli* cell which can apparently also utilize membrane coupling factor to link energy from glycolysis to membrane energy needs.

In four different experiments we found that the aerobic uptake of proline by ATPase-defective mutants was consistently lower, being 20–50% that of wild type. One possible explanation of this finding is that ATPase contributes to, but is obviously not essential for, aerobic transport.

As shown in Fig. 4, anaerobic uptake of proline by ATPase mutants is restored by addition of NO_3^- which behaves as a terminal electron acceptor replacing oxygen; also we have observed that anaerobic growth of these mutants is restored by addition of NO_3^- to the medium. It thus seems likely that anaerobic respiration of NO_3^- supplies energy for active transport.

Finally, our findings are in agreement with those recently reported by Schairer and Haddock[5] who observed that respiratory poisons such as KCN completely abolish uptake of the β-galactoside, (TMG), in ATPase defective strains. These workers concluded that ATPase is necessary for coupling of ATP hydrolysis to the accumulation of TMG in the absence of respiration. Thus ATPase or coupling factor activity appears essential for anaerobic active transport of certain sugars as well as amino acids. The question of whether ATP functions directly as energy source for anaerobic transport must await future biochemical experiments. While this paper was in preparation Butlin *et al.*[14] published their finding that *unc* A mutants are impaired in anaerobic growth. They also describe a new class of uncoupled mutants (*unc* B) and discuss the role of coupling factor proteins in oxidative phosphorylation in *E. coli*.

ACKNOWLEDGMENTS

We especially thank Francisco Luna for preparation of the ATPase mutants. Research supported by a grant from the National Science Foundation (GB-35331). M. N. is the recipient of a grant from the Centre National de la Recherche Scientifique and a travel grant under the Fulbright–Hays Program for studies in the laboratory of Prof. M. D. Kamen, whom we thank for encouragement and support.

REFERENCES

1 Harold, F. M. (1972) *Bacteriol. Rev.* 172–216
2 Butlin, J. D., Cox, G. B. and Gibson, F. (1971) *Biochem. J.* 124, 75–81
3 Hong, J.-S. and Kaback, H. R. (1972) *Proc. Natl. Acad. Sci. U.S.* 69, 3336–3340
4 Simoni, R. D. and Shallenberger, M. K. (1972) *Proc. Natl. Acad. Sci. U.S.* 69, 2663–2667
5 Schairer, H. U. and Haddock, B. A. (1972) *Biochem. Biophys. Res. Commun.* 48, 544–551
6 Kanner, B. I. and Gutnick, D. L. (1972) *J. Bacteriol.* 111, 287–289

7 Roth, J. R. (1970) in *Methods in Enzymology* (Tabor, H. and Tabor, C. W., eds), Vol. 27, pp. 3–34, Academic Press, New York
8 Evans, Jr, D. J. (1969) *J. Bacteriol.* 100, 914–922
9 Fiske, C. H. and SubbaRow, J. (1925) *J. Biol. Chem.* 66, 375–400
10 Shapiro, B. M. and Stadtman, E. R. (1970) in *Methods in Enzymology* (Tabor, H. and Tabor, C. W., eds), Vol. 27, pp. 910–922, Academic Press, New York
11 Lowry, O. H., Rosebrough, N. J., Farr, A. L. and Randall, R. J. (1951) *J. Biol. Chem.* 193, 265–275
12 Kobayashi, H. and Anraku, Y. (1972) *J. Biochem. Tokyo* 71, 387–399
13 Lombardi, F. J. and Kaback, H. R. (1972) *J. Biol. Chem.* 247, 7844–7857
14 Butlin, J. D., Cox, G. B. and Gibson, F. (1973) *Biochim. Biophys. Acta* 292, 366–375

Biochimica et Biophysica Acta, 314 (1973) 276–283

BBA 46600

THE RESPIRATORY CHAIN OF *AZOTOBACTER VINELANDII*

II. THE EFFECT OF CYANIDE ON CYTOCHROME *d*

H. F. KAUFFMAN and B. F. VAN GELDER

Laboratory of Biochemistry, B. C. P. Jansen Institute, University of Amsterdam, Plantage Muidergracht 12, Amsterdam (The Netherlands)

(Received April 18th, 1973)

SUMMARY

1. Cyanide causes a slow disappearance of the oxidized band (648 nm) of cytochrome *d* in particles of *Azotobacter vinelandii* and inhibits the appearance of the reduced band (631 nm). No effect of cyanide is found on the reduced band of cytochrome *d*.

2. The kinetics of the disappearance of the 648-nm band of cytochrome *d* with excess cyanide deviates from first-order kinetics at lower temperatures (22 °C) indicating that at least two conformations of the enzyme are involved. At higher temperatures (32 °C) the observed kinetics of the cyanide reaction are first order with a $k_{on}=0.7\ M^{-1}\cdot s^{-1}$ and with an estimated k_{off} of approximately $5\cdot10^{-5}\ s^{-1}$.

3. The value for the k_{off} ($7\cdot10^{-4}$–$14\cdot10^{-4}\ s^{-1}$ at 32 °C) determined from the rate of reduction of cyanocytochrome *d* by $Na_2S_2O_4$ or NADH is one order of magnitude larger than the k_{off} value found when the enzyme is in its oxidized state.

4. No effect of cyanide is found on the spectrum of cytochrome a_1.

INTRODUCTION

In a previous paper[1] on the respiratory chain of *Azotobacter vinelandii*, it has been concluded from spectra of particles reduced by internal substrates that the oxidized (648 nm) and the reduced (631 nm) absorption bands of cytochrome *d* are only indirectly related. Therefore we proposed a second oxidized conformation of cytochrome *d*, that scarcely absorbs in the red region. In order to study the properties of both conformations we investigated the effect of ligand binding to the oxidase part of the chain.

Microspectroscopic studies[2–6] of aerobically grown microorganisms revealed the disappearance of the oxidized band of cytochrome *d* upon addition of cyanide without the formation of the reduced band, and a shift by carbon monoxide of the reduced band 7 nm to the red. In contrast, cytochrome *cd*, isolated from anaerobically nitrate-grown *Pseudomonas aeruginosa*, shows hardly any spectral change upon

Abbreviations: TMPD, *N,N',N,N'*-tetramethyl-*p*-phenylenediamine; DCIP, 2,6-dichlorophenolindophenol.

addition of cyanide, and CO causes a flattening of the reduced (625 nm) absorption band[7].

In the branched respiratory chain as proposed by Jones and Redfearn[8], cyanide is an effective inhibitor of cytochrome a_1, but has less effect on cytochrome *d* in the particles of *A. vinelandii*. However, no spectroscopic studies were carried out on the oxidase to support their suggestion. We have, therefore, investigated the effect of cyanide on the absolute spectra of cytochrome *d* in particles of *A. vinelandii* and the kinetics of the spectral changes.

METHODS

Phosphorylating particles were prepared as described by Pandit-Hovenkamp[9] and stored in 40 mM phosphate buffer (pH 7.2)–0.25 M sucrose–40 mM KCl at 77 °K.

Spectra, recorded on a Perkin–Elmer spectrophotometer Model 356, were measured with particles suspended in 30 mM phosphate buffer (pH 7.6)–5 mM $MgCl_2$–1 mM EDTA. When absolute spectra were recorded the effect of light scattering was diminished by using a sonified clay–powder suspension in the reference cell[1]. The spectra were normalized as described in a previous paper[1] taking 600 and 725 nm as reference points. For calculating the contribution of the separate electronic transitions to the composite oxidized absorption band, spectra were analysed using a Dupont 310 Curve Resolver.

Chemicals were Analar grade, mainly obtained from British Drug Houses, except those used for the culture medium, that were less highly purified.

RESULTS

The effect of 2 mM cyanide on the spectrum of oxidized particles as a function of time is shown in Fig. 1. It is clear that cyanide causes a diminishing of the absorption band at 648 nm without the appearance of a band at 631 nm of reduced cytochrome *d*. In a previous paper[1] it was shown that the composite oxidized band can be resolved into three Gaussian curves with peak positions at 635, 648 and 670 nm. On resolving the spectra of Fig. 1 in this way it appears that the decrease of the composite band is largely due to a decrease of the Gaussian 648-nm absorption band of oxidized cytochrome *d*. The band at 670 nm also diminishes but more slowly, whereas the 635-nm band is hardly affected. Spectrum No. 5 of Fig. 1, remaining 46 min after addition of cyanide, has a peak at 645 nm. On resolution of this spectrum, it was found that 95% of the initial Gaussian band remains at 635 nm, 75% of that at 670 nm and only 10% of that at 648 nm. After 20 h incubation (spectrum No. 6), the two broad bands at 635 and 670 nm have further decreased.

In order to determine whether the decrease of the 635- and 670-nm bands is due to an effect of cyanide or to reduction, the reducing agent ascorbate *plus* TMPD was added to particles preincubated with 2 mM cyanide for 1 h, in which the residual broad absorption band consisted mainly of the Gaussian 635- and 670-nm bands. After the addition of the reducing agent, spectrum No. 7 of Fig. 1 is rapidly formed with a very broad and flat band centered around 650 nm. Therefore, it is likely that the decrease of the Gaussian absorption bands at 635 and 670 nm in the presence of

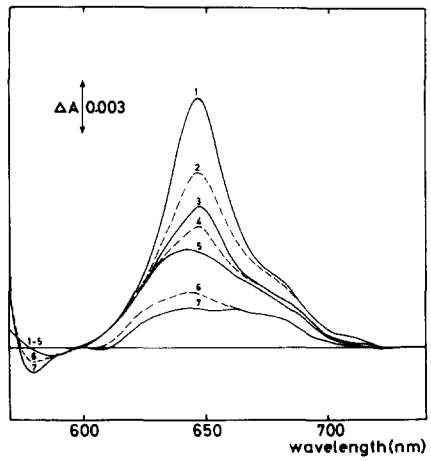

Fig. 1. The effect of cyanide on the spectrum of cytochrome *d* as a function of incubation time. Particles (0.7 mg protein/ml) were suspended in phosphate–$MgCl_2$–EDTA solution (pH 7.6) at 32 °C. The reference cell contained an appropriate clay-powder suspension to diminish the effect of light scattering. Spectra: 1, particles in the absence of cyanide; 2–6, after 11.5, 17.5, 26 and 46 min and 20 h incubation with 2 mM cyanide, respectively; 7, after 1 h cyanide (2 mM) pre-incubation and addition of ascorbate (7.5 mM), *N,N,N',N'*-tetramethyl-*p*-phenylenediamine (TMPD) (0.25 mM) followed by 1 min bubbling of oxygen. Scan speed 240 nm/min. The spectra are normalized (see Methods).

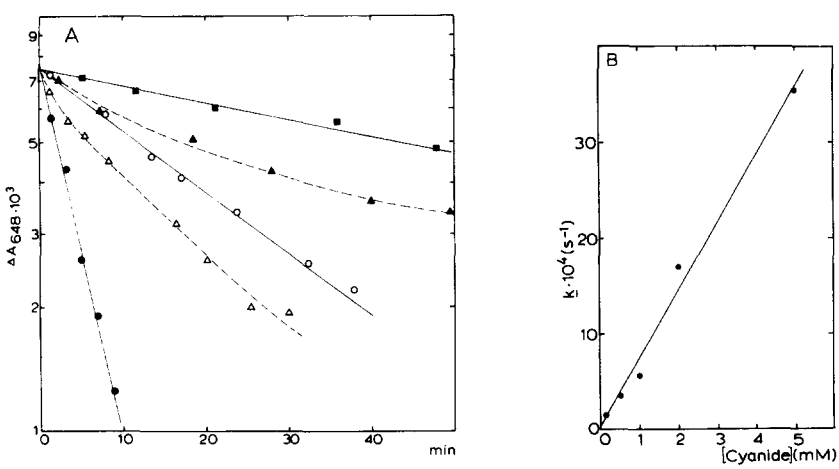

Fig. 2. Reaction of cyanide with oxidized cytochrome *d*. Particles (0.7 mg protein/ml) were diluted in phosphate–$MgCl_2$–EDTA solution *plus* variable cyanide concentrations. Intensities of the absorbance of cytochrome *d* at 648 nm were calculated by means of a Curve Resolver (see Methods). A. Time course of the reaction at 32 °C: ●—●, 5 mM cyanide; ○—○, 1 mM cyanide; ■—■, 0.1 mM cyanide, and at 22 °C: △----△, 5 mM cyanide; ▲----▲, 2 mM cyanide. B. Effect of cyanide concentration on the first-order rate constant at 32 °C.

cyanide is caused by reduction. This is supported by the observation that in the presence of cyanide, ferricyanide prevents the disappearance of these bands, but not that at 648 nm.

The disappearance of the Gaussian 648-nm band of cytochrome *d* follows first-order kinetics for different cyanide concentrations at 32 °C, as is shown in Fig. 2A, where the $\log \Delta A_{648\ nm}$ is plotted as a function of time. By plotting the observed pseudo first-order constants, which equal k_{on} [cyanide]$+k_{off}$, against cyanide concentrations (Fig. 2B), a second-order rate constant of 0.7 $M^{-1} \cdot s^{-1}$ can be calculated from the slope of the straight line. The k_{off}, estimated from the intersection point with the ordinate, has a value of approximately $5 \cdot 10^{-5}$ s^{-1}.

Fig. 2A shows that at 22 °C the decrease of the 648-nm band is no longer first order. Therefore, it must be concluded that a second reaction preceding or following the binding of cyanide is involved (see also Van Buuren *et al.*[10] and Van Buuren[11]). The convex lines in the plot of $\log \Delta A_{648\ nm}$ against time at 22 °C, can be explained by assuming that the second reaction approaches equilibrium. The marked effect of temperature on the deviation from first-order kinetics suggests the involvement of a conformational change in one of the reactions. On the basis of these data, combined with our observation[1] of two oxidized conformations of cytochrome *d*, we like to propose the following mechanism:

$$d_{648} \rightleftharpoons d_x \overset{CN}{\rightleftharpoons} d_x\text{–CN}$$

where d_{648} and d_x denote conformations of cytochrome *d* absorbing at 648 nm and hardly absorbing in the red, respectively (*cf.* also ref. 1).

It may be concluded that cyanide (2 mM) does not affect the ligand field of the heme of reduced cytochrome *d*, since after an incubation for 5 h under anaerobiosis no change in the 631-nm band is observed. This is in agreement with observations made by Negelein and Gerischer[2] with *Azotobacter chroococcum* and Tissières[5] with *Aerobacter aerogenes*. However, after opening the cuvette and aerating the solution, a rapid decrease of the 631-nm band is observed without the formation of the 648-nm absorption band. Therefore, it is concluded that cyanide can react rapidly with cytochrome *d* when oxygen is introduced.

Cyanide-liganded cytochrome *d* has little absorption in the red and its rate of reduction is inhibited, when compared to that in the absence of cyanide[2–6]. This makes it possible to study the relationship between the oxidized (648 nm) and reduced (631 nm) absorption bands of the non-liganded cytochrome. In Table I the intensities of both bands are compared as a function of the preincubation time with cyanide. It is clear that the decrease in intensity of the absorbance at 631 nm, measured directly after the addition of dithionite, corresponds with that at 648 nm. This demonstrates again that the two bands are intimately related, as was shown in a previous paper[1].

When dithionite is added to particles in which cytochrome *d* is present as cyanocytochrome *d*, prepared by the action of 2 mM cyanide in the presence of ascorbate *plus* TMPD and O_2, a slow appearance of the reduced band of cytochrome *d* (631 nm) is observed. This represents the decay of cyanocytochrome *d*, and is shown in a first-order plot in Fig. 3. From the slope of the straight line a first-order rate constant

($1.4 \cdot 10^{-3}$ s^{-1}) can be calculated, that is independent of the cyanide concentration used (not shown).

Under anaerobic conditions the reduction of cyanocytochrome *d* by NADH (Fig. 3) shows after a lag period, which is possibly due to traces of oxygen present,

TABLE I

THE PERCENTAGES OF THE OXIDIZED AND REDUCED ABSORPTION BANDS OF CYTOCHROME *d* AS A FUNCTION OF THE PREINCUBATION TIME WITH CYANIDE

Spectra were measured directly before ($A_{648\ nm}$) and after addition of dithionite ($A_{631\ nm}$). Conditions as described under Fig. 1.

Preincubation time (*min*)	[*Cyanide*] (*mM*)	$\%A_{648\,nm}$	$\%A_{631\,nm}$
0	0.1	100	100
40	0.1	76	73
86	0.1	59	54
160	0.1	44	43
55	5	0	0

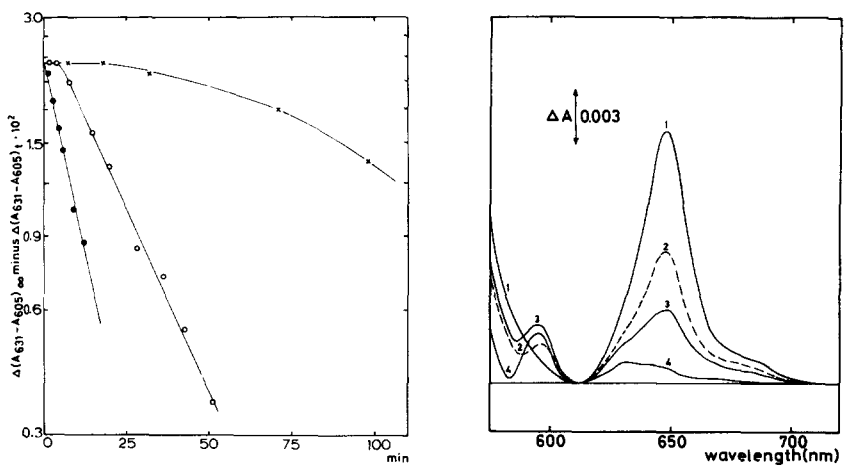

Fig. 3. Rate of reduction of cyanocytochrome *d* with different substrates. Cyanocytochrome *d* was prepared by aerobic incubation of particles (1.15 mg protein/ml) with cyanide (2 mM) for 10 min after which ascorbate (7.5 mM) *plus* TMPD (0.25 mM) were added. After evacuation (6 min) substrate was added from a side arm. The reference cuvette contained an appropriate clay–powder suspension. The degree of reduction of cytochrome *d* was calculated from spectra, normalized as described in Methods. The $\Delta(A_{631-605\ nm})_\infty$ value was obtained from a dithionite-reduced sample in the absence of cyanide. Spectra were scanned with a speed of 240 nm/min. ×—×, no addition; ●—●, *plus* dithionite; ○—○, *plus* 2 mM NADH.

Fig. 4. The effect of cyanide on the spectra of cytochrome *d* and cytochrome a_1 as a function of time. Particles (1.3 mg protein/ml) were suspended in phosphate–$MgCl_2$–EDTA solution at 21 °C. The reference cell contained an appropriate clay–powder suspension. Spectra were normalized as described in the previous paper[1] taking 610 and 710 nm as reference points. Scan speed 240 nm/min. Spectra indicated: 1, in the absence of cyanide; 2 and 3, after 5 and 12 min incubation with 10 mM cyanide, respectively; 4, 15 min preincubation with cyanide followed by the addition of ascorbate (7.5 mM) *plus* TMPD (0.75 mM) and bubbling with oxygen for 1 min.

also first-order kinetics with a k value of $7 \cdot 10^{-4}$ s^{-1}. The control experiment, with ascorbate *plus* TMPD, at anaerobiosis also shows reduction, but the lag period is substantially longer and no first-order kinetics are obtained. From this it may be concluded that cyanocytochrome *d* is reduced by substrates under anaerobic conditions either directly or *via* non-liganded heme in equilibrium with the cyanide compound.

In the particles used in the previously described experiments no clear absorption maximum of cytochrome a_1 could be detected. Nevertheless, the activity of these particles is as high as for other particles containing a substantial amount of cytochrome a_1 (3.1 and 4.1 μatoms O/min per mg protein for ascorbate *plus* 2,6-dichlorophenolindophenol (DCIP) and NADH, respectively, as substrates). Therefore, one wonders whether cytochrome a_1 is an integral part of the respiratory chain of *A. vinelandii*.

In the model of the chain as proposed by Jones and Redfearn[8] cytochrome a_1 functions as a cyanide-sensitive terminal oxidase. Therefore, we investigated the spectroscopic effect of cyanide on a batch of particles, isolated from bacteria cultured for 38 h, which contained a substantial amount of cytochrome a_1. As illustrated in Fig. 4, the addition of cyanide to oxidized particles causes a decrease of the absorbance at 648 nm (spectra Nos 2 and 3) in time, and a concomitant reduction of cytochrome a_1, as judged from the increase in absorbance at 596 nm. The maximal reduction of cytochrome a_1 is reached after addition of ascorbate *plus* TMPD (spectrum No. 4). Addition of potassium ferricyanide brought about a fast reoxidation of cytochrome a_1 (not shown), indicating that cyanide does not affect cytochrome a_1 since it remains easily oxidizable and reducible.

DISCUSSION

The disappearance of the oxidized (648 nm) band of cytochrome *d* without appearance of a reduced (631 nm) band after the addition of cyanide is in accordance with the observation[1] that these two bands are indirectly related. It was proposed that a second oxidized conformation of cytochrome *d*, termed cytochrome d_x, exists that scarcely absorbs in the red region. Furthermore, the 648-nm band of oxidized cytochrome *d* was ascribed to a charge transfer from a ligand to the iron[1]. The effect of cyanide on cytochrome *d* resembles the observation of Brill and Williams[12], that charge-transfer bands of ferric hemoproteins disappear in the presence of cyanide. Thus, the disappearance of the 648-nm band of cytochrome *d* can be explained as a binding of cyanide to cytochrome *d*, thereby preventing the charge transfer.

Based on the kinetics of the binding of cyanide to oxidized cytochrome *d*, and the effect of temperature on the rate of binding, a mechanism is proposed, in which a change of cytochrome *d* from the d_{648} to the d_x conformation is followed by the binding of cyanide to cytochrome d_x. This is supported by the observation that at turnover conditions, thereby promoting the d_x conformation[1], the binding of cyanide to cytochrome *d* was highly facilitated[13]. It is interesting to note that the kinetics of cyanide binding to oxidized cardiac cytochrome *c* oxidase[10,11,14–16] are of the same type as was found for cytochrome *d* at 22 °C. But, in contrast to cytochrome *c* oxidase[10,11], reduced cytochrome *d* shows no spectral change on the addition of cyanide.

Dithionite or NADH under anaerobic conditions are able to reduce cyanocytochrome *d*. For the decay of cyanocytochrome *d* first-order rate constants of $7 \cdot 10^{-4}$–$14 \cdot 10^{-4}$ s^{-1} at 32 °C could be calculated. The value of k is at least one order of magnitude larger than the k_{off} value ($5 \cdot 10^{-5}$ s^{-1}) which was calculated from the reaction of cyanide with oxidized cytochrome *d*. This difference can be explained in two ways. Firstly, reduction of the heme *d* occurs in cyanocytochrome *d*, after which the cyanide is split off from the reduced heme with a higher k_{off} value. Secondly, a conformational change of the cytochrome *d* molecule, brought about by the reduction of other components of the chain, and thus giving rise to a higher value for the dissociation rate constant of the oxidized heme *d*. The latter explanation is similar to that given by Van Buuren *et al.*[10] and Van Buuren[11] for the dissociation of cyanide from cyanocytochrome aa_3.

The reduction of cytochrome a_1 in the presence of cyanide and oxygen and its reoxidation after ferricyanide addition, showed that cyanide does not affect the heme of cytochrome a_1 and thus is unable to function as a cyanide-sensitive oxidase as was proposed earlier[8]. This is supported by the observation that a cyanide-sensitive ascorbate *plus* DCIP activity is found even in particles in which no cytochrome a_1 is detectable or that had been purified with Triton X-100[17].

The apparent effect of cyanide on oxidized cytochrome *d* in particles of *A. vinelandii* seems to be in contrast with the observations on isolated cytochrome *cd* from anaerobically nitrate-grown *Ps. aeruginosa* and *Micrococcus denitrificans*[18]. Although generally in literature[19,20] no distinction is made between cytochromes *d* from aerobically or anaerobically grown organisms, a comparison of the different properties of these two types of cytochromes, which are summarized in Table II, shows that the two enzymes differ considerably in physical and chemical properties. The apparent functional difference of the two enzymes, being an oxidase[8,21] or nitrite reductase[22,23], respectively, is expressed in different effects of ligand binding. The difference in peak positions of the pyridine hemochrome and alkaline heme *d* spectra[7] also indicate that the prosthetic groups are not identical, as was already proposed by Newton[18].

TABLE II

DIFFERENCES BETWEEN CYTOCHROMES *d* FROM AEROBICALLY AND ANAEROBICALLY NITRATE-GROWN ORGANISMS

Properties	*Cytochrome d*	*Cytochrome cd*
Function	Oxidase[8, 21]	Nitrite reductase[22, 23]
Growth condition	Aerobe	Anaerobe *plus* nitrate
Effect of oxygen during growth	Low $[O_2]$→ high [cyt. *d*] High $[O_2]$→ low [cyt. *d*][24, 25]	Enzyme is depressed, another oxidase is formed[26–28]
Oxidized absorption band	645–648 nm[1–6]	630–635 nm[7, 18, 22, 23, 29]
Reduced absorption band	630–632 nm[1–6]	625 nm[7, 18, 22, 23, 29]
Oxidized cytochrome *plus* cyanide	648-nm band disappears[1–6], this paper	Small spectral effects[7]
Reduced enzyme *plus* CO	634–636 nm[2–6]	625-nm band flattens[7]
Pyridine hemochrome	612–613 nm[1, 30]	618–620 nm[7, 29, 31]
Reduced alkaline haem *d*	618 nm[30]	626 nm[7, 29, 31]

ACKNOWLEDGEMENTS

We wish to thank Prof. E. C. Slater for his interest, Mrs Dr H. G. Pandit-Hovenkamp, Dr A. O. Muijsers, Dr L. J. M. Eilermann and Dr K. J. H. van Buuren for their advice and stimulating discussions and Mr B. van Swol for his expert technical assistance. This work was supported in part by a grant from the Netherlands Organization for the Advancement of Pure Research (Z.W.O.) under the auspices of the Netherlands Foundation for Chemical Research (S.O.N.).

REFERENCES

1 Kauffman, H. F. and Van Gelder, B. F. (1973) *Biochim. Biophys. Acta* 305, 260–267
2 Negelein, E. and Gerischer, W. (1934) *Biochem. Z.* 268, 1–7
3 Keilin, D. (1934) *Nature* 133, 290–291
4 Fujita, A. and Kodama, T. (1934) *Biochem. Z.* 273, 186–197
5 Tissières, A. (1951) *Biochem. J.* 50, 279–288
6 Tissières, A. (1956) *Biochem. J.* 64, 582–589
7 Horio, T., Higashi, T., Matsubara, H., Kusai, K., Nakai, M. and Okunuki, K. (1958) *Biochim. Biophys. Acta* 29, 297–302
8 Jones, C. W. and Redfearn, E. R. (1967) *Biochim. Biophys. Acta* 143, 340–353
9 Pandit-Hovenkamp, H. G. (1967) in *Methods in Enzymology* (Estabrook, R. W. and Pullman, M. E., eds), Vol. 10, pp. 152–157, Academic Press, New York
10 Van Buuren, K. J. H., Nicholls, P. and Van Gelder, B. F. (1972) *Biochim. Biophys. Acta* 256, 258–276
11 Van Buuren, K. J. H. (1972) *The Binding of Cyanide to Cytochrome* aa_3, Ph. D. Thesis, University of Amsterdam, Gerja, Waarland
12 Brill, A. S. and Williams, R. J. P. (1961) *Biochem. J.* 78, 246–253
13 Eilermann, L. J. M. (1973) *Some Aspects of Energy Conservation in Azotobacter vinelandii*, Ph. D. Thesis, University of Amsterdam, Gerja, Waarland
14 Van Buuren, K. J. H., Zuurendonk, P. F., Van Gelder, B. F. and Muijsers, A. O. (1972) *Biochim. Biophys. Acta* 256, 243–257
15 Nicholls, P., Van Buuren, K. J. H. and Van Gelder, B. F. (1972) *Biochim. Biophys. Acta* 275, 279–287
16 Antonini, E., Brunori, M., Greenwood, C., Malmström, B. C. and Rotilio, G. C. (1971) *Eur. J. Biochem.* 23, 396–400
17 Mueller, T. J. and Jurtshuk, Jr, P. (1972) *Fed. Proc.* 31, 888 Abs
18 Newton, N. (1969) *Biochim. Biophys. Acta* 185, 316–331
19 Bartsch, R. G. (1968) *Annu. Rev. Microbiol.* 22, 181–200
20 Kamen, M. D. and Horio, T. (1970) *Annu. Rev. Biochem.* 39, 673–700
21 Castor, L. N. and Chance, B. (1959) *J. Biol. Chem.* 234, 1587–1592
22 Yamanaka, T., Ota, A. and Okunuki, K. (1961) *Biochim. Biophys. Acta* 53, 294–308
23 Yamanaka, T. and Okunuki, K. (1963) *Biochim. Biophys. Acta* 67, 379–393
24 Harrison, D. E. F. (1972) *Biochim. Biophys. Acta* 275, 83–92
25 Ackrell, B. A. C. and Jones, C. W. (1971) *Eur. J. Biochem.* 20, 29–35
26 Lam, Y. and Nicholas, D. J. D. (1969) *Biochim. Biophys. Acta* 180, 459–472
27 Sapshead, L. M. and Wimpenny, J. W. T. (1972) *Biochim. Biophys. Acta* 267, 388–397
28 Azoulay, E. and Couchoud-Beaumont, P. (1965) *Biochim. Biophys. Acta* 110, 301–311
29 Horio, T., Higashi, T., Yamanaka, T., Matsubara, H. and Okunuki, K. (1961) *J. Biol. Chem.* 236, 944–951
30 Barrett, J. (1956) *Biochem. J.* 64, 626–639
31 Yamanaka, T. and Okunuki, K. (1963) *Biochim. Biophys. Acta* 67, 407–416

Biochimica et Biophysica Acta, 314 (1973) 284–297

BBA 46592

PURIFICATION OF CYTOCHROME b_6 A TIGHTLY BOUND PROTEIN IN CHLOROPLAST MEMBRANES

ALLAN L. STUART* and AARON R. WASSERMAN

Department of Biochemistry, McGill University, Montreal, P.Q. (Canada)

(Received March 19th, 1973)

SUMMARY

Purification of cytochrome b_6 was pursued to further develop rational technology for purification, proof of purity, and study of properties of membrane proteins. Cytochrome b_6 was purified —the first time from any source— from spinach chloroplast membranes; yield of pure cytochrome b_6 was 30% of that found in ethanol-extracted particles. The three-step procedure (pH 8) employed: (I) extraction in Triton X-100–4 M (optionally 2 M) urea, (II) chromatography in a Bio-Gel A-1.5m Column (Triton X-100–4 M urea). Without this step, subsequent electrophoresis failed. (III) Preparative disc gel electrophoresis.

Properties of cytochrome b_6: Cytochrome b_6 migrated in undenatured form as a single band in disc electrophoresis (pH 8, 7 or 8.9). None of the limited, accepted properties of the cytochrome in particles was altered by the purification procedure: Reduced b_6 has absorption maxima (22 °C) at 434, 536, and 563 nm; at −199 °C the α absorption region shows two peaks of equal intensity at 561 and 557 nm. Cytochrome b_6 is reduced by dithionite (not by ascorbate) and is autoxidizable. The prosthetic group of b_6 is protohaemin and is fully extractable by acid–acetone. No non-haem iron is present. The millimolar extinction coefficient of reduced b_6 (563 − 600nm) per mole of haem is 21. The protein equivalent weight is 40000 g per mole of haem. Cytochrome b_4 is an intrinsically aggregatable molecule. The reduced cytochrome does not react with CO except when Triton X-100 is present.

INTRODUCTION

The purification of tightly bound membrane proteins with retention of their known properties has long hindered and challenged many areas of Biology. The chloroplast grana of higher plants contain three cytochromes —f (a peak at 554 nm), b_{559} (α peak at 559 nm) and b_6 (α peak at 562) — all tightly bound membrane proteins which are not released by extraction with salt solution or by prior delipidation of the membrane. Consequently, purification of the chloroplast cytochromes was pursued with the hope that technology might gradually developed which was applicable generally to the purification, proof of purity, and study of membranes proteins. Purification of cytochrome f (ref. 1) and cytochrome b_{559} (ref. 2) with evidence for

* This research constituted part of a thesis to be submitted in partial fulfillment of the requirements for the Ph. D. degree at McGill University.

purity was recently reported from this laboratory though the development of new methods, some of which may be generally applicable to the purification of membrane proteins. However, both procedures relied on an empirical intermediate purification step of binding most of the protein impurities to DEAE-cellulose. Purification of cytochrome b_6 was therefore undertaken with the hope of devising a different, more generally useful intermediate purification step.

The 563-nm peak of cytochrome b_6 was observed in chloroplast by Davenport[3] in 1952; it was designated as b_6 and further examined by Hill[4] in 1954. No success was subsequently reported for nearly 20 years in either the purification of cytochrome b_6 or even its extraction in stable from form particles.

This paper reports the complete purification of cytochrome b_6 and some of its properties. The initial step of the procedure (extraction using aqueous Triton X-100–4 M (or 2 M) urea, pH 8) and the final step (disc electrophoresis in aqueous Triton X-100, pH 8) were derived with some modification from the cytochrome b_{559} and *f* procedures from this laboratory[2,1]. An innovation and critical step in the b_6 procedure is the successful use of a Bio-Gel Z-1.5m column containing Triton–4 M urea as an effective preliminary chromatographic step which enables the following electrophoretic step to succeed.

METHODS

"Total chloroplast particle fraction" was prepared from spinach leaves and stored frozen (−15 °C) in physiologically active form as previously described[1]. Washed "ethanol-extracted particles" were then prepared from thawed suspensions of "total chloroplast particle fraction"[2].

Disc gel electrophoresis with non-ionic detergent was performed as described earlier[1] except that the resolving gel buffer was 0.38 M Tris–HCl, pH 8, rather than 8.9 to increase cytochrome stability; other changes are noted, where appropriate, under Results. Location of protein bands in gels by staining and spectrophotometric location of cytochrome in gel slices were also described previously[1]. Content of cytochrome b_6 (using its α maximum at 563 nm) was assayed in ethanol-extracted particles and during purification by difference spectrophotometry (reduced with dithionite *vs.* ascorbate). (Ascorbate reduces cytochromes *f* and b_{559} but not cytochrome b_4; dithionite reduces all three cytochromes.) Absorption spectra were recorded during purification using a Phoenix–Chance scanning spectrophotometer. The response of the instrument was linear (calibrated with solutions of horse-heart cytochrome *c*) down to its detection limit of about 0.0002 absorbance unit (1-cm cell). Accuracy of the Phoenix–Chance absorbance values was checked by cross-calibration *via* cytochrome *c* with a Cary Model 15 recording spectrophotometer and Beckman DU spectrophotometer. Absorbance spectra at 22 °C of pure cytochrome b_6 were recorded on the Cary model 15 spectrophotometer; spectra at the temperature of liquid nitrogen (−199 °C) were recorded with the Phoenix–Chance instrument equipped with low-temperature accessory (optical Dewar flask, 2-mm cells). One (absorbance) unit of cytochrome b_6 is defined as that amount of reduced protein which when dissolved in 1 ml gives an absorbance at 22 °C of 1 (1-cm light path) at its α maximum at 563 nm relative to the absorbance at 600 nm.

Haem content was assayed as the reduced pyridine haemochromogen by the

method of Appleby[5]. Acid–acetone extraction of the haem of cytochrome b_6 was performed (and assayed as the reduced pyridine haemochromogen[5]) by the method of Basford *et al.*[6]. Biuret protein determinations were performed by the method of Gornall *et al.*[7] with crystalline bovine serum albumin as standard; the biuret color of pure cytochrome b_6 samples was corrected for haem contribution by an alkaline control containing cytochrome b_6. Total iron was analyzed by the method of Doeg and Ziegler[8] with pure iron wire as standard. Chlorophyll content of particles was determined by the method of Arnon[9].

Bio-Gel A-1.5m, a non-ionic Agarose Gel, was purchased from Bio-Rad Laboratories, Rockville Centre, N.Y. Sephadex G-25 and G-200 were purchased from Pharmacia Canada Ltd (Montreal). Diaflo membranes (used in a Diaflo Ultrafiltration Pressure-concentrating Cell, under N_2) were from Amicon Corp., Lexington, Mass. Millipore filters were products of Millipore Corporation, Bedford, Mass.

Sonic disturption: The instrument, manufactured by Blackstone Ultrasonics, Inc., Sheffield, Pa. consisted of probe model BP2 with 5/8-inch probe tip and generator model SS-2 capable of maximum power output of 200 W. During sonic disruption of suspensions, it was set to position 40, out of a possible range of 100, and tuned to maximum pitch. Further details are given in Step 1 of the purification procedure in Results.

RESULTS

Experiments to develop the purification procedure for cytochrome b_6

Quantitative (90–100%) extraction of the cytochrome b_6 content of ethanol-extracted chloroplast particles into an optically clear aqueous dispersion was accomplished by sonication at 0 °C in a medium containing 2% Triton–4 M urea–0.05 M Tris–HCl buffer, pH 8. If the medium was not supplemented with sulfhydryl reagents such as 2 mM dithiothreitol or 10 mM cysteine, b_6 was stable at 0 °C for at least 2–3 days. Using the approach developed in this laboratory[1], the optically clear dispersion of cytochrome b_6 in Triton–urea was applied to an analytical disc-electrophoretic 5 or 7% resolving gel (with or without a 4% stacking gel) with Triton X-100 as supplement in all media. A series of experiments was performed in which the Triton content in disc electrophoresis was varied from a low of 0.1% up to a high concentration of 2%. In all cases, disc electrophoresis failed: the extract did not stack properly and cytochrome b_6 did not penetrate the resolving gel, nor was b_6 adequately separated from other proteins present. It was, thus, uncertain whether the original extract contained cytochrome b_6 as separate molecules or as polydispersed aggregates, perhaps bound to other proteins. It was consistently observed that a brown-protein material formed a layer at the top of the first gel in its path. Operationally, a "trouble fraction" was hypothesized, *i.e.* some protein fraction other than the chloroplast cytochromes which prevented proper electrophoretic resolution in disc electrophoresis containing Triton X-100. In work in our laboratory on cytochrome b_{559} the same phenomenon had previously been observed during the purification of b_{559}: an intermediate complete binding in Triton–urea medium (pH 8) of the brown-protein fraction to DEAE-cellulose was required to allow subsequent proper electrophoresis of b_{559}. It was thus probable that more than a reduction of the total protein content of the original extract had to be accomplished; rather,

complete removal of the brown-protein fraction ("trouble fraction") was required. A variety of attempts were made to purify cytochrome b_6 (in either Triton–urea medium or in 2% Triton alone). Two criteria were applied: (1) at least 2 fold purification and (2) subsequent proper resolution of cytochrome b_6 in analytical disc gel electrophoresis containing 1% Triton X-100. $(NH_4)_2SO_4$ fractionation failed completely; both b_6 and the most of protein in the extract precipitated together between 15 and 20% saturation of $(NH_4)_2SO_4$ at pH 8. Purification *via* fractionation with sequential of calcium phosphate gel also failed. Unlike cytochrome *f* or cytochrome b_{559}[2] which pass through a DEAE-cellulose column in Triton-urea-Tris medium (pH 8), cytochrome b_6 was bound to DEAE-cellulose together with most of the contaminating protein, including all of the brown-protein fraction. Recovery of b_6 from the column by supplementing the eluting medium with NaCl at a fixed concentration (ranging from 0 to 2 M in separate experiments) produced poor recovery and negligible purification. Attempts were then made to bind "trouble fraction" but not b_6 on DEAE-cellulose by increasing the ionic strengh of the applied sample before binding from a low of 0.025 M to a high of 0.125 M in separate column experiments. No purification was achieved, although recovery of b_6 was quantitative with the extracts applied in 0.125 M ionic strength.

On the further assumption that cytochrome b_6 migth exist as separate molecules in the original extraction medium (2% Triton–4 M urea–0.05 M Tris–HCl buffer, pH 8), *i.e.* not bound to other proteins, and that the brown "trouble fraction" might merely be clogging the top surface of polyacrylamide gels, purification experiments were pursued using molecular-sieving materials. Both b_6 and the total protein content (including "trouble fraction") were quantitatively retained by the Diaflo membranes XM50 (50000-dalton exclusion limit), XM100 (100000 daltons), XM300 (300000 daltons), and Millipore filters of 0.05-μm and 0.10-μm porosity. Both cytochrome b_6 and "trouble fraction" quantitatively passed through the more porous 0.22- and 0.45-μm Millipore filters. In a column of Sephadex G-200, containing Triton–urea–Tris medium, b_6 was slightly retarded but the procedure achieved no effective separation of b_6 from the excluded brown-protein fraction. (The exclusion limit for proteins on Sephadex G-200 in aqueous medium is 800000 daltons; the exclusion limit of Sephadex G-200 for proteins in aqueous Triton–urea medium is not known.) All of the above sieving materials failed, but the slight retardation of b_6 on Sephadex G-200 suggested that a molecular-sieving material of higher exclusion limit might suffice. Accordingly, purification of the extract was attempted on a column of Bio-Gel A-1.5m in the same medium. (Bio-Gel A-1.5, has an exclusive limit of $1.5 \cdot 10^6$ daltons; the exclusion limit for proteins in Triton–urea is not known.) The brown-protein fraction was completely excluded and completely separated from the retarded single cytochrome b_6 and single cytochrome *f* fractions. The brown-protein fraction represented about 30–50% of the applied protein but contained no cytochromes. 70–80% of the cytochrome b_6 applied to the column was routinely recovered with purification, on a Biuret-protein basis, of 18-fold. The cytochrome b_4 fraction when applied in Triton–urea medium was then found to stack and separate satisfactorily in analytical disc gel electrophoresis containing Triton X-100; no urea supplements were required for the gel media and electrode buffer. Optimum conditions for efficient electrophoretic purification of cytochrome b_6 were then obtained by controlled experiments in which individual parameters of disc-gel electrophoresis were varied, followed

TABLE I

PURIFICATION OF CYTOCHROME b_6

Fraction	*Color*	*Total volume (ml)*	*Total units* of cytochrome b_6*	*Total protein (mg)*	*Specific content (units/mg protein)*	*Recovery of cytochrome b_6 (%)*	*Purification (-fold)*
1. Unextracted green particles**	Dark green	375	15.3***	6285	0.0024	100	–
2. Ethanol-extracted particles in Triton X-100–4 M urea	Brown	110	15.3	4230	0.0036	100	1.5
3. Concentrated 100000 × *g* supernatant	Dark brownish-green	25	14.0	1555	0.0090	93	3.8
4. Eluent from Bio-Gel A-1.5 m column	Light green	88	9.8	61.3	0.16	65*	67
5. Polyacrylamide gel electrophoresis eluent after concentration	Orange	10	4.6 (4.9)*	9.4	0.49 (0.52)*	30**	200

* Determined by difference spectra (see Methods).

** These particles contained 750 mg of chlorophyll.

*** Determined from ethanol-extracted particles assuming no loss during extraction. Cytochrome content in green particles could not be reliably measured because of optical limitations.

§ 70–80% of the units applied to the column were routinely recovered.

§§ Recovery after electrophoresis was routinely at least 80% of the applied units. Concentrating the eluents after steps 4 and 5 by dry Sephadex G-25 contributed the bulk of the loss in this case, although each concentration can incur, with greater care, less than 10% loss.

§§§ Numbers in parentheses employ units of cytochrome b_6 from absolute spectra (563–600 nm).

by spectrophotometric assay of the resolved b_6 band and by inspection of the stain pattern of resolved protein bands. These optimum conditions are presented in Step 3 of the purification procedure for cytochrome b_6 in the following section.

Purification of cytochrome b_6

All steps were performed at 0–4 °C. The procedure, as described, is for a preparation using chloroplast particles originally containing about 750 mg of chlorophyll and about 6300 mg of protein. A typical preparation is summarized in Table I.

Step 1— extraction of cytochromes. A pellet of washed "ethanol-extracted particles" containing 0.05 M Tris–HCl buffer, pH 8, was resuspended by hand homogenization in about 10 pellet volumes (100 ml) of 2% Triton X-100, 4 M urea, 0.05 M Tris–HCl buffer, pH 8. The Triton to protein ratio (mg/mg) was at least 0.4. Final volume was usually 110–115 ml. The suspension was sonicated for 2 min total time (four 30-s sonication periods in ice interspersed with 1-min cooling intervals) and then centrifuged twice, each time at $27000 \times g$ for 15 min. The supernatant was further centrifuged, this time at $100000 \times g$ for 60 min, to remove non-cytochrome components. After spectrophotometric assay for content of cytochrome b_6 and cytochromes b_{559} and f, the extract was concentrated twice with dry Sephadex G-25 to reduce the volume to about 25 ml. Recovery of b_6 after extraction and concentration with Sephadex was essentially complete.

Step 2— partial purification by chromatography on a Bio-Gel A-1.5m column containing Triton–4 M urea. A 5.0 cm × 84 cm column of Bio-Gel A-1.5m (200–400 mesh) was prepared and equilibrated with the extraction medium (2% Triton X-100, 4M urea, 0.05 M Tris–HCl, pH 8). The 25-ml extract from Step 1 was applied and chromatographed using the same extraction medium in a descending direction at a flow rate of 60 ml/h. Large size, non-cytochrome components —which otherwise severely interfered with purification in Step 3 (disc electrophoresis)— were effectively removed as an excluded front fraction. Cytochrome b_6 moved as a single retarded fraction (peak at 924 ml *vs* V_0 for the column of 528 ml $-K_{AV} = 0.36$) which was virtually completely separated from cytochrome f ($K_{AV} = 0.59$). (Due to the lack of thiols, which stabilize b_{559}[2] but inactivate b_6, no b_{559} is observed in the eluted fractions.) The tubes containing cytochrome b_6 were then pooled, supplemented to 10% glycerol and then concentrated once or twice with dry Sephadex G-25 to achieve a volume of about 15 ml.

Step 3— Final purification via preparative disc-gel electrophoresis (0.5% Triton X-100). A Kontes Glass Co. Preparative Electrophoresis Apparatus (250-ml chamber) was used. Electrode buffer was Tris–glycine, pH 8.3 (0.005 M Tris base, 0.039 M glycine) *plus* 0.5% Triton X-100. The running gel (9%, 100 ml volume) contained 10% glycerol, 0.5% Triton X-100 and 0.38 M Tris–HCl buffer, pH 8.0. Prewashing of the gel with electrode buffer was performed for 2 h at 20 mA, 300 V prior to applying the sample. (Note 1: without prewashing, the b_6 recovery was reduced and significant of a second (artifactual) faster-moving b_6 band were produced. Note 2: because of the prewashing, the usual pH 6.7 stacking gel was necessarily omitted.) The 15-ml sample, greenish brown in color, was then applied (without supplementation with sucrose) and electrophoresis at 20 mA, 300 V was performed for a total time of

about 40 h. After the cytochrome had penetrated the gel (about 12–16 h) the electrophoresis was briefly stopped and a chlorophyll layer (light green) remaining above the gel was carefully pipetted off; electrophoresis was then resumed until the sharp, orange b_6 band had penetrated 1 cm into the gel. After cutting out the orange b_6 band, the gel slice was fragmented in a hand homogenizer together with about 40 ml of 0.05 M Tris–HCl, pH 8, 10% glycerol (no Triton X-100). The suspension was diluted with additional amounts of this medium so that the total amount of fluid added was about 10 times (about 60 ml) that of the original volume of the gel slice. The gel suspension was stirred about 3 h, then centrifuged ($27000 \times g$, 15 min), and the supernatant was concentrated with dry Sephadex G-25. The concentrated b_6 solution contained about 0.3% Triton X-100, estimated from the volume of the gel slice and its Triton concentration of 0.5%, from the known dilution factor during extraction from the slice, and from the known -fold concentration after treatment with dry Sephadex G-25. (Triton X-100 micelles are quantitatively concentrated together wit protein by dry Sephadex G-25; unpublished studies in this laboratory.) Overall yield of pure b_6 was 30% of that present in ethanol-extracted particles.

Stability

Cytochrome b_6 was stable for at least 3 months when stored frozen (−15 °C) in 0.05 M Tris-HCl buffer, pH 8, containing 10% glycerol or stable for at least 7 days in liquid solution at 0 °C. In contrast with cytochrome b_{559}, whose stability is best preserved by thiols such a 1–5 mM dithiothreitol, and with cytochrome *f*, whose stability is enhanced by thiols, cytochrome b_6 (otherwise a relatively stable molecule) is slowly inactivated by 1–5 mM dithiothreitol even at 0 °C. (By inactivation we mean the abolition of the b_6 spectrum; no new absorption peaks are observed.)

Proof of purity

Analytical disc gel electrophoresis (pH 8) of b_6 in undenatured, non-aggregated form in medium containing Triton X-100 showed no contamination by either cytochromes *f* or b_{559} or any other protein (*cf.* Fig. 1 and its legend). Additional

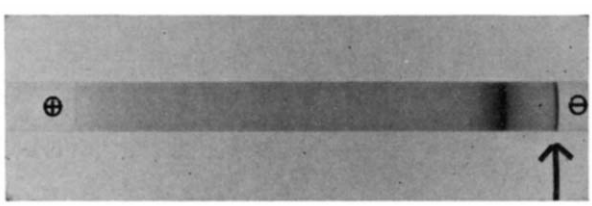

Fig. 1. Analytical disc gel electrophoresis (18 h) of pure cytochrome b_6. No stacking gel; 9% running (pH 8) prerun for 1 h with electrode buffer to wash gel. Electrode buffer was 5 mM Tris base–0.039 M glycine (pH 8.3) *plus* 1% Triton X-100; 9% gel medium was 0.38 M Tris–HCl (pH 8) *plus* 2% Triton X-100, 10% glycerol. (When the applied sample was directly after the purification procedure, an estimated concentration of Triton X-100 of 0.3% was already present. When the applied sample had previously been dialyzed seven days against Tris buffer, it was supplemented to about 0.5% Triton X-100.) Prior to staining the band was visibly orange colored before reduction and gave a typical b_6 spectrum. No protein or cytochrome was seen in the front fraction or anywhere else in the gel. The arrow indicates the top of the gel, where no protein stain was visible.

disc gel electrophoretic experiments performed either at pH 7.0 or 8.9 also showed no impurities. Instability of b_6 in acetate buffer (pH 5.5) precluded a purity test at pH 5.5. The absorption spectrum of reduced cytochrome b_6 (22 °C) also shows

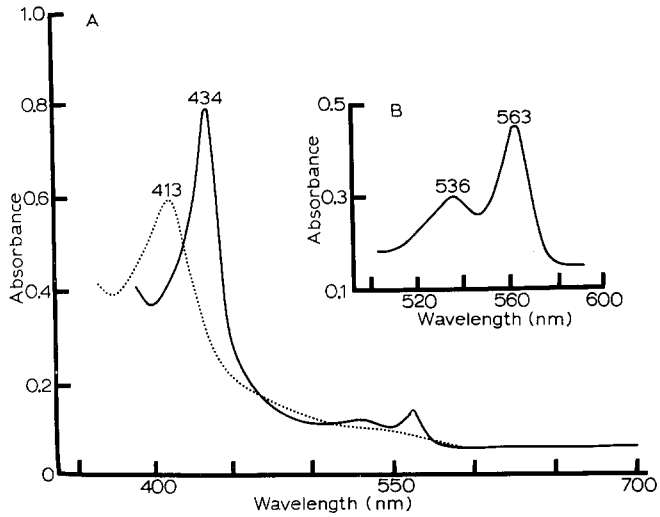

Fig. 2. Absolute reduced (dithionite) (solid line) and absolute oxidized (untreated) absorbance spectra of pure cytochrome b_6 (22 °C). For insert (B), the sample aliquot was 4 times the concentration of that in A, so as to reveal more detail. Solution medium was 0.05 M Tris–HCl, pH 8.

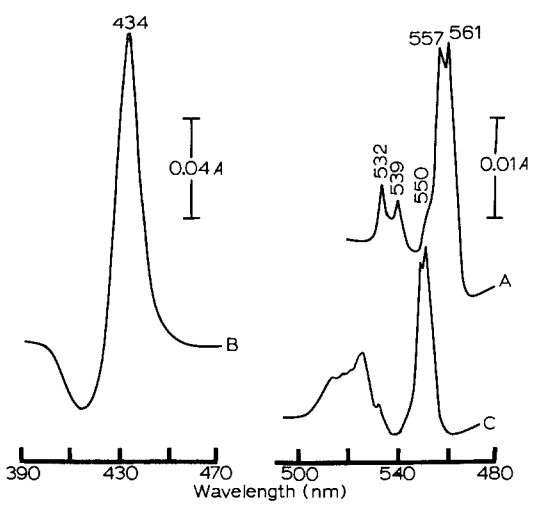

Fig. 3. Absorbance difference spectrum (reduced (dithionite) *vs.* oxidized (untreated)] of pure cytochrome b_6 at the temperature of liquid nitrogen (−199 °C). A and B. Cytochrome b_6. Magnification in A is 4 times that in B. The concentration of the sample was such that it gave an absorbance of 0.040 (563–600 nm) in a 1-cm cell at 22 °C. Dialysis for 5 days removed sufficient Triton X-100 to allow optical measurements at −199 °C; b_6 was stable during this dialysis. C. Horse heart ferrocytochrome *c* spectrum (−199 °C) as reference to demonstrate validity of the technique as performed. Medium in A, B and C was 0.05 M Tris–HCl, pH 8, 50% glycerol. The slit width must be as narrow as possible for good optical resolution.

no contamination by cytochrome *f* and b_{559} (Fig. 2). Furthermore, a difference spectrum (not shown) of ascorbate *vs.* ferricyanide (oxidized) at −199 °C, which would normally reveal any native b_{559} or *f* present (but not b_6), in fact showed no absorption peaks. The absorption difference spectrum of b_6) [reduced by dithionite *vs* oxidized (untreated)] recorded at −199 °C is presented in Fig. 3. Two peaks (561 nm, 557 nm) are seen in the α absorption region. If the peak at 557 nm were contributed by a small contaminating of cytochrome b_{559}, additional peaks of $b_{559}{}^2$ would be expected at 513, 529, and 536 nm (β region) and especially the intense

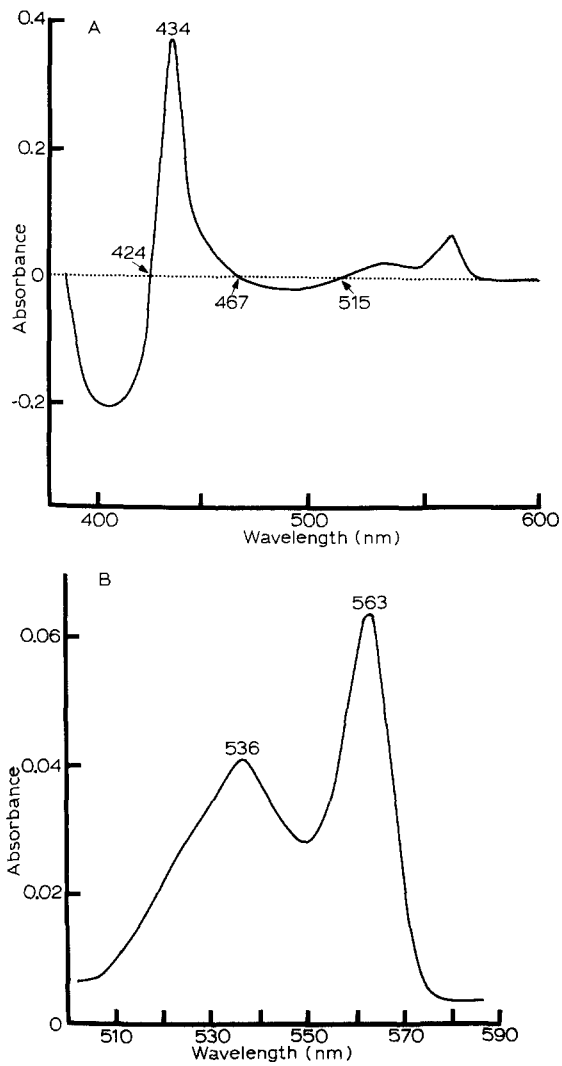

Fig. 4. Difference spectrum at 22 °C of pure cytochrome b_6 (reduced (with dithionite) *minus* oxidized (untreated)). The spectrum in B was recorded at 10 times the magnification of that in A to show the α and β peaks in greater detail. Solution medium was 0.05 M Tris–HCl buffer, pH 8.

Soret peak of b_{559} at 429 nm. The absence of the latter b_{559} peaks would suggest that, at −199 °C, both the peak at 561 nm and that at 557 nm are contributed by b_6 itself.

Absorption spectra

Absolute reduced and absolute oxidized spectra (22 °C) of b_6 are presented in Fig. 2. (The absorption spectra were unaffected by Triton X-100.) The low-temperature difference spectrum (Fig. 3) indicates that b_6 exhibits two peaks at −199 °C in the α region, 561 and 557 nm. This supports the tentative suggestion made by Boardman and Anderson[10] on b_6 in chloroplast particles. The absorption difference spectrum of b_6 (22 °C) is presented in Fig. 4.

Like b_6 in chloroplast particles, purified b_6 is autoxidizable and is reduced by dithionite, but not by ascorbate. (Either ascorbate or dithionite can reduce cytochrome f and cytochrome b_{559}.) No time lag was observed during reduction by dithionite. Reduction was complete within the time required to record the spectra at 22 °C (*i.e.* about 30 s to record the α and β peaks).

Haem prosthetic group, millimolar extinction coefficient, protein equivalent weight, iron content

The absorption spectrum of the reduced pyridine haemochromogen of pure b_6 was identical with that of protohaemin, showing maxima at 556, 526 and 423.5 nm. The haem of b_6 was quantitatively extracted by acid–acetone with recovery of 95% of the haem.

Using the coefficient of the reduced pyridine haemochromogen of $\Delta\varepsilon_{mM}=23.4$ (556 − 539 nm)[5] the millimolar extinction coefficient of cytochrome b_6 was determined as $\Delta\varepsilon_{mM}=21$ (563 − 600nm) per mole of haem. Cytochrome b_6 contained 47.(5) nmoles of haem per A unit and 40000 g of Biuret protein per mole of haem. $\Delta A_{563-600\,nm}$ per mg Biuret protein was 0.52. Total iron content of cytochrome b_6 was 47 (±4%) nmoles of iron per A unit. The equivalence of total iron and haem iron indicates that b_6 contains no significant amount of non-haem iron.

Quantitative (reversible) reaggregation upon depletion of Triton X-100

The intrinsic reaggregatability of cytochrome b_6 was examined by the disc-electrophoretic approach used in this laboratory[1,11]. Pure b_6 containing initially less than 0.3% Triton X-100 was dialyzed against 0.05 M Tris–HCl buffer, pH 8, for an aribitrary dialysis time of seven days with daily changes of the Tris buffer. The cytochrome was quantitatively stable and soluble during this dialysis period. When the dialyzed sample was examined by analytical disc gel electrophoresis (pH 8) using a washed 9% gel (*cf.* legend of Fig. 1 for details) but without Triton X-100 either in the sample or in the electrophoretic system, the cytochrome was quantitatively reaggregated in that none of it was able to penetrate the 9% running gel. When the dialyzed sample was supplemented with 0.5% Triton X-100 and examined by disc gel electrophoresis (pH 8) with 0.5% Triton X-100 in the system, the entire cytochrome b_6 sample dissociated and migrated in the 9% gel as a single electrophoretic band which exhibited the usual b_6 absorption spectrum. Cytochrome b_6 was also non-destructively dissociated by Triton X-100 at pH 7 and pH 8.9.

Non-reaction of cytochrome b_6 with CO after depletion of Triton X-100

Samples of pure cytochrome b_6 — sufficiently dialyzed (as in the above section) so that quantitative reaggregation was observed — showed no reaction with CO. As shown by Hill[4], native cytochrome b_6 in chloroplast particles also showed no CO reaction. However, when the pure sample was dissociated by the addition of 0.5% Triton X-100 (final concentration) complete reaction with CO occurred as shown spectrophotometrically in Fig. 5. The minimum concentration of Triton X-100 needed

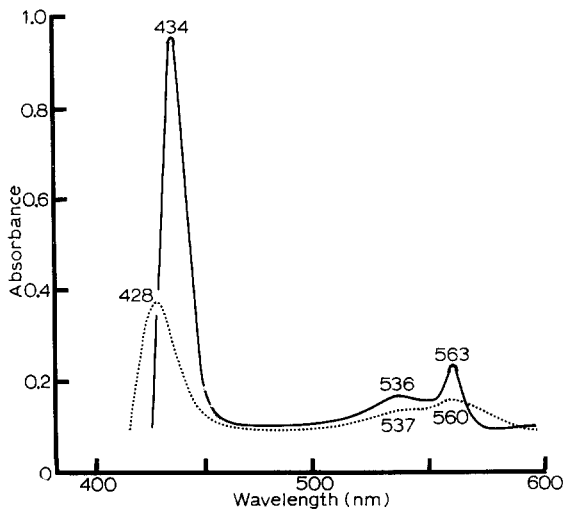

Fig. 5. The effect of CO on the difference spectrum (reduced (with dithionite) *versus* oxidized (untreated)) of pure cytochrome b_6 (22 °C) in the absence and presence of 0.5% Triton X-100. The sample had been dialyzed against 0.05 M Tris–HCl buffer, pH 8, for 7 days to deplete its concentration of Triton X-100. The sample was stable and soluble during this dialysis. After reduction with dithionite, CO was bubbled through the reduced sample for 3 min and the spectrum then recorded. ——, no Triton X-100 added; spectrum is unaltered by CO. · · · ·, 0.5% Triton X-100 (final concentration) added, after bubbling with CO, and the spectrum was recorded 1 min later. Calculated aborbance ratios are $A_{563\text{ nm}}/A_{560\text{ nm}} = 1.9$; $A_{434\text{ nm}}/A_{428\text{ nm}} = 3.2$, thus indicating a drop in absorbance upon reaction with CO. (Addition of Triton X-100 alone (no CO), not shown, had no effect on the normal b_6 spectrum.)

to induce CO reactivity is not known but is probably considerably less than 0.5%. (The results of this section do not establish or imply that monomeric, *i.e.* dissociated cytochrome b_6 is intrinsically CO reactive, except of course in the presence of Triton; nor, conversely, can one infer that the cytochrome in the chloroplast is necessarily in aggregated form.)

DISCUSSION

The purification procedure suffers none of the problems usually encountered in the extraction and purification of most "hydrophobic", tightly bound membrane proteins: (1) Extraction of b_6 was easily accomplished and was complete, and no alteration of the cytochrome's accepted properties was observed. Further, if Bio-Gel A-1.5m is indeed an inert molecular-sieving material, then b_6 was in molecular

form, not bound to protein contaminants, in the original extraction medium of Triton–4 M urea, pH 8. (2) The cytochrome moved as a single fraction either in the Bio-Gel chromatography or in the more-discriminating method of disc electrophoresis. Multiple fractions, multiple forms or streaking of b_6 was not encountered. A second substantial band of b_6 (exhibiting the same absorption spectrum as the normal band) was an artifact not an "isozyme" whose formation was avoided by "pre-washing" the disc-electrophoretic resolving gel. (3) The purification steps were few and essentially quantitative (70–80% recovery, routinely, in the Bio-Gel step and at least 80% recovery, routinely, from preparative disc electrophoresis). (4) As in the work in our laboratory on cytochrome *f*, we have had no success in effectively chromatographing cytochrome b_6 on the ion exchanger DEAE-cellulose (or on any other charged support medium). This difficulty may possibly be attributable to aggregation of b_6 as well as of other proteins present induced by charges in the ion exchanger and/or in the eluting salt solution. To our knowledge, the Bio-Gel step is the first demonstration of chromatography of a desired membrane protein in undenatured form in a crude extract. (5) Purification of cytochrome f[1] in this laboratory demonstrated that disc electrophoresis in non-ionic detergent could serve in effect as a much-needed chromatographic method for a membrane protein both as a final preparative step and as a subtle method for "proof of purity". The procedures for all three chloroplast cytochromes have now successfully employed these methods, thus validating their general promise for other membrane proteins.

The experiments in the first section of Results indicate that removal of a "trouble fraction" from the initial Triton–4 M urea dispersion was required to allow cytochrome b_6 to penetrate disc electrophoretic gels. Only chromatography by molecular sieving in Bio-Gel A-1.5m (Triton–urea) succeeded in removing this apparently large molecular weight fraction despite a variety of attempts by other methods. Since cytochrome b_6 is small enough to penetrate a 9% electrophoretic gel, the requirement for sieving out the "trouble fraction" *via* a large-pore Bio-Gel A-1.5m sieving material (rather than *via* Sephadex G-200) remains at present an enigma. The Bio-Gel procedure and the concept of a "trouble fraction" (or disc-gel plugging fraction) may prove useful for purification of other membrane proteins.

Bendall[12] in a brief report proposed that chloroplasts contained a second b_6 component with an absorption peak at 559 nm (presumably at room temperature) together with the usual 563-nm (b_6) component. (Both were reduced by dithionite Although no definitive comment can yet be made by us, the following observations may be of interest: (1) We have never observed any b_6 component either in particles or soluble extracts other than the conventional b_6 component at 563 nm. (2) Assay of conventional, ascorbate-reducible b_{559} in solvent-extracted chloroplasts has not been reliable (in our laboratory) except in Triton–urea medium, pH 8. Solvent-extracted particles in suspension with or without Triton X-100 (but lacking 4 M or 2 M urea) are not always fully permeable to ascorbate. (Dithionite appears to encounter no permeability barrier.) The same particles in Triton–2 M or 4 M urea — either by suspension in Triton–urea, pH 8, or by adding 2 or 4 M urea during assay to particle suspensions in Triton alone — show their expected full amount of ascorbate-reducible b_{559}. The latter observation also poses a reservation to the proposal of a second, low-potential form of b_{559} in particles (*i.e.* a form not-reducible by ascorbate, *e.g.* see Cox and Bendall[13].)

We have observed two alpha absorption peaks (561, 557 nm) at −199 °C in our cytochrome b_6 preparation. Based on all available evidence, does the 557-nm peak represent an unresolved bound impurity? (1) It is universally accepted that two α peaks at −199 °C can be produced by two different cytochrome molecules whose absorption spectra are otherwise poorly resolved and show considerable asymmetry at 22 °C. However, a single pure cytochrome molecule also can exhibit two major α peaks at −199 °C even though only one α peak is found at 22 °C. One such example is cytochrome *f* which at −199 °C shows both a 551.5 nm peak and a very considerable peak at 548 nm. No one has yet suggested that the latter peak represents a major or minor impurity. Thus, the presence of two α absorption peaks (−199 °C) for a preparation is, by itself, an equivocal criterion for impurity and additional evidence must be examined. (2) No ascorbate-reducible b_{559} was present in the cytochrome b_6 preparation (−199 °C). (3) Pure cytochrome b_{559} has absorbance maxima (22 °C) at 559 nm (α), 530 nm (β) and 429 nm (Soret). At −199 °C it shows absorbance peaks in a difference spectrum at 556 nm (α), 529 (principal β) (as well as minor β peaks at 513 and 536 nm) and an intense Soret Peak at 429 nm. The above preparation of cytochrome b_{559} was completely ascorbate reducible. From additional, more extensive studies on cytochrome b_{559} in this laboratory (Garewal, H. S. and Wasserman, A.R., unpublished) we have no reason to question either the reliability of the above absorption data or whether it is representative (within experimental error) of the cytochrome b_{559} content of chloroplast grana. If the ascorbate-reducible form, unprotected by thiols, is converted artifactually or otherwise to one or more forms of lower potential (*i.e.* forms reducible by dithionite but not by ascorbate), we would expect any such "dithionite-reducible form "either to retain all of the characteristic absorption peaks of cytochrome b_{559} or to have shifts in maxima for all three principal maxima. There is no precedent for any cytochrome retaining the position and sharpness of its α peak while at the same time suffering alteration or elimination of its β and Soret peaks. If all, or even 15% of the height of the 557 nm peak (−199 °C) in Fig. 3 is presumed to be contributed by a "dithionite-reducible form" of b_{559}, we would expect to see the principal beta of b_{559} at 529 nm or at least some shoulder at 529 nm and to see either a peak or shoulder near 429 nm. This, however, is not seen. Further, such contamination by b_{559} would, at 22 °C, either produce a considerable shoulder on the left side of the alpha peak or, for larger contamination, shift the 563 nm peak to a shorter wavelength (perhaps to 560 or 561 nm). Inspection of Figs 2B and 4B shows no such signs of contamination. From currently available data on pure b_{559} as well as the present data on cytochrome b_6, we must therefore conclude that the peaks at 557 and 561 nm (−199 °C) are intrinsic properties of pure cytochrome b_6. A corollary of this conclusion would be that any particulate preparation containing b_6 and presumably free of b_{559} would show both peaks (−199 °C) with almost equal intensity and that particulate preparations containing both b_6 and b_{559} would show greater absorbance at 557 nm than at 561 nm. (4) Using another approach, experiments in progress on the polypeptide subunits of our cytochrome b_6 preparation (Stuart, A. and Wasserman, A. R., unpublished) and of pure cytochrome b_{559} (Garewal, H.S. and Wasserman, A.R., unpublished) show that about 75% of the mass of cytochrome b_6 consists of chains unequivocally absent in cytochrome b_{559}; the remaining 25% of the protein mass of b_6 also appears to consist of a chain not found in b_{559} but this requires further verification.

We have not yet examined the redox potential of pure cytochrome b_6. The redox potential of cytochrome b_6 in particles is in dispute, having been reported variably as -60 mV[4], recalculated later as 0.0 mV[14], -180 (± 20) mV[15] and -100 mV[16].

No acceptable enzyme assay exists for cytochrome b_6; at this time the immediate physiological reductant or oxidant for the cytochrome in photosynthesis is unknown.

ACKNOWLEDGEMENTS

This work was supported by an operating grant (to A.R.W.) from the Medical Research Council of Canada. We thank our former colleagues, Jasbir Singh and Harinder S. Garewal, for their advice and encouragement.

REFERENCES

1 Singh, J. and Wasserman, A. R. (1971) *J. Biol. Chem.* 246, 3532–3541
2 Garewal, H. S., Singh, J., and Wasserman, A. R. (1971) *Biochem. Biophys. Res. Commun.* 44, 1300–1305
3 Davenport, H. E. (1952) *Nature* 170, 1112–1114
4 Hill, R. (1954) *Nature* 174, 501–503
5 Appleby, C. A. (1969) *Biochim. Biophys. Acta* 172, 88–105
6 Basford, R. E., Tisdale, H. D., Glenn, J. L., and Green, D. E. (1957) *Biochim. Biophys. Acta* 24, 107–115
7 Gornall, A. G., Bardawill, C. J., and David, M. M. (1949) *J. Biol. Chem.* 177, 751–766
8 Doeg, K. A. and Ziegler, D. M. (1962) *Arch. Biochem. Biophys.* 97, 137–140
9 Arnon, D. I. (1949) *Plant Physiol.* 24, 1–15
10 Boardman, N. K. and Anderson, J. M. (1967) *Biochim.Biophys. Acta* 143, 187–203
11 Singh, J. and Wasserman, A. R. (1970) *Biochim. Biophys. Acta* 221, 379–382
12 Bendall, D. S. (1968) *Biochem. J.* 109, 46p–47p
13 Cox, R. P. and Bendall, D. S. (1972) *Biochim. Biophys. Acta* 283, 124–135
14 Hill, R. and Bendall, D. S. (1967) in T. W. Goodwin (Editor), *Biochemistry of Chloroplasts*, Vol. 2, P. 559–564, Academic Press, London
15 Fan, H. N. and Cramer, W. A. (1970) *Biochim. Biophys. Acta* 216, 200–207
16 Nelson, N. and Neumann, J. (1972) *J. Biol. Chem.* 247, 1817–1824

Biochimica et Biophysica Acta, 314 (1973) 298–311

BBA 46602

ENERGY TRANSDUCTION IN PHOTOSYNTHETIC BACTERIA

VI. RESPIRATORY SITES OF ENERGY CONSERVATION IN MEMBRANES FROM DARK-GROWN CELLS OF *RHODOPSEUDOMONAS CAPSULATA*

A. BACCARINI MELANDRI, D. ZANNONI and B. A. MELANDRI

Istituto Botanico, Università di Bologna, Bologna (Italy)

(Received March 12th, 1973)
(Revised manuscript received June 15th, 1973)

SUMMARY

Membranes prepared from *Rhodopseudomonas capsulata* grown heterotrophically in the dark perform phosphorylation linked to oxidation of NADH and succinate, with $P/2e^-$ ratios of about 0.5 and 0.15, respectively. The localization of the sites of energy conservation was investigated by observing the respiration-induced quenching of the fluorescence of atebrine.

Energization of the membrane can be demonstrated when NADH is oxidized by O_2, ferricyanide or Q_1, when succinate is oxidized by O_2 or by oxidized diaminodurene, and during the oxidation of reduced diaminodurene.

Antimycin A completely inhibits energization between succinate and O_2 or succinate and diaminodurene; however, it only inhibits partially NADH or succinate oxidases and energization between NADH and O_2. KCN inhibits NADH oxidase in a biphasic way: the first level of inhibition is observed at concentrations which block the oxidation of exogenous cytochrome *c* or of diaminodurene and energization between succinate or ascorbate–diaminodurene and O_2. The second level corresponds to the inhibition of the antimycin-insensitive oxidase.

The results are interpreted as evidence of the presence in these bacteria of a respiratory chain branching after the dehydrogenase system, one arm of the chain being sensitive to antimycin A and low concentrations of KCN and capable of energy conservation, the other being represented by a completely uncoupled system.

INTRODUCTION

The respiratory system of facultative photosynthetic bacteria has received relatively little attention in comparison with the large amount of research dealing with their photosynthetic apparatus. Nevertheless aerobic metabolism can be no less important than photometabolism since these organisms are capable of high rates of growth in the dark in the presence of oxygen[1].

Our present limited knowledge on the composition and function of the respir-

atory chain of non-sulfur purple bacteria is concerned primarily with the nature of the electron transport components and their interaction with substrates[2–6]. Very little information is available so far on the localization of energy-conserving sites in the respiratory electron chain of *Athiorodaceae*. It has been demonstrated that the inhibition of cyclic phosphorylation by antimycin A in *Rhodosporillum rubrum* photosynthetic membranes can be overcome by low concentrations of phenazine methosulfate; on this basis it has been proposed that a site of energy conservation is located between an antimycin-sensitive component and reaction center bacteriochlorophyll[7]. However, this evidence could not be reproduced in *Rps. capsulata*[8]. Evidence for a second site in cyclic photophosphorylation, again in *Rh. rubrum*, has been obtained fom the demonstration of cross-over effects and from the demonstration that ATP or PP_i induce reverse electron flow reactions between a *b*-type and a *c*-type cytochrome[9]. In addition, a third site was postulated by Keister *et al.* [10] between NADH and fumarate, in order to rationalize the mechanism of energy-dependent reduction of NAD^+ by succinate. All these observations were further supported in the work by Isaev *et al.*[11], who were able to demonstrate energy conservation coupled to oxidation of NADH by oxygen or of succinate by ferricyanide or upon illumination in the presence of antimycin A and ascorbate–*N,N,N',N'*-tetramethyl-*p*-phenylenediamine.

Membranes prepared from facultative photosynthetic bacteria, grown aerobically, perform oxidative phosphorylation utilizing NADH or succinate as substrates[12,13]; however the low $P/2e^-$ ratios usually obtained in these preparations are a technical hindrance in elucidating further the sequence of redox reactions of the electron transport carriers and the associated energy-converting steps. Recently this problem has been approached in photosynthetic membranes of *Rps. rubrum* by an indirect method, namely measuring the distribution of permanent anoins as a probe of membrane energization[11]. In this study we have attempted to localize the energy coupling sites of respiration in membranes from *Rps. capsulata*, grown aerobically, by means of respiration-induced quenching of atebrine fluorescence. This phenomenon, which has been shown to be related to energization of phosphorylating membranes[14,15], has been studied by us in parallel with measurements of phosphate esterification in the presence of suitable electron flow inhibitors and electron donors and acceptors.

MATERIALS AND METHODS

Photosynthetic cultures of *Rps. capsulata*, strain St. Louis (American Type Culture Collection 23 782) were grown in the medium described by Ormerod *et al.*[16], transferred to a small flask (25 ml) containing the same medium and grown for many generations in the dark with continuous mechanical shaking. A small inoculum of these aerobic cultures was then transferred to Fernbach bottles and strongly aerated by bubbling air through the cultures and shaking with a mechanical rotatory device. After 20 h the bacteria, which appeared to be slightly pinkish, were harvested, washed once with 0.1 M glycylglycine (pH 7.2) containing 8 mM $MgCl_2$ and broken in a French pressure cell operating at 16000 lb/inch^2. The cell extract was freed of the largest debris and unbroken cells by centrifugation for 20 min at $40000 \times g$ and the membrane fraction was sedimented at $150000 \times g$ for 40 min. The membrane

fragments were suspended in the same buffer and kept in ice. All the experiments were performed within a few hours of preparation of the membranes. The degree of coupling of the system was found to be considerably decreased after 8–15 h of storage. Oxidation of NADH and reduction of ferricyanide or cytochrome *c* were measured spectrophotometrically at 340 nm, 420 nm and 550 nm, respectively, using a Cary Model 15 double beam spectrophotometer. The rates of oxidation of succinate, ascorbate–diaminodurene and ascorbate–cytochrome *c* were measured polarographycally using a Yellow Springs O_2 electrode (Model 5400). The routine reaction mixture for all these assays contained (in a volume of 2 ml for the spectrophotometric measurements and 6.8 ml for the polarographic): glycylglycine (pH 7.2), 100 mM; $MgCl_2$, 10 mM; EDTA, 1 mM; bovine serum albumin, 1 mg/ml; and particles (0.1 to 0.2 mg protein/ml). The various reactions were started by addition of NADH, 0.15 mM; sodium succinate, 20 mM; sodium ascorbate, 3 mM; oxidized mammalian cytochrome *c*, 0.012 mM; or diaminodurene, 0.12 mM. The amounts of other electron donors, electron acceptors and inhibitors are indicated for each experiment (see Results).

When necessary, anaerobic conditions were achieved by flushing the reaction mixture containing all the reagents except particles and bovine serum albumin, with N_2 for 10 min; these last two components were added from the side arm of the Thunberg cuvette after the flushing was completed. Other additions were made with microliter syringes through a rubber septum.

Phosphorylation was assayed by measuring the incorporation of $^{32}P_i$ into glucose 6-phosphate as previously described[17]. For routine experiments, when NADH or succinate were the substrates used, the procedure followed was the one described in ref. 18; otherwise experimental conditions are described under Results.

Measurements of fluorescence were made at a 90° with a filter fluorimeter[19].

Proteins were assayed by the method of Lowry *et al.*[20].

RESULTS

NADH and succinate oxidases and associated phosphorylations

Membranes prepared from *Rps. capsulata*, grown heterotrophically under the conditions described above, synthetize ATP coupled to the oxidation of NADH and succinate. Although the oxidase rates can vary considerabley in different preparations, the $P/2e^-$ ratios measured in membranes from cells harvested in the early stationary phase of growth fall between 0.4 and 0.5 for NADH and between 0.15 and 0.2 for succinate. As previously reported[18], phosphorylation linked to both substrates is completely inhibited by uncouplers and oligomycin; NADH-dependent activities are also sensitive to rotenone.

The effect of KCN on NADH and succinate oxidase activities and coupled phosphorylations is shown in Fig. 1. The rate of NADH oxidation shows a clear biphasic dependency upon KCN concentration, suggesting the presence of two different sites of action of the inhibitor. The concentrations of KCN at which the two phases are 50% inhibited are approximately 5.10^{-6} and 6.10^{-4} M, respectively. By contrast, the inhibition of succinate oxidation appears to be monophasic with an apparent K_i of approximately $5 \cdot 10^{-5}$ M.

Phosphorylation rates show similar patterns of inhibition: the NADH-

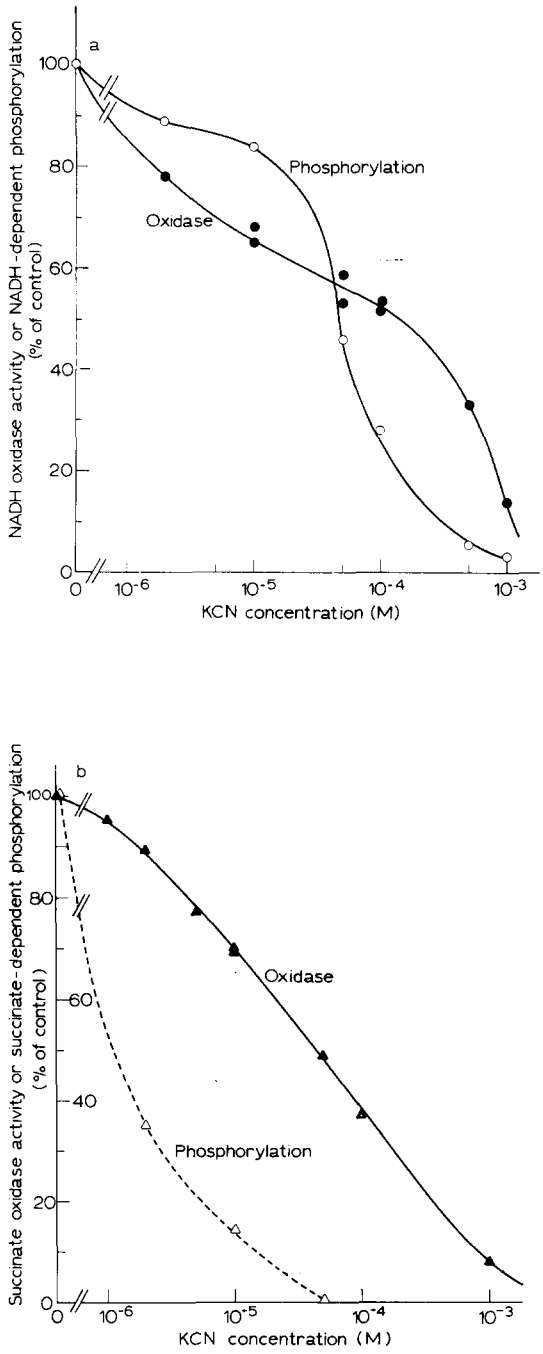

Fig. 1. Profile of NADH (a) or succinate (b) oxidases and related phosphorylation activities as a function of KCN concentration. NADH and succinate oxidases, in the absence of inhibitor, were 13.9 and 4.5 μmoles/h per mg protein, respectively; under similar conditions NADH- or succinate-dependent oxidative phosphorylation were 6.4 and 1.3 μmoles/h per mg protein.

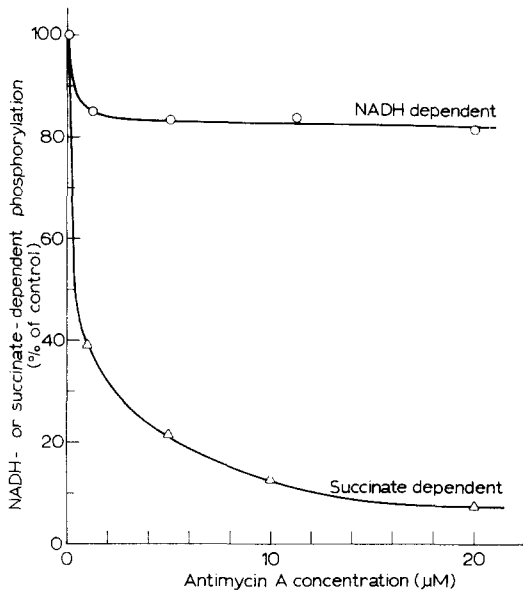

Fig. 2. Effect of antimycin A on NADH or succinate-linked oxidative phosphorylation. Control activities were 7.6 μmoles/h per mg protein for NADH-dependent phosphorylation and 1.4 μmoles/h per mg protein for succinate-dependent phosphorylation.

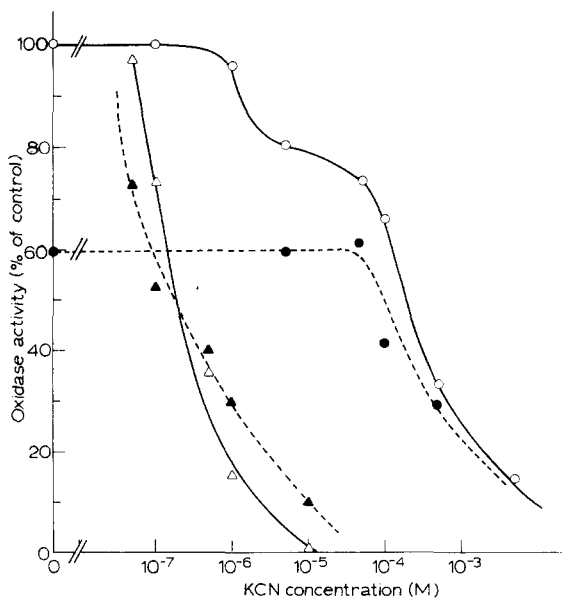

Fig. 3. Inhibition by KCN of NADH (○—○), ascorbate–cytochrome *c* (▲- - -▲), and ascorbate–diaminodurene (△—△) oxidases as a function of inhibitor concentration. Control activities were: 36 μmoles/h per mg protein for NADH oxidase; 8.7 μmoles/h per mg protein and 24 μmoles/h per mg protein for ascorbate–cytochrome *c* and ascorbate–diaminodurene oxidases, respectively. The curve indicated as ●—● refers to the rate of NADH oxidase in presence of antimycin A (20 μM).

dependent activity is rather insensitive to KCN at concentrations below 10^{-5} M, whereas the succinate dependent one is 70% inhibited at this concentration.

Oxidative phosphorylation shows similar difference in sensitivity to antimycin A (Fig. 2): in the presence of the inhibitor the maximum inhibition of NADH-dependent phosphorylation is only 18% of the control (ocasionally inhibition reaches values of 30%), while at the same concentration phosphorylation coupled to succinate oxidation is nearly completely inhibited. In agreement with the results previously reported with respiratory membranes from *Rsp. rubrum*[2] and *Rps. capsulata*, strain Kb1 (ref. 4), both NADH and succinate oxidases are only inhibited maximally between 50 and 60% by antimycin A.

These observations together with the results described above may be interpreted as evidence fo two pathways of oxygen consumption. Indeed it can be shown (Fig. 3) that the residual NADH oxidase activity measured in the presence of antimycin A is completely insensitive to KCN concentrations lower than $5 \cdot 10^{-5}$ M. However KCN was extremely effective in inhibiting the oxidation of substrates with more positive potentials such as sodium ascorbate *plus* mammalian cytochrome *c* or sodium ascorbate *plus* diaminodurene: these oxidases were 50% inhibited at 10^{-7} M and $5 \cdot 10^{-7}$ M, respectively.

Oxidation of NADH and succinate by different electron acceptors

The data presented in Table I show the rates of NADH and succinate oxidations by O_2 or, in anaerobiosis, in the presence of different exogenous electron acceptors and their sensitivity to antimycin A and rotenone. The results confirm and extend the data previously published by Klemme *et al.*[4]., with membrane preparations

TABLE I

EFFECT OF ANTIMYCIN A AND ROTENONE ON VARIOUS REACTIONS CATALYZED BY RESPIRATORY MEMBRANES FROM *RPS. CAPSULATA*

The measurements were performed as described under Materials and Methods. The concentrations of the various electron acceptors used were; ferricyanide, 2.5 mM; equine cytochrome *c*, 0.027 mM; Q_1, 0.05 mM; sodium fumarate, 3 mM. The activities are expressed as μmoles of substrate oxidized/h per mg of protein

Electron donor	*Electron acceptor*	*Activity (μmoles/h per mg)*	*Plus antimycin A (10 μM)*		*Plus rotenone (8 μM)*	
			Activity (μmoles/h per mg)	%	*Activity (μmoles/h per mg)*	%
NADH	O_2	13.9	6.9	50	0.4	2.9
NADH*	Ferricyanide	109	114	104	75	68.5
NADH**	Cytochrome *c*	5.9	0.8	13.6	0.3	5.1
NADH*	O_1	14.3	15.5	110	2.9	20.3
NADH*	Fumarate	0.08	Not inhibited		Inhibited	
Succinate	O_2	4.5	2.6	58	–	—
Succinate*	Ferricyanide	10.8	3.2	30	—	—
Succinate**	Cytochrome *c*	1.7	0.25	14.7	—	—

* Activities measured in anaerobiosis.

** Activities measured in the presence of $4 \cdot 10^{-3}$ M KCN.

from *Rps. capsulata*, strain Kb1. All NADH-dependent reactions are sensitive to rotenone though to different degrees; NADH–ferricyanide and NADH–Q_1 reductases are inhibited by 31 and 80%, respectively. Antimycin A is generally less effective but exerts a more selective action: this inhibitor does not affect the oxidation of NADH by "Site I" electron acceptors, like Q_1 and fumarate, but drastically inhibits the reduction of exogenous cytochrome *c*.

Succinate oxidation both by ferricyanide and cytochrome *c* is strongly inhibited by antimycin A (70 and 85%, respectively) but an antimycin A-insensitive pathway is responsible for about 50% of the overall oxidation rate present with both NADH and succinate oxidases.

Membrane energization by partial reactions of respiration

The study of the relationship between different partial reactions of the respiratory chain (Table I) and energization of the membranes was accomplished using atebrine as a probe for the high energy state. It has indeed been demonstrated that the fluorescence of this dye is largely quenched in the presence of energized vesicular phosphorylating systems[14,15]. More specifically it has been suggested that the quenching is related to an active uptake of this diamine into the inner compartment of the vesicle, following acidification of this phase. For this reason the quenching of certain fluorescent amines (with a pK higher than 10) has been proposed as a tool for a direct measurement of the transmembrane pH difference[21].

Recent experiments have demonstrated that in a liposome system[22] this model holds quantitatively for the monoamine 9-aminoacridine (pK=10), but only qualitatively for the diamine atebrine (pK_1=7.9; pK_2=10.5; see ref. 21), but we have chosen atebrine as a probe in this study because of its faster response and

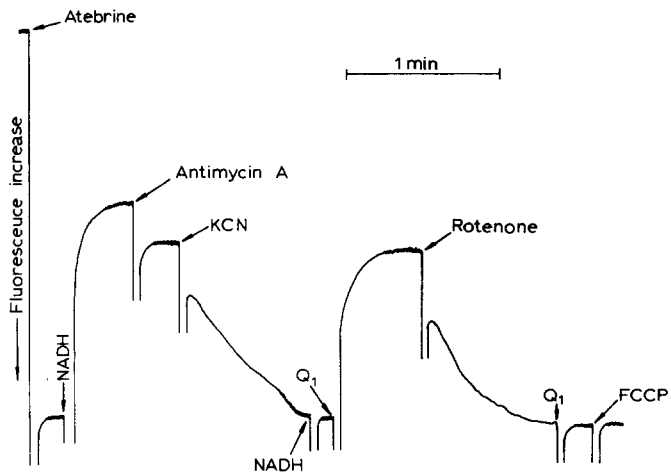

Fig. 4. Quenching of the fluorescence of atebrine induced by oxidation of NADH by oxygen or by an artificial electron acceptor (Q_1). The assay contained, in a final volume of 2.5 ml: glycylglycine (pH 8.0), 100 μmoles; $MgCl_2$, 12.5 μmoles; KCl, 250 μmoles; bovine serum albumin, 1.25 mg; EDTA, 2.5 μmoles; valinomycin, 4 μg; atebrine, 10 nmoles and respiratory membranes corresponding to 1 mg of protein. The following additions were made: NADH, 0.5 μmole; KCN, 1 μmole; Q_1, 0.1 μmole; rotenone, 20 nmoles; antimycin A, 25 nmoles; carbonyl cyanide *p*-trifluoromethoxyphenylhydrazone (FCCP), 25 nmoles.

higher sensitivity to small pH differences. However all the results presented below can also be obtained using 9-aminoacridine. Valinomycin and KCl, which have been shown to enhance the rate and extent of atebrine fluorescence quenching, were used throughout these experiments.

The effect of different inhibitors and electron acceptors on the quenching of atebrine fluorescence induced by the oxidation of NADH is shown in Figs 4 and 5. Addition of NADH to an aerobic suspension of respiratory membranes of *Rps. capsulata* (Fig. 4) causes a decrease in fluorescence which is only slightly reversed by antimycin A; $4 \cdot 10^{-4}$ M KCN completely abolishes the quenching. If at this point an artificial electron acceptor such as Q_1 is added, a decrease in fluorescence is observed which is completely sensitive to rotenone.

The experiments illustrated in Fig. 5 indicate that in the presence of KCN the oxidation of NADH by ferricyanide is also able to induce a considerable quenching of the fluorescence of the dye. The energization is inhibited by rotenone, but is insensitive to antimycin A. Since we have shown that the oxidation of NADH by Q_1 or ferricyanide is not completely sensitive to rotenone, it must be concluded that these dehydrogenase reactions proceed through multiple pathways which are not all equivalent in energy conservation.

From this first set of results it appears clear that the oxidation of NADH by

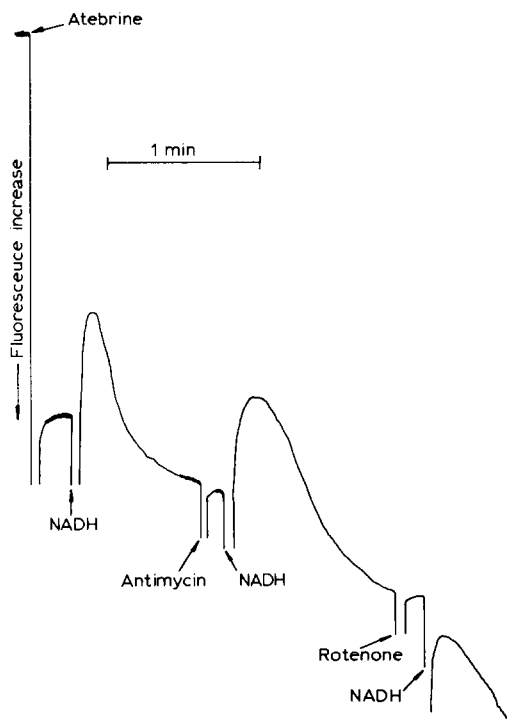

Fig. 5. Membrane energizatior dependent on oxidation of NADH by ferricyanide. Conditions as in Fig. 4, except that the assay contained 5 μmoles of potassium ferricyanide and 1 μmole of KCN before the addition of atebrine. The shifting of the baseline is due to the reduction of ferricyanide and the resulting decrease in absorbance of the excitation light.

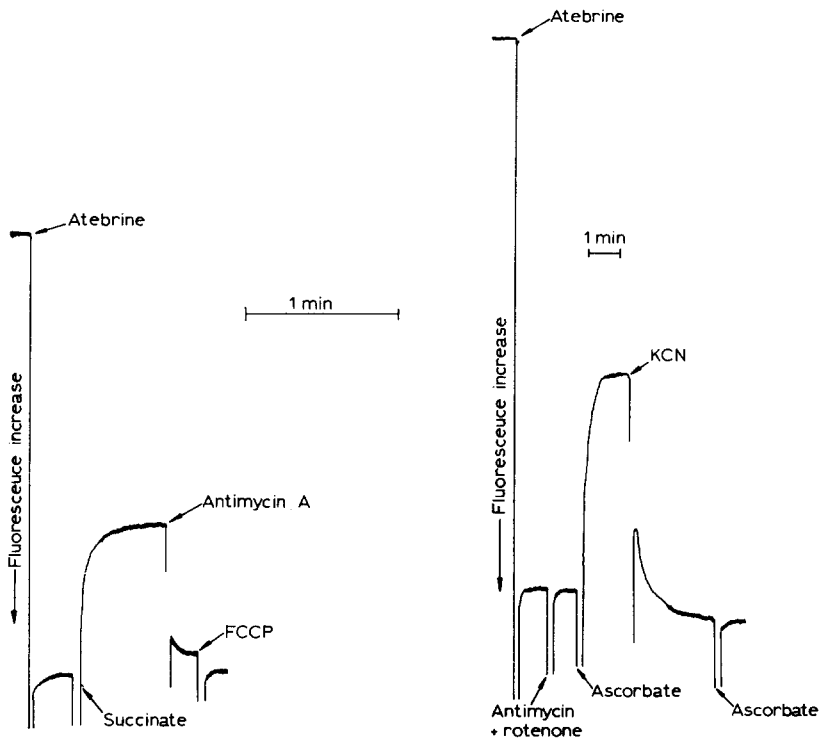

Fig. 6. Quenching of atebrine fluorescence revealing energization of the membrane linked to oxidation of succinate. Conditions as in Fig. 4; sodium succinate added, 20 μmoles.

Fig. 7. Quenching of atebrine fluorescence revealing energization of the membrane depending on oxidation of ascorbate–diaminodurene. Conditions as in Fig. 4 except that diaminodurene (0.1 μmole) was already present in the assay mixture before the addition of atebrine. The amount of sodium ascorbate added was 2.5 μmoles.

O_2 or, in the presence of KCN, by Q_1 or ferricyanide leads to energization of the membrane and that this state is easily revealed by the use of atebrine.

The effect of the addition of succinate on the fluorescence of atebrine is shown in Fig. 6. The quenching induced by addition of succinate to an aerobic suspension of membranes is smaller than that obtained in the presence of NADH and is completely reversed by antimycin A. These results agree with those obtained by measuring directly the rates of NADH- or succinate-dependent oxidative phosphorylation in the presence or absence of this electron transport inhibitor.

Using the same technique we also studied the response to other electron donors of a more positive oxidation reduction potential. In the presence of antimycin A and rotenone the ascorbate–diaminodurene couple induces a significant decrease in fluorescence (Fig. 7); the reversal of the quenching by KCN indicates a locus of membrane energization between this electron donor system and oxygen.

Though the effects of antimycin A on the energization linked to oxidation of succinate or ascorbate–diaminodurene clearly differentiate between the site of entry of electrons from these two-electron donors into the respiratory chain, it is possible

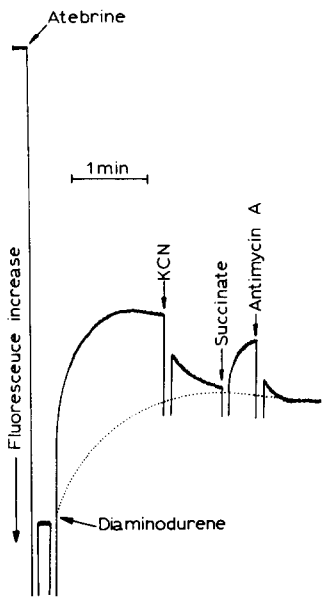

Fig. 8. Energization of the membrane depending on oxidation of reduced diaminodurene by oxygen and reduction of oxidized diaminodurene by succinate. The assay contained respiratory particles corresponding to 1.5 mg protein. The following additions were made: diaminodurene, 1 μmole; KCN, 1 μmole; succinate, 5 μmoles; antimycin A, 20 nmoles. The displacement of the baseline is due to the increase in absorbance of the excitation light following oxidation of reduced diaminodurene; this phenomenon is resolved from the true quenching of fluorescence due to energization of the membrane, if the latter is eliminated by the addition of 20 nmoles of gramicidin (dotted line).

in principle, that in both cases the effect observed is related to the same energy converting site. It is unlikely that the effects of ascorbate–diaminodurene are due to a direct interaction of ascorbate with the electron transport chain because substrate amounts of diaminodurene ($E'_0 = +0.245$ V) alone are capable of inducing a measurable energization, which is sensitive to KCN (Fig. 8). Moreover the presence of two different coupling sites between succinate and O_2 was confirmed by the following experiment: A substrate amount of reduced diaminodurene was extensively oxidized by respiratory membranes (in an energy yielding process) and the reaction was blocked by the addition of KCN (4.10^{-4} M), which at this concentration completely inhibits the coupled oxidation of succinate (Fig. 1b). At this stage, addition of succinate was able to induce a second energization cycle which was now completely inhibited by antimycin A. Thus diaminodurene can act both as an electron donor in the reduced form and an electron acceptor from succinate in the oxidated state and these two reactions are both coupled to energization.

Oxidative phosphorylation by segments of the respiratory chain

We have been able to show that partial oxidation reactions of the respiratory chain which can energize the membrane are also able to drive ATP synthesis (Table II). Incorporation of $^{32}P_i$ into ATP could be demonstrated when an anaerobic suspension of membranes was supplemented with NADH and Q_1; the reaction was inhibited by oligomycin and uncouplers.

TABLE II

TYPICAL OXIDASE AND PHOSPHORYLATION ACTIVITIES OF RESPIRATORY MEMBRANES FROM *RPS. CAPSULATA*

The experimental conditions used for measuring NADH- and succinate-dependent activities were described under Materials and Methods. The measurement of NADH–Q_1 reductase and linked phosphorylation were performed in anaerobic Thunberg cuvettes as follows: a reaction mixture containing all the components, except NADH, carrier-free $^{32}P_i$ and Q_1 was made anaerobic by flushing with nitrogen. In order to avoid any incorporation of $^{32}P_i$ due to oxidation of NADH by traces of oxygen still present in the reaction mixture, NADH was added first to the measuring cuvette, followed by addition of carrier-free $^{32}P_i$. The reaction was started by adding Q_1 (0.1 mM) and the oxidation of NADH was monitored spectrophotometrically; 0.1 ml of cold 25% trichloroacetic acid was added to both reference and measuring cuvettes after all Q_1 was reduced. The values presented for ascorbate–diaminodurene and ascorbate–cytochrome *c* oxidases and associated phosphorylations were obtained by measuring both activities directly in the oxygen electrode chamber. All components, including diaminodurene or cytochrome *c*, were already present before the reaction was started by the addition of ascorbate; a few seconds after starting the reaction, carrier-free $^{32}P_i$ was added and the reaction was allowed to reach the complete exhaustion of oxygen. A 2-ml sample was then added to precooled centrifuge tubes containing 0.2 ml of 25% trichloroacetic acid. All measurements were run in duplicate; control experiments in the presence of oligomycin or in the absence of the substrate were also performed. Special care was also used for the extraction of the inorganic phosphate: after addition of carrier glucose 6-phosphate (0.3 mM) the phosphomolybdate complex was extracted twice with isobutanol–benzene (1:1 by vol.) saturated with water followed by two other extractions, one with isobutanol and one with ethyl ether.

Electron donor	*Electron acceptor*	*Oxidase rate (μmoles/h per mg)*	*Substrate oxidized (nmoles)*	*ATP formed (nmoles)*	*P/2e⁻*
NADH	O_2	26.7	467	228	0.46
Succinate	O_2	9.4	363	55	0.15
Diaminodurene–ascorbate	O_2	20.9	2680*	157	0.06
NADH	Q_1	22.3	225	53	0.23
Cytochrome *c*–ascorbate	O_2	6.45	3360*	154	0.05

* Measured as natoms of oxygen consumed.

Similarly, phosphorylation coupled to oxidation of ascorbate–diaminodurene could be obtained and the incorporation was again inhibited by oligomycin and uncouplers, but was completely insensitive to antimicyin A and rotenone. Synthesis of ATP, which was insensitive to antimycin A, was also obtained by oxidation of ascorbate *plus* mammalian cytochrome *c* (compare ref. 4, Table V). This reaction represents another and more direct demonstration of energy conservation linked to cytochrome oxidase. Energy conservation at this site could not be confirmed using atebrine because the Soret band of cytochrome *c* overlapped the atebrine absorption spectrum too heavily.

The experimental $P/2e^-$ ratios obtained with the different oxidative phosphorylating systems are summarized in Table II; the numerical values indicated are typical of those consistently obtained with NADH or succinate dependent phosphorylations, but are merely indicative for the other systems due to the low $P/2e^-$ ratios obtained. It should be noted however that the experimental $P/2e^-$ values associated with the oxidation of ascorbate–diaminodurene are consistently lower

than that measured with succinate in spite of the higher rates of oxidation of the ascorbate–diaminodurene couple.

DISCUSSION

All the results described above have been obtained in membrane preparations from *Rps. capsulata*, strain St. Louis, grown heterotrophically in the dark under the conditions described; at the present we do not know if these properties hold also for photosynthetically grown cells since no data are available. Therefore, the following discussion will be primarily concerned with the properties of the respiratory system in cells grown aerobically and will not attemtp to consider the interrelationship between the photosynthetic and respiratory electron transport chain.

Before discussing the sites of energy conservation it is necessary to comment briefly about the effect of antimycin A and KCN on the different oxidase activities.

Antimycin A inhibits succinate or NADH oxidases by only about 50%. It almost completely blocks cytochrome *c* reduction by either NADH or succinate in the presence of $4 \cdot 10^{-3}$ M KCN. The inhibition of the NADH oxidase by KCN is biphasic in the concentration range between 10^{-6} and $5 \cdot 10^{-3}$ M. The first phase of the KCN inhibition is saturated at concentrations comparable to those which completely inhibit oxidation of ascorbate–cytochrome *c* or ascorbate–diaminodurene. The second phase corresponds to the inhibition of that portion of the NADH oxidase activity which is insensitive to antimycin A.

Succinate oxidation is also inhibited by KCN concentrations ranging from 10^{-6} and $5 \cdot 10^{-3}$ M but no biphasicity is clearly observable. Finally the presence of a slow but definite rate of reduction of fumarate by NADH confirms that the two dehydrogenase systems must interact through some common component.

The simplest way of explaining these results is to assume that NADH and succinate oxidation proceed to oxygen through a branched pathway, with the branch point situated on the substrate side of the antimycin A block. According to this model, cytochrome *c* only donates or accepts electrons after the site of antimycin A inhibition on the pathway which is sensitive to low concentrations of KCN. The other arm of the branched chain, assumed to be that which is blocked by high concentrations of cyanide, may be merely the result of an autooxidizable component of the respiratory chain.

On the basis of this scheme the energization data are readily interpreted. Energization linked to NADH oxidation, which is also largely present when antimycin A or low concentrations of KCN are added, must be located at least partially before the antimycin A-sensitive site. The demonstration of energization associated with NADH oxidation by Q_1, or ferricyanide which is insensitive to KCN or antimycin A, can be considered as direct evidence for this site.

On the other hand the greater sensitivity to antimycin A and cyanide of succinate-linked energization indicates that all the energy-conserving steps coupled to the oxidation of this substrate must involve electron flow through a pathway which contains the sites of action of these two inhibitors. The exact number of these sites is difficult to assess. The experimentally determined $P/2e^-$ ratios for succinate oxidation are always higher than those observed for the oxidation of ascorbate–diaminodurene or ascorbate–cytochrome *c*. An estimation of the number

of coupling sites on this basis cannot be very accurate, since the experimental $P/2e^-$ ratios can depend on the rate of oxidation[23]. It should be noted, however, that the rate of succinate oxidation is always considerably lower than that of cytochrome *c* or diaminodurene oxidases. It appears therefore that there is more than one coupling site linked to oxidation of succinate.

Oxidation of the couples ascorbate–diaminodurene or ascorbate–cytochrome *c* induces an energization of the membrane which is insensitive to antimycin A in contrast to the energization dependent upon succinate oxidation; this energization was also confirmed by direct measurements of $^{32}P_i$ incorporation both using ascorbate–diaminodurene or ascorbate–cytochrome *c* as electron donors. In addition we have shown that it is possible to obtain an energy-dependent quenching of atebrine fluorescence by adding substrate amounts of reduced diaminodurene, which, once oxidized, can act as an electron acceptor from succinate in an energy-yielding reaction. These two reactions which are sensitive to KCN and antimycin A, respectively, possibly represent a direct demonstration of the presence of two coupling sites.

The present study has shown that the measurement of atebrine fluorescence during energization can be used to localize energy coupling sites in preparations of phosphorylating membranes characterized by low $P/2e^-$ ratios. In addition this study demonstrates that, if the proposed model for the mechanism of the quenching is correct[21], a good correlation can be demonstrated between proton translocation and phosphorylation in every site of energy conservation of aerobic bacterial membranes, as required by the chemioosmotic coupling hypothesis.

In summary, the picture that can be drawn from these observations bears considerable similarity to that of the electron transport chain of mammalian mitochondria, with in addition a very active non-phosphorylating pathway insensitive to antimycin A and sensitive to high concentrations of KCN. The presence of branched chains has been proposed also for other respiratory systems[24–26].

Our conclusions partially disagree with the proposal by Klemme and Schegel[4] that ATP formation is linked only to succinate oxidation. It has to be noted however that in their studies a different strain of *Rps. capsulata* (Kb1) was used, along with a more disruptive procedure for breaking the cells, *i.e.* sonication.

It is not possible to suggest a physiological role for the non-phosphorylating pathway at present. The antimycin A-insensitive oxygen consumption could be an expression of a second, non-phosphorylating terminal oxidase or, as suggested above, due to the autooxidizability of some electron carrier. In either case, the presence of this pathway would explain the low $P/2e^-$ ratios routinely observed in these preparations. In this connection it should be recalled that in intact photosynthetic cells of *Rsp. rubrum*, respiration can be totally inhibited by light and the inhibition be reversed by uncouplers[27]. Though the nature of the endogenous substrate of respiration is unknown, these data may be interpreted as showing that "*in vivo*" only a phosphorylating respiratory chain exists.

After this manuscript was completed we became aware (H. Gest, personal communication) that a number of respiratory mutants of *Rps. capsulata* have been isolated by Marrs and Gest[28]. The scheme we have proposed above agrees remarkable well with the characteristics of growth and the properties of respiration observed in these mutants. However, it was observed that mutants with a lesion on the final

cytochrome *c* oxidase are still capable of aerobic growth on a medium containing malate. This observation suggests that an alternative pathway of respiration, possibly identical with the antimycin A-insensitive pathway described in this paper is operative also "*in vivo*" at least under the extreme conditions existing in these mutants.

ACKNOWLEDGEMENTS

The technical assistance of Mr Luciano Maragna is gratefully acknowledged. We wish to express our gratitude to Dr A. R. Crofts and Mr R. J. Codgell, University of Bristol, for critically reading the manuscript and to Dr H. Gest, Indiana University, for supplying preprints of his manuscripts This work was supported by Grant No. 70.01741.04 from Consiglio Nazionale delle Ricerche (Italy).

REFERENCES

1 Horio, T. and Kamen, M. D. (1970) *Ann. Rev. Microbiol.* 24, 409
2 Taniguchi, S. and Kamen, M. D. (1965) *Biochim. Biophys. Acta* 96, 395–428
3 Thore, A., Keister, D. L. and San Pietro, A. (1969) *Arch. Mikrobiol.* 67, 378–396
4 Klemme, J.-H. and Schlegel, H. G. (1969) *Arch. Mikrobiol.* 68, 326–354
5 Whale, F. R. and Jones, O. T. G. (1970) *Biochim. Biophys. Acta* 223, 146–157
6 Sasaki, T., Motokawa, Y. and Kikuchi, G. (1970) *Biochim. Biophys. Acta* 197, 284–291
7 Baltscheffsky, H. and Ardwidsson, B. (1962) *Biochim. Biophys. Acta* 65, 425–428
8 Klemme, J.-H. and Schlegel, H. G. (1968) *Arch. Mikrobiol.* 63, 154–169
9 Baltscheffsky, M. (1969) *Arch. Biochem. Biophys.* 121, 46–53
10 Keister, D. L., Yike, N. J. (1967) *Arch. Biochem. Biophys.* 121, 415–422
11 Isaev, A. A., Liberman, E. A., Samilov, V. D., Skulachev, V. P. and Tsofina, T. M. (1970) *Biochim. Biophys. Acta* 216, 22–29
12 Geller, D. M. (1962) *J. Biol. Chem.* 237, 2947–2954
13 Yamashita, J., Yoshimura, S., Matuo, Y. and Horio T. (1967) *Biochim. Biophys. Acta* 143, 154–172
14 Kraayenhof, R. (1970) *FEBS Lett.* 6, 161–165
15 Azzi, A., Fabbro, A., Santato, M. and Gherardini, P. L. (1971) *Eur. J. Biochem.* 21, 404–410
16 Ormerod, J. G., Ormerod, K. S. and Gest, H. (1961) *Arch. Biochem. Biophys.* 94, 449–463
17 Baccarini Melandri, A., Gest, H. and San Pietro, A. (1970) *J. Biol. Chem.* 245, 1224–1226
18 Melandri, B. A., Baccarini Melandri, A., San Pietro, A. and Gest, H. (1971) *Science* 174, 514–516
19 Melandri, B. A., Baccarini Melandri, A., Crofts, A. R. and Cogdell, R. J. (1972) *FEBS Lett.* 24, 141–145
20 Lowry, O. H., Rosebrough, N. J., Farr, A. L. and Randall, R. J. (1951) *J. Biol. Chem.* 193, 265–275
21 Schuldiner, S., Rottemberg, H. and Avron, M. (1972) *Eur. J. Biochem.* 25, 64–70
22 Deamer, W. D., Prince, R. C. and Crofts, A. R. (1972) *Biochim. Biophys. Acta* 274, 323–335
23 Tsou, C. A. and van Dam, K. (1969) *Biochim. Biophys. Acta* 172, 174–176
24 Jones, C. W. and Redfearn, E. R. (1967) *Biochim. Biophys. Acta* 143, 340–353
25 Bendall, D. S. and Bonner, W. D. (1971) *Plant Physiol.* 47, 236–245
26 Lambowitz, A. M., Smith, E. W. and Slayman, C. W. (1972) *J. Biol. Chem.* 247, 4850–4858
27 Oelze J. (1972) in *Proc. 2nd Int. Congr. on Photosynthesis Research, Stresa, 1971* (Forti, G., Avron, M. and Melandri, B. A., eds), Vol. I, pp. 649–654, Dr W. Junk N. V. Publishers, The Hague
28 Marrs, B. and Gest, H. (1973) *J. Bacteriol.* 114, 1045–1051

Biochimica et Biophysica Acta, 314 (1973) 312–319

BBA 46601

KINETICS OF ATP FORMATION AND PROTON EFFLUX BY ACID–BASE TRANSITION IN CHLOROPLASTS

YUICHIRO NISHIZAKI

Institute for Agricultural Research, Tohoku University, Sendai (Japan)

(Received March 12th, 1973)

SUMMARY

The relationship between the kinetics of ATP formation and proton release in chloroplast suspensions by acid–base transition were studied by means of a stopped-flow spectrophotometer. The time course of ATP synthesis shows two-phase kinetics, fast and slow, corresponding to the two-phase efflux of protons from the chloroplasts. Under certain conditions of the experiments, about 50% of the H^+ gradient is constantly utilized for ATP formation in both phases. However, the ratio of ATP formed to the amount of protons leaked out, changes depending on the rate constants of proton efflux.

INTRODUCTION

Exposing broken chloroplast fragments first to pH 4 media, containing permeant organic acid such as succinate and then to base at pH 8, is known to cause a transient high-energy state which results in ATP formation[1]. Energy in this acid–base transition experiment was suggested to be supplied by the H^+ gradient across the thylakoid membranes[2].

In the previous papers[3,4], the kinetics of proton efflux in chloroplast suspensions by the acid–base transition were studied by means of a stopped-flow apparatus. Rapid recording with bromocresol purple as a pH indicator showed that the time course of proton release consisted of two phases, fast and slow[4]. The fast phase was suggested to be due to the rapid release of protons from the matrix of thylakoid membranes, and the slow phase to the efflux through the membrane of organic acid (and/or protons) previously absorbed from the initial acid medium. This phase was followed by the additional slower component of proton loss[3,4].

The time course of phosphorylation by the acid-base transition has been followed chemically by stopping the reaction at appropriate intervals[1]. However, the relationship between the time course of ATP formation and the protein efflux from the chloroplasts has not yet been precisely established. In this report, the time course of pH changes was followed to observe the above relationship by means of a stopped-flow spectrophotometer with bromocresol purple, which has been shown not to be bound to membrane[5,6], as a pH indicator.

Abbreviation: DCMU, 3-(3,4-dichlorophenyl)-1,1-dimethylurea.

METHODS

Chloroplasts were isolated from market spinach as described earlier[7], and finally suspended at about 0.4 mg of chlorophyll per ml in 10 mM NaCl. 0.2 ml of this suspension was mixed with 0.2 ml of a solution at pH 4.0 containing 25 mM succinic acid, 10 mM $MgCl_2$, and 75 μM 3-(3,4-dichlorophenyl)-1,1-dimethylurea (DCMU) in a reservoir of the stopped-flow apparatus maintained at a constant temperature (usually 3.5–4.0 °C). The acidified chloroplasts were incubated for 15–20 s, 0.25 ml of which were then rapidly picked up into one of the two syringes in the apparatus. The other syringe contained an equal volume of 30 μM bromocresol purple, 8 mM Na_2HPO_4, and NaOH solution sufficient to neutralize the succinic acid and bring the final pH to about 8. When phosphorylation was to be followed, 0.4 mM ADP was added in the latter syringe. No buffer was used in the base stage. Variations of the reaction mixture components are indicated in the figure. Chlorophyll was determined by the method of Arnon[8].

The stopped-flow spectrophotometer SPS-1 used was the same as before[4], and the changes in the absorbance of bromocresol purple at 594 nm after mixing were recorded with the memoriscope MS-5019A[4]. Two syringes were driven by compressed N_2 at 1–2 kg/cm^2 for mixing and the dead time[4] was under 2 ms, usually 1–1.2 ms.

The pH changes of the chloroplast suspension were calculated from the absorbance–pH curves of bromocresol purple at 594 nm; absorbance changes of more than 0.02 could be detected per 0.1 pH unit at the pH used. Also, the changes in H^+ concentration (ΔH^+, μequiv/mg chl) were calculated from the pH values according to direct titrations of the buffer capacities of the chloroplast suspension (the reaction mixture components present) with acid and with NaOH at each time of the experiments.

To follow the time course of ATP formation in rapid reactions such as those in the present experiments, it is difficult to determine ATP yield directly by luciferase assay and by incorporation of phosphate. Jagendorf and Uribe[1] showed that the major part of the observed phosphate incorporation by acid–base transition experiments had represented net synthesis of ATP when the basic reaction mixture contained ADP, P_i and Mg^{2+}. Further, in his experiments with chloroplasts, Schwartz[9] made use of the fact that at pH 8.0 one proton is consumed irreversibly in the synthesis of ATP.

$$ADP^{3-} + HPO_4^{2-} + H^+ \rightarrow ATP^{4-} + H_2O$$

Both theoretical and experimental considerations of this method were made by Nishimura *et al.*[10].

Thus in the present experiments the time course of ATP formation was measured, according to Schwartz, following its associated alkalinization (less acidification) of the chloroplast suspension during the course of efflux of protons after mixing when ADP was present. The presence of ADP, P_i or Mg^{2+} alone did not alter the rate of proton efflux to any significant extent.

RESULTS

As reported previously[4], the release of protons by acid–base transition showed

two-phasic time courses at the low temperature used. The two phases could be discriminated from the recorded time course of the ΔH^+ changes as shown in Fig. 4 in ref. 4. In this report, the fast and the slow phases will be designated as Phase I and Phase II, respectively.

Time courses of the ΔH^+ and ATP formation

In Fig. 1 the time courses of the ΔH^+ of the chloroplast suspension after mixing either with or without the addition of ADP are compared. One syringe contained 12.5 mM succinate at pH 4.0 with chloroplasts (0.2 mg chlorophyll/ml) and 5 mM $MgCl_2$, and the other contained 30 μM bromocresol purple, 8 mM sodium phosphate, either with or without 0.4 mM ADP, and NaOH so that the final pH after mixing the contents of the two syringes could be 8.4.

As can be seen in Fig. 1, the tracing shows a sharp increase in H^+ concentration in the suspension immediately after mixing (Phase I), followed by a slow increase (Phase II) as a function of time until an equilibrium was attained in about 10 s. In the fast tracing of ΔH^+ (Fig. 1B), the transition from Phase I to Phase II could be clearly observed. When ADP was present, there was less change in H^+ concentration in both Phases I and II, indicating a consumption of H^+ for the formation of ATP[9,10]. The differences of H^+ concentration between the two curves (−ADP and +ADP) are equivalent to the concentrations of ATP formed in this process.

Fig. 2 shows an experiment in which one syringe contained the strong mineral acid, HCl, instead of succinic acid, to bring the pH of the chloroplast suspension to 4.0. In this case, practically the same increase in H^+ concentration in Phase I was

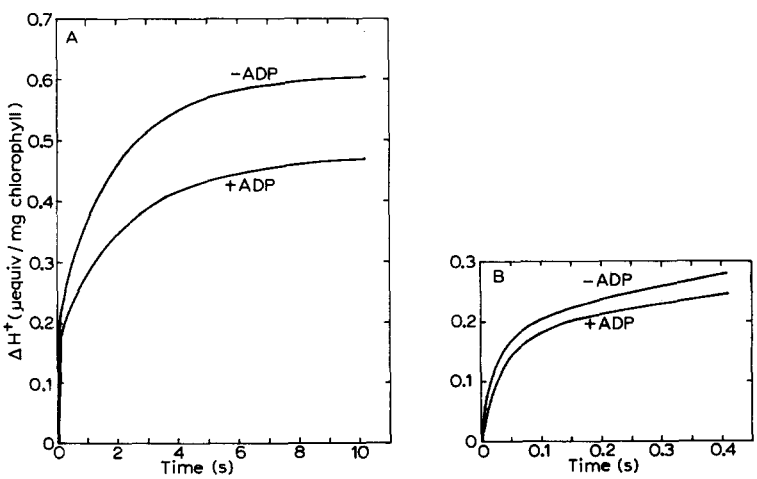

Fig. 1. Efflux of protons after mixing. The ΔH^+ curves are reproduced from the oscillograph tracing of pH change (see Methods). Initial chloroplasts at pH 4.0 with 12.5 mM succinic acid, 5 mM $MgCl_2$, and 38 μM DCMU. The base solution contained 30 μM bromocresol purple and sufficient NaOH to neutralize succinic acid to bring the final pH to 8.4 with and without ADP (0.4 mM). Chlorophyll concentration was 0.1 mg/ml after mixing. Temperature, 4 °C. (A) Slow recording. (B) Fast recording to follow transition from Phase I to Phase II.

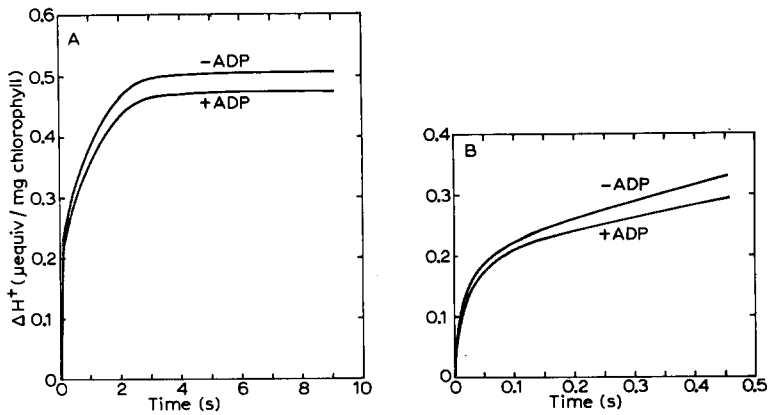

Fig. 2. Efflux of protons when HCl was substituted for succinic acid in the acid stage. Final pH 8.0. Other conditions were the same as in Fig. 1.

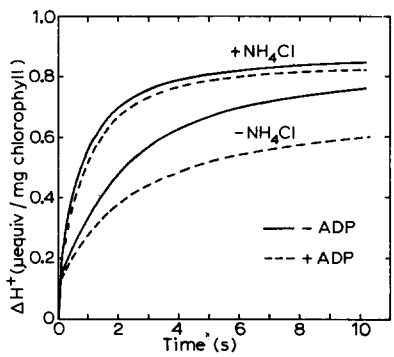

Fig. 3. Efflux of protons with and without NH_4Cl (10 mM in acid stage) together with and without ADP. Final pH 8.3. Other conditions were the same as in Fig. 1. When NH_4Cl was present, practically no difference was observed between the time courses of proton efflux with and without ADP.

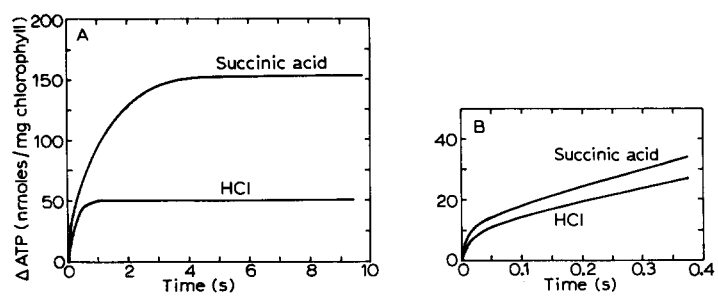

Fig. 4. Time courses of ATP formation calculated from Figs 1 and 2.

observed as in Fig. 1, but in Phase II (Fig. 2A) less H^+ was released from the chloroplasts and the equilibrium was attained much faster, that is, in about 2–3 s.

When an uncoupler such as NH_4Cl was present (added in the acid stage at

10 mM), the time course of proton efflux was practically independent of whether ADP was added or not in the base stage as shown in Fig. 3.

Time courses of ATP formation, calculated from Figs 1 and 2, are shown in Fig. 4. Identical kinetics for the ATP formation were found when HCl was used in the initial acidification in place of succinic acid immediately after mixing (Fig. 4B, Phase I). However, though the ATP formation completely stopped before 1 s had elapsed in HCl-treated chloroplasts (Fig. 4A), it continued for about 4 s and much more ATP was formed before the equilibrium was attained when succinic acid was used in the acid stage (Phase II). All of these facts are consistent with the observations that succinic acid which entered the thylakoid vesicles in the acid stage served as a proton reservoir in the base stage, resulting in a large amount of ATP formation in an acid–base experiment[2].

Considerable amounts of protons are found to have leaked out after the completion of ATP formation when ΔH^+ and ATP curves are compared in Figs 1, 2 and 4. In other words, some H^+ gradient between the inside and the outside of the thylakoid membrane still existed when ATP formation was completely stopped.

Fig. 5 gives the changes of ATP formation with temperature. At 4° C, the rate of ATP formation was less than at 20 °C. However, the increase of the ATP concentration was continued much longer (about 5 s) at 4 °C than at 20 °C (less than 2 s), resulting in a crossing of the two curves and finally more ATP was formed at 4 °C. This is consistent with the results that the rate constants of the proton release in Phase II increased markedly under higher temperatures (Table III in ref. 3 and Table I in ref. 4) and also with the fact that higher rate constants for Phase II of proton release associated with the lower yield of ATP[3].

Estimation of the efficiency of the utilization of the H^+ gradient

Both Phases I and II of proton efflux, and also the associated ATP formations, followed apparent first-order kinetics when plotted on a semi-logarithmic scale as shown in Fig. 6.

If the concurrent ATP synthesis does not affect the rate constant of the proton

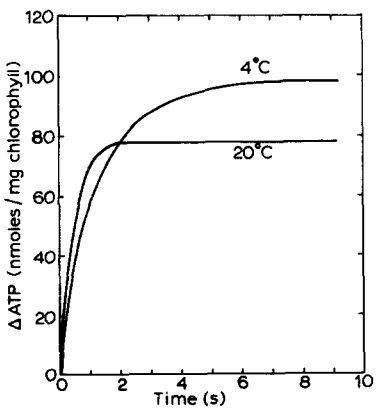

Fig. 5. Time course of ATP formation at two different temperatures (4 and 20 °C). Final pH 8.1. Other conditions were the same as in Fig. 1.

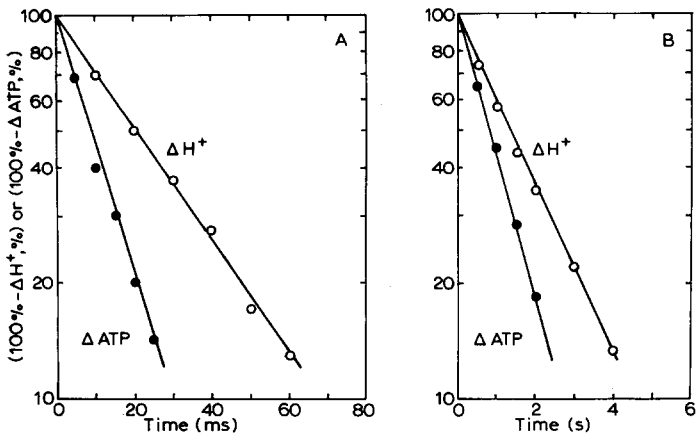

Fig. 6. Semi-logarithmic plot of proton efflux (−ADP) and ATP formation (+ADP) in Phase I (A) and Phase II (B). Ordinate shows (100%−ΔH$^+$, %) or (100%−ΔATP, %).

release in the absence of ATP formation, the processes taking place during the period of acid–base-induced phosphorylation can be assumed, as a first approximation, to be

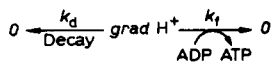

where k_d and k_f represent the first-order rate constants of the two processes, efflux of protons and ATP formation, competing with each other for the common "driven force" represented by the H$^+$ gradient (*grad* H$^+$) which is established at zero time in the base stage. This is a modification of the scheme suggested by Izawa[11], and Jagendorf and Uribe[2]. In this case, the rate constant calculated directly from the apparent kinetics of ATP formation, corresponds to the combined rate constants k_d+k_f, and the rate constant k_d can be calculated from the kinetics of proton efflux without adding ADP. The efficiency of *grad* H$^+$ trapping for ATP formation is estimated at $k_f/(k_d+k_f)$. Typical data thus obtained under several conditions are summarized in Tables I and II.

TABLE I

APPARENT FIRST-ORDER RATE CONSTANTS FOR PHASE I

Experimental procedures were the same as in Fig. 1. Acid stage: 12.5 mM succinic acid, 38 μM DCMU, 5 mM $MgCl_2$, pH 4.0. Base solution: 30 mM NaOH, 8 mM P_i, 30 μM bromocresol purple, 0.4 mM ADP. Final pH 8.0 (Expt 1) and 8.5 (Expt 2).

Expt	*Temp.* (°C)	*ADP*	*Rate constant* (s^{-1})			$k_f/(k_d+k_f)$
			ΔH^+ (k_d)	ΔATP (k_d+k_f)	k_f	k
1	3.5	−	30.1			
		+	—	63.0	32.9	0.52
2	4.0	−	34.7			
		+	—	77.0	42.3	0.55

TABLE II

APPARENT FIRST-ORDER RATE CONSTANTS FOR PHASE II

Initial pH 4.0. Final pH 8.4 (Expts 1 and 2), 8.1 (Expt 3). Other procedures were the same as Table I.

Expt	*Acid stage*	*Temp.* (°C)	*ADP*	*Rate constant* (s^{-1})			$k_f/(k_d+k_f)$
				$\Delta H^+(k_d)$	$\Delta ATP\,(k_d+k_f)$	k_f	
1	HCl	3.5	−	1.16			
			+	—	2.31	1.15	0.50
	Succinic acid	4.0	−	0.50			
			+	—	0.87	0.37	0.43
2	Succinic acid	4.0	−	0.43			
			+	—	0.82	0.39	0.48
		20	−	0.99			
			+	—	1.82	0.83	0.46
3	Succinic acid	4.0	−	0.53			
			+	—	0.99	0.46	0.47

The efficiency of trapping of the H^+ gradient for Phase I was $k_f/(k_d+k_f)=0.54 \pm 0.06$ (four experiments) and for Phase II 0.47 ± 0.02 (five experiments). Similar efficiency (about 50%) was obtained irrespective of temperature, rate constant, and the kind of acid used in the acid stage, both in Phases I and II. These values of about 50% efficiency coincide with that of X_E (a high energy state) capture obtained by Izawa[11] in the experiments of post-illumination ATP formation. This suggests the possibility that the H^+ gradient itself in the acid–base transition experiment is identical with X_E in the post-illumination experiment.

On the other hand, the stoichiometric relationship between the amount of H^+ released and ATP formed during the processes of phosphorylation after the acid–base transition, differed appreciably in Phase I and Phase II. In Phase I the ratios of H^+ released to ATP formed were 16 (HCl in the acid stage, 160 nequiv to 10 nmoles per mg chlorophyll)–8 (succinic acid, 135 nequiv to 18 nmoles). When these ratios are corrected for the estimated efficiency of H^+ gradient utilization (54% in Phase I) the values fall to 8.6 and 4.3, respectively. In Phase II, though the ratio was 6.7 (215 nequiv to 32 nmoles) in HCl-treated chloroplasts, fairly constant values of 3.4–2.9 (385 nequiv to 135 nmoles) were obtained with succinic acid as H^+ carrier (4 °C). Corrected values for the efficiency (47% in Phase II) fall to 3.1 (HCl) and 1.6–1.4 (succinate). At higher temperatures the ratio increased, indicating a lower ATP formation than at lower temperatures. Thus the stoichiometry is suggested to be changed under different conditions.

DISCUSSION

In summarizing together the results presented in this paper and in the previous ones[3,4], the time courses for the approach to equilibrium pH in the chloroplast

suspension after the acid–base transition showed apparent first-order kinetics, with three distinct components: (a) the fast phase (Phase I) of the rapid loss of protons from the matrix of thylakoid membranes having a half-life of about 20–40 ms (ref. 4), (b) the major portion of proton efflux from the inside of the thylakoid vesicles (Phase II), having a Q_{10} of 2 and a half-life of about 1.5–3 s (refs 3 and 4), and (c) a minor residual portion (Phase III) of the proton loss, having a Q_{10} of 1.2 and a half-life of about 5 s (ref. 3). As Phase III is assumed to be a simple loss of protons, having no relationship with ATP formation[3], a discussion of this is omitted here.

As shown in Figs 1, 2, 4, and 5, ATP formation started immediately after mixing, even during the process of proton dissociation from the thylakoid membrane (Phase I)[4]. The time course of ATP formation itself also has two components depending on the two-phasic time course of proton efflux (Fig. 4B). Both of the components followed apparent first-order kinetics closely depending on the first-order efflux of protons from the thylakoid vesicles both in Phases I and II (Fig. 6).

Since the production of the H^+ gradient may play a decisive role in the phosphorylation process[12], it is important to appreciate what proportion of the whole H^+ gradient may participate in the formation of ATP. The estimated efficiencies of the utilization of the H^+ gradient for the phosphorylation of ADP were 54% in Phase I and 47% in Phase II (Tables I and II). This is practically in accord with the efficiency of X_E capture (56%) obtained in the post-illumination phosphorylation experiments[11], though the Phase I component is not present in the latter. Comparable efficiency of X_E and H^+ gradient trapping under different procedures of the experiments suggests that the H^+ gradient may be identical with the X_E.

The efficiency of the utilization of the H^+ gradient is not changed when HCl is substituted for succinic acid in the acid stage in spite of the large rate constants of the H^+ efflux after the acid–base transition (Table II). The same situation is true at higher temperatures. However, the actual ratios of ATP formed to the amounts of protons released vary with the rate constants of the proton efflux. The larger the rate constants, the smaller the quantity of ATP formed in agreement with the previous observations[3]. Continued maintenance of an adequate H^+ gradient must be a necessary prerequisite for continued ATP synthesis.

ACKNOWLEDGEMENT

This work was supported in part by a grant from the Ministry of Education of Japan.

REFERENCES

1 Jagendorf, A. T. and Uribe, E. (1966) *Proc. Natl. Acad. Sci. U. S.* 55, 170–177
2 Jagendorf, A. T. and Uribe, E. (1966) *Brookhaven Symp. Biol.* 19, 215–241
3 Nishizaki, Y. and Jagendorf, A. T. (1971) *Biochim. Biophys. Acta* 226, 172–186
4 Nishizaki, Y. (1972) *Biochim. Biophys. Acta* 275, 177–181
5 Jackson, J. B. and Crofts, A. R. (1969) *Eur. J. Biochem.* 10, 226–237
6 Chance, B., Crofts, A. R., Nishimura, M. and Price, B. (1970) *Eur. J. Biochem.* 13, 364–374
7 Nishizaki, Y. and Jagendorf, A. T. (1969) *Arch. Biochem. Biophys.* 133, 255–262
8 Arnon, D. I. (1949) *Plant Physiol.* 24, 1–15
9 Schwartz, M. (1968) *Nature* 219, 915–919
10 Nishimura, M., Ito, T. and Chance, B. (1962) *Biochim. Biophys. Acta* 59, 177–182
11 Izawa, S. (1970) *Biochim. Biophys. Acta* 223, 165–173
12 Mitchell, P. (1966) *Biol. Rev.* 41, 445–502

Biochimica et Biophysica Acta, 314 (1973) 320–327

BBA 46603

ENERGY TRANSFER IN PHOTOSYNTHESIS

KONRAD COLBOW*

Fachbereich Biologie, Universität Konstanz, Konstanz (Germany)

(Received March 14th, 1973)

SUMMARY

The results of recent spectroscopic measurements on chlorophyll *a* in bilayers and lipid vesicles stimulated a re-examination of energy transfer in photosynthesis. The Förster resonance transfer mechanism is believed to be applicable under reasonable assumptions despite recent criticism. The Förster parameter was newly determined to be $R_0 = 65$ Å; previous uncertainty due to unknown transition moment orientation can be avoided by assuming the black film dichroic result to be applicable in vivo. The effect due to the still incompletely known thylakoid structure and chlorophyll aggregation is discussed qualitatively. Agreement with experimental fluorescence lifetimes and quantum efficiencies may be obtained with a reasonable choice of parameters.

I. INTRODUCTION

Chlorophyll *a* and its auxiliary pigments absorb light energy and transfer 97% of it to a reagent center, where water is split (System II) and the reducing agent NADPH is produced (System I). In a dark reaction CO_2 is then incorporated into sugar. About 3% of the absorbed light is re-emitted as fluorescence. Emerson and Arnold's flashing light experiments have shown that there are about 2500 chlorophyll molecules per O_2 released, and there is evidence that 8 photons are required per O_2 released, which then implies that we have 300 chlorophyll *a* molecules per reaction center (50 for bacteria). A detailed and elementary discussion of this subject may be found elsewhere[1,2].

The decay time and yield of fluorescence depends either on the efficiency of energy uptake by the reaction center[3,4], or on the time required for light energy to reach the reaction center[2,5–7], or possibly on both. Bay and Pearlstein and Pearlstein[6,7] discussed the second possibility using the Förster[8,9] theory of energy transfer between adjacent pigment molecules by dipole–dipole resonance interaction. Using somewhat extreme values, Robinson[3] was critical of applying Förster's theory, which assumes negligible back transfer of excitation from acceptor to donor molecule. This will hold if the lifetime forthermal degradation is short compared to the Förster transfer time between nearest neighbors. At a two-dimesional chlorophyll *a* separation of 11 Å both times are comparable[3], and we are dealing with a boundary situation

* On sabbatical leave on an Alexander van Humboldt Fellowship from the Department of Physics, Simon Fraser University, Burnaby, B.C., Canada, where all inquiries are to be sent to.

where the application of Forster's theory (R^{-6} rate) and Perrin's theory (R^{-3} rate) are both doubtful[10]. Thus, it is rather important to calculate R_0 in Förster's theory[8] with the highest possible accuracy. The calculation was previously done from absorption and fluorescence data of chlorophyll *a* in ether[2,5,8–10]. *In vivo* data are difficult to estimate due to the presence of several pigments, and absorption band shifts due to interaction of pigment molecules with each other and with other molecules of the medium[11]. The present paper is motivated by four new developments: (1) Recent bilayer (black film) experiments[12,13] showed that the red transition moment of chlorophyll *a* makes an angle $\beta_R = 36.5°$ with the plane of the bilayer. It will be argued that the same is true *in vivo*, and the consequences of this assumption are investigated in detail. (2) Recent experiments by the author[14] determined the fluorescence and absorption parameters of chlorophyll *a* in lipid vesicles. This data should provide, in combination with the black film experiments[12,13], a better model system than ether solution spectra, for a new calculation of R_0 in Förster's theory. (3) Montroll[15] derived expressions for the mean number of steps the excitation takes in a random walk to reach the reaction center. This makes computer calculations[3,7] unnecessary and gives roughly the same answers. Equal jump time to each nearest neighbor was assumed. (4) Much recent work[16,17] indicates that chlorophyll *a* aggregation is important and may in fact account for most of the changes of *in vivo* spectra compared to solution spectra. This has an important effect on energy transfer to the reaction center.

II. THE MODEL

Many different models have been proposed for the structure of the chloroplast thylakoids[18–25]. We shall assume a simple fluid lipid bilayer model[22,23], in which the globular proteins have little influence on energy transfer between chlorophyll molecules. The latter are assumed to be in the lipid bilayer (Fig. 1), anchored at the membrane–water interface by the hydrophilic cyclopentane ring (V). Analogous to the black film dichroism results[12,13] we shall assume that the red transition moment makes an angle of $\beta = 36.5°$ with the membrane surface. The red transition moment lies along the diagonal of the conjugated porphyrin ring (I to III in Fig. 2). From blue dichroism in black films and the knowledge that the red and blue transition moments are perpendicular[26] it follows that the porphyrin head makes an angle $\gamma = 48°$ with the membrane surface[12,13]. We believe the same angular arrangement is present *in vivo*, since it provides the simplest explanation for the weak dichroism in all but the 695-nm absorption band[21,26]. We do not necessarily believe the bilayer model assumed (Fig. 1) to be the correct one. The difference between the assumed model and those advocated by Calvin[24] or Kreutz[21], is only important for the comparatively small transfer across the plane of the membrane, to be discussed in section VI. The major energy transfer to the reaction center is in either case a two-dimensional problem. The still disputed point is whether to believe a lipid thickness of 40 Å obtained from electron microscopy[23], or a 21-Å thickness obtained from X-ray scattering[21]. No use was made of the quantasomes[5,18,27] introduced by Park on the basis of electron microscopy; they may be artifacts[18].

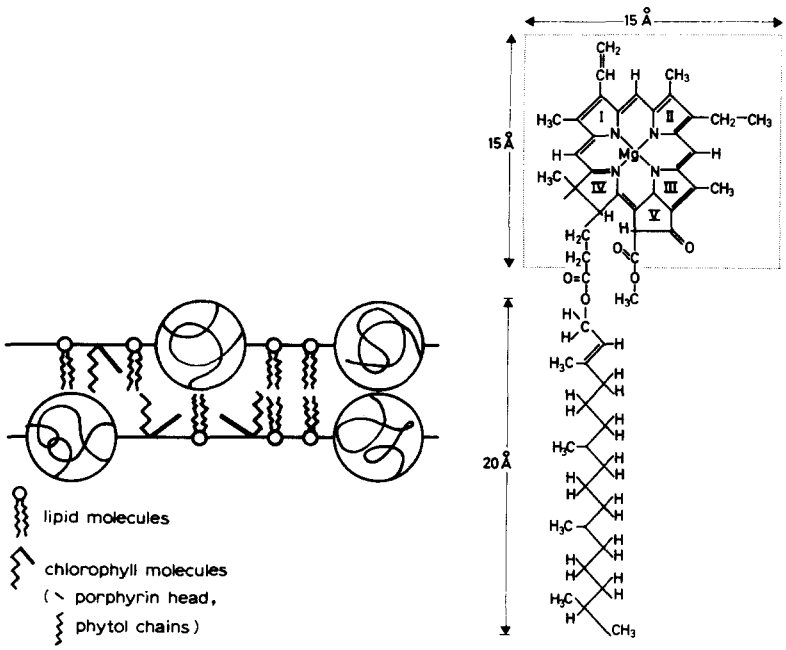

Fig. 1. Lipid bilayer model. According to Muelhethaler[23] the lipid molecules form a bilayer 40 Å thick. The coiled up spherical proteins (60 Å diameter) are immersed about 20 Å into the lipid. We have also shown chlorophyll molecules with their porphyrin head at an angle of 48° to the membrane surface and their phytol chains perpendicular to the surface.

Fig. 2. Structure of chlorophyll *a*. The molecule is believed to be anchored by the group V (cyclopentane ring) to the water–lipid interface; the red transition moment points from ring I to III and makes an angle of 36.5° with the membrane surface.

III. THE PAIRWISE ENERGY TRANSFER RATE (F'RSTER'S THEORY)

This pairwise energy transfer rate by dipole–dipole resonance interaction between two molecules distance R apart may be written in the form[8–10]

$$\frac{1}{\tau_J} = \frac{1}{\tau_0}\left(\frac{R_0}{R}\right)^6 \tag{1}$$

Here

$$R_0^6 = \frac{9K^2(\ln 10)^2 c\tau_0}{16\pi^4 n^2 N'^2 \nu_0^2} J\nu \tag{2}$$

Assuming a mirror image between red absorption and fluorescence band the overlap integral takes the form[8,9]

$$J_\nu = \int_0^\infty \varepsilon(\nu)\varepsilon(2\nu_0 - \nu)\,\mathrm{d}\nu \tag{3}$$

Here ε is the extinction coefficient ($l \cdot mole^{-1} \cdot cm^{-1}$) on a wave number scale (cm^{-1}), n the index of refraction, c the velocity of light, $N' = 6.023 \cdot 10^{20}$ molecules $\cdot$ mmole^{-1}, and ν_0 is the mean wave number of the absorption and fluorescence peak.

$$K^2 = (2\pi)^{-2} \iint d\psi \, d\psi' (\cos\phi_{ad} - 3\cos\phi_a \cos\phi_d)^2 \tag{4}$$

becomes an average over dipole directions for the energy acceptor (a) and donor (d), with ϕ_{ad} the angle between them and ϕ_a, ϕ_d the angle each one makes with the line connecting them. K^2 can vary between 0 and 4 and has the value 2/3 for a completely random arrangement[8,9]. Many expressions in the literature differ from Eqn 2 by a factor of π or 2π and are in our opinion in error (see also ref. 27). Förster obtained the value $R_0 = 80$ Å ($J_\nu = 2.1 \cdot 10^{12}$ cm$^3 \cdot$ mmole^{-2}) for chlorophyll *a* at low concentration in ethyl ether[8,9]. More recent estimates[2,5,10] use the shorter natural lifetime $\tau_0 = 15.2$ ns, and obtain $R_0 = 70$ Å under the assumption of three-dimensional random dipole directions[2,6,10].

Using the model outlined in Section II and Fig. 1, where the red transition moment is free to rotate, while maintaining an angle of β with the plane of the membrane we obtained for an average over dipole directions (Eqn 4)

$$K^2 = \sin^4\beta + \tfrac{5}{4}\cos^4\beta \tag{5}$$

Using the black film result[12,13] $\beta = 36.5°$ one finds $K^2 = 0.647$, which is quite close to the completely random value of 2/3. We shall neglect for the present, transfer between chlorophyll *a* molecules across the plane of the bilayer (see Section VI).

The overlap integral J_ν (Eqn 3) was re-evaluated using spectra of chlorophyll *a* in lipid vesicles recently obtained by the author[14]. For comparison the calculations were also performed on spectral data from chlorophyll *a* in ether and ethanol, where our data is in close agreement with previous work[14,29]. Let us assume a Gaussian line profile, which gives a good fit to the fluorescence and the red absorption band down to 0.1 of peak height. Thus

$$\varepsilon(\nu) = \varepsilon_m \exp\{-\tfrac{1}{2}\alpha^2(\nu - \nu_a)^2\} \tag{6}$$

and from Eqn 3

$$J_\nu = \varepsilon_m{}^2 (\sqrt{\pi}/\alpha) \exp\{-\alpha^2 \nu_s{}^2/4\} \tag{7}$$

where ε_m is the extinction at the absorption maximum ν_a (cm^{-1}), ν_s the Stoke shift, and $\alpha = (2 \ln 2)^{\frac{1}{2}}/\nu_{\frac{1}{2}}$. For the half width at half peak height $\nu_{\frac{1}{2}}$ the high energy side was taken for the fluorescence band and the low energy side for the absorption band. Both agree within 10% from each other and also from the slightly wider halfwidths on the low energy side in fluorescence and high energy side in absorption. The relevant values together with the calculated J_ν (Eqn 7) are given in Table I. R_0 (Eqn 2) was then calculated using an index of refraction for the lipid[6] of $n = 1.45$, a lifetime[10] $\tau_0 = 15.2$ ns and $K^2 = 0.647$.

IV. MEAN CHLOROPHYLL SPACING AND EXCITATION TRAPPING

Based on the dimensions of a quantasome, Bay and Pearlstein[5] used a mean chlorophyll *a* separation *in vivo* of 11 Å under the assumption of a two-dimensional

TABLE I

FLUORESCENCE AND ABSORPTION PARAMETERS, THE OVERLAP INTEGRAL J_ν (EQN 6), AND THE FÖRSTER ENERGY TRANSFER PARAMETER R_0 (EQN 2) FOR CHLOROPHYLL *a*

Parameter	*Ether*	*Ethanol*	*Lipid vesicle*
Absorption max., ν_a (cm^{-1})	15149	15056	14945
Fluorescence max., ν_f (cm^{-1})	14988	14872	14846
Stoke shift, ν_s (cm^{-1})	161	184	100
Halfwidth, $\nu_{\frac{1}{2}}$ (cm^{-1})	188	232	260
Extinction coefficient ε_m ($l \cdot mole^{-1} \cdot cm^{-1}$)	85100	69400	62000
J_ν (10^{12} $cm^3 \cdot mmole^{-2}$)	1.59	1.35	1.43
R_0 (Å)	66.0	64.4	65.1

arrangement and 17 Å in a three-dimensional arrangement. Neglecting for the moment chlorophyll aggregation effects, we would prefer a value of 15 ± 1 Å for the mean two-dimensional separation within one plane. This corresponds to an available surface area of 200 $Å^2$ to 250 $Å^2$ per porphyrin ring, which is in agreement with several estimates[30–32,21] and is consistent with chlorophyll making up 21% of the lipid-soluble fraction of thylakoid membranes[21,27]. The differences between 15 Å and 11 Å is important. Using 11 Å and $R_0 = 70$ Å one obtains (Eqn 1) a nearest neighbor transfer rate of $1/\tau_J = 4.4 \cdot 10^{12}$ s^{-1}, which is of the same magnitude as the vibrational relaxation rate ($3 \cdot 10^{12}$ s^{-1})[33]. Thus Robinson's criticism[3,10] of the application of Förster's theory is justified. However, with a mean spacing of 15 Å and $R_0 = 65.1$ Å (Table I) the nearest neighbor transfer rate is $0.44 \cdot 10^{12}$ s^{-1}, which is sufficiently below the vibrational relaxation rate to justify the application of Förster's theory. Now let us assume we have per reaction center N equally spaced chlorophyll *a* molecules in a plane; effects due to chlorophyll aggregation will be considered in the next section. Further we shall assume that the reaction center permanently traps and utilizes the excitation energy with high efficiency, once it arrives there. This may or may not be true[1–6,10,33]. Thus the fluorescence efficiency and decay time depend on the mean trapping time

$$\langle \tau_T \rangle = \langle n \rangle \tau_J \tag{8}$$

wher $\langle n \rangle$ is the mean number of steps before trapping in a random walk. This problem has been discussed in two dimensions for a square lattice by Pearlstein[7] and Robinson[3]; and Knox[34] has treated it for square and triangular lattices by direct machine inversion of the transfer matrix. More recently Montroll[15] has solved the problem in terms of an asymptotic series in $1/N$. For the special case of equal probability for a random walker to go to any nearest neighboring point on a given step, he finds for a square lattice

$$\langle n \rangle = \pi^{-1} N \ln N + 0.19506\, N \tag{9}$$

plus higher order terms which we shall neglect. In the region of interest Montroll's expression is in close agreement with machine computations. For example for $N = 324$,

a reasonable value for plants, we obtain $\langle n \rangle = 659$ steps from Eqn 9 compared to 670 steps from machine computation by Robinson[3]. For $N = 50$, a likely value for bacteria, the corresponding numbers are 72 and 74 steps, respectively.

Using $N = 300$ and a nearest neighbour transfer rate of $0.44 \cdot 10^{12}$ s^{-1}, the mean trapping time (Eqn 8) is $\langle \tau_T \rangle = 1.37$ ns, and the corresponding fluorescence efficiency $\phi = 100 \langle \tau_T \rangle / \tau_0 = 9\%$. These values are considerably larger than previous estimates[5] and closer to *in vivo* experimental values of fluorescence lifetimes, which range from 0.4 to 2 ns, and fluorescence efficiencies of 3 to 6%[1,5,33]. In fact the calculated values are somewhat large in view of the fact that the calculation assumes all traps open, a situation which corresponds to the minimum values of both $\langle \tau_T \rangle$ and ϕ.

V. THE EFFECT OF CHLOROPHYLL AGGREGATION

Let us now take into account that the chlorophyll molecules are not located on a lattice corresponding to the mean spacing. A proper treatment using the correct chlorophyll distribution, even if it were known, would seem too difficult mathematically. The red absorption band of chlorophyll *a in vivo* may be separated into at least three bands with maxima at 673, 683 and 695 nm[1,2,11,17,21,33]. There is strong evidence that this multiplicity of peaks is due to chlorophyll aggregation, rather than different interactions with lipids of proteins[1,17,21,33]. There is general agreement that the 683-band is due to a dimer[21,33] and the 695-nm band may be a stacked chlorophyll polymer[21,35]. Whether the 673-nm band is due to a different chlorophyll dimer[21], or represents the monomer[33] is an important unanswered question. The suggestion that the 673-nm band represents a dimer as well comes from the solution spectra shift to 663 nm in many solvents[29], which may then be taken to represent the monomer[21]. In general about 20% of the red absorption is in the 695-nm band; the ratio of 673-nm to 683-nm absorption may vary from 3:1 to 1:3 depending on plant and growing condition[11,17].

For simplicity let us now assume that all the chlorophyll is in dimer form. Placing 150 dimers per reaction center on a square lattice with twice 225 Å^2 area per dimer, one obtains a mean dimer spacing of 23.5 Å instead of the 15-Å monomer spacing (Section IV). The excitation requires on the average 268 steps to reach the trap (Eqn 9 with $N = 150$). The overlap integral (Eqn 7) should not change too much; thus if we use again $R_0 = 65.1$ Å and $\tau_0 = 15.2$ ns, we obtain a nearest neighbor transfer rate of $0.30 \cdot 10^{11}$ s^{-1}, and a mean trapping time of 9 ns (Eqn 8). This trapping time is too large by a factor of about 10, probably since the natural lifetime of chlorophyll *a* dimers is smaller than the monomer lifetime of 15.2 ns corresponding to a smaller fluorescence efficiency[33,36].

VI. ENERGY TRANSFER BETWEEN TWO LAYERS

The transfer of energy from one layer to the next nearest layer may be important since it might represent the possibility of energy transfer from System II to System I. If we take the bilayer model (Fig. 1) with a membrane thickness[23] of 40 Å, and assume the porphyrin center is on each side (15/2) sin 48° (Å) inside the membrane surface (Figs 1 and 2), then the effective thickness for energy transfer between two layers is $d = 29$ Å. On the basis of the thylakoid model by Kreutz[21] one finds

$d=76$ Å and from the model by Calvin[24] $d=162$ Å. The problem of the exact structure of the thylakoid membrane probably still needs further clarification.

The energy transfer rate between two layers by the Förster mechanism is

$$W_a = C \int_0^\infty \gamma\rho(\rho^2+d^2)^{-3}d\rho = C\gamma_a/4d^4 \tag{10}$$

where $C=2\pi\sigma\tau_0{}^{-1}R_0{}^6$ and $\sigma=$density of chlorophyll monomer or dimer per unit area, depending on the assumptions made regarding chlorophyll aggregation. ρ is the distance in the plane of the membrane. The angular factor γ is the K^2 given by Eqn 4, and

$$\gamma_a = \tfrac{2}{3}(\sin^2\beta+\tfrac{1}{2}\cos^2\beta)^2 \tag{11}$$

Taking[12,13] $\beta=36.5°$ for the angle the red transition moment makes with the plane of the membrane we find $\gamma_a=0.687$ compared to an angular factor of $\gamma_i=0.647$ for transfer within one plane and an average value of 2/3 for a three-dimensional random arrangement of chlorophylls. The ratio of across-plane to in-plane energy transfer is then

$$W_a/W_i = (\gamma_a/\gamma_i)(r_0/d)^4 \tag{12}$$

An upper limit for this ratio comes about from the assumption that all chlorophyll is in dimer form (Section V), corresponding to a mean dimer spacing of $r_0=23.5$ Å, and the smallest possible choice for the transfer plane separation of $d=29$ Å. In this case the ratio is 0.46 and the across-plane transfer rate is relatively large. However for $d=50$ Å across-plane transfer rate is already down to 5% of the in-plane transfer.

VII. CONCLUSION

We have followed through the assumption that the red transition moment of chlorophyll *a in vivo* makes an angle of 36.5° with the membrane surface, as observed[12,13] by dichroism in black lipid bilayers. This assumption is further strengthened by the weak red dichroism observed *in vivo*. Together with new spectroscopic measurements on chlorophyll *a* in lipid vesicles, this enabled us to calculate a more precise value (65 Å) for the Förster energy transfer parameter, which is in the range of previous estimates. Recent criticism of using the Förster theory is rejected on the basis of previous choices for the chlorophyll nearest neighbor distance. Aggregation effects will further improve the conditions for applying Förster's theory to energy transfer *in vivo*. With a reasonable choice of parameters one may fit the fluorescence lifetime and efficiency data *in vivo*. However, a detailed comparison with experiments is difficult due to present uncertainty about thylakoid structure and chlorophyll aggregation.

ACKNOWLEDGEMENTS

The author would like to thank Professors L. N. M. Duysens, J. C. Goedheer, W. Kreutz and P. Läuger for useful discussions. The award of an Alexander von Humboldt Fellowship is gratefully acknowledged.

REFERENCES

1 Rabinowitch, E. and Govindjee (1969) in *Photosynthesis*, Wiley, New York
2 Duysens, L. N. M. (1964) *Prog. Biophys. Mol. Biol.*, 14, 1–104
3 Robinson, G. W. (1967) *Brookhaven Natl. Lab. Symp.* 19, 16–48
4 Paillotin, G. (1972) *J. Theor. Biol.* 36, 223–235
5 Bay, Z. and Pearlstein, R. M. (1963) *Proc. Natl. Acad. Sci. U.S.* 50, 1071–1078
6 Pearlstein, R. M. (1964) *Proc. Natl. Acad. Sci. U.S.* 52, 824–830
7 Pearlstein, R. M. (1967) *Brookhaven Natl. Symp.* 19, 8–15
8 Förster, T. (1947) *Z. Naturforsch.* 2b, 174–182
9 Förster, T. (1951) in *Fluorescenz Organischer Verbindungen*, pp. 176–177 Vandenhoeck and Ruprecht, Göttingen
10 Hoch, G. and Knox, R. S. (1968) in *Photophysiology* (Giese, A. C., ed.), Vol. 3, pp. 225–251, Academic Press, New York
11 French, C. S. (1960) in *Handbuch der Pflanzenphysiologie* (Ruhland, W., ed.), Vol. 5, pp. 252–297, Springer, Berlin
12 Cherry, R. J., Hsu, K. and Chapman, D. (1972) *Biochim.Biophys. Acta* 267, 512–522
13 Steinemann, A., Stark, G. and Läuger, P. (1972) *J. Membrane Biol.* 9, 177–194
14 Colbow, K. (1973) *Biochim. Biophys. Acta*, 318, 4–9
15 Montroll, E. W. (1969) *J. Math. Phys.* 10, 753–765
16 Katz, J. J. (1972) *Adv. Food. Res. Suppl.* 3, 103–122
17 Brown, J. S. (1972) *Annu. Rev. Plant Physiol.* 23, 73–86
18 Branton, D. (1968) in *Photophysiology* (Giese, A. C., ed.), Vol. 3, pp. 197–224, Academic Press, New York
19 Lucy, J. A. (1968) in *Biological Membranes* (Chapman, D., ed.), pp. 233–288, Academic Press, New York
20 Leslie, R. B. (1968) in *Biological Membranes* (Chapman, D., ed.), pp. 289–346, Academic Press, New York
21 Kreutz, W. (1970) *Adv. Bot. Res.* 3, 53–169
22 Singer, S. J. and Nicolson, G. L. (1972) *Science* 175, 720–731
23 Muehlethaler, K. (1969) in *Biochemistry of Chloroplasts* (Goodwin, T. W., ed.), Vol. 1, pp. 49–64, Academic Press, New York
24 Calvin, M. (1959) *Brookhaven Symp. Biol.* 11, 160–168
25 Robertson, J. D. 1960) *Prog. Biophys. Biophys. Chem.* 10, 343–418
26 Goedheer, J. C. (1966) in *The Chlorophylls* (Vernon, L. P. and Seely, G. R., eds), pp. 147–184 Academic Press, New York
27 Park, R. B. (1966) in *The Chlorophylls* (Vernon, L. P. and Seely, G. R., eds), pp. 283–211, Academic Press, New York
28 Drexhage, K. H., Zwick, M. M. and Kuhn, H. (1963) *Z. Electrochem., Ber. Bunsenges. Physik. Chem.* 67, 62–67
29 Seely, G. R. and Jensen, R. G. (1965) *Spectrochim. Acta* 21, 1835–1845
30 Goedheer, J. C. (1957) Thesis, Utrecht
31 Thomas, J. B., Minnaert, K. and Elbers, P. F. (1955) *Acta Bot. Neerl.* 5, 315–321
32 Wolken, J. J. and Schwertz, F. A. (1953) *J. Gen. Physiol.* 37, 111–119
33 Clayton, R. K. (1965) in *Molecular Physics in Photosynthesis*, Blaisdell, New York
34 Knox, R. S. (1968) *J. Theor. Biol.* 21, 244–259
35 McRae, E. G. and Kasha, M. (1964) in *Physical Processes in Radiation Biology* (Augenstein, G. L., Maeson, R. and Rosenberg, B., eds), pp. 23–42, Academic Press, New York
36 Lavorel, J. (1957) *J. Phys. Chem.* 61, 1600–1605

Biochimica et Biophysica Acta, 314 (1973) 328–339

BBA 46594

THE SITE OF KCN INHIBITION IN THE PHOTOSYNTHETIC ELECTRON TRANSPORT PATHWAY

S. IZAWA*, R. KRAAYENHOF**, E. K. RUUGE*** and D. DEVAULT

Johnson Research Foundation, School of Medicine, University of Pennsylvania, Philadelphia, Pa. 19174 (U.S.A.)

(Received March 19th, 1973)

SUMMARY

Treatment of chloroplasts with high concentrations of KCN inhibits reactions which involve Photosystem I (*e.g.* electron transport from water or diaminodurene to methylviologen), but not those assumed to by-pass Photosystem I (*e.g.* electron transport from water to quinonediimides). The spectrophotometric experiments described in this paper showed that KCN inhibits the oxidation of cytochrome *f* by far-red light without blocking its reduction by red light. Both optical and EPR experiments indicated that KCN does not inhibit the photooxidation of P700 but markedly slows down the subsequent dark decay (reduction). Reduction of P700 by Photosystem II is prevented by KCN. It is concluded that KCN blocks electron transfer between cytochrome *f* and P700, *i.e.* the reaction step which is believed to be mediated by plastocyanin. In KCN-poisoned chloroplasts the slow dark reduction of P700 following photooxidation is greatly accelerated by reduced 2,6-dichlorophenolindophenol or by reduced *N*-methylphenazonium methosulfate (PMS), but not by diaminodurene. It appears that the reduced indophenol dye and reduced PMS are capable of donating electrons directly to P700, at least partially by-passing the KCN block.

INTRODUCTION

It has long been recognized that high concentrations of KCN inhibit the Hill reaction in isolated chloroplasts[1]. Trebst[2] found that salicylaldoxime and KCN inhibit not only the Hill reaction but also Photosystem I-dependent photophosphorylation, and suggested that a blocking of electron transport may have occurred rather close to Photosystem I. However, the data were also explainable by assuming that

Abbreviations: DCMU, 3-(3,4-dichlorophenyl)-1,1-dimethylurea; DCIP, 2,6-dichlorophenolindophenol; HEPES, *N*-2-hydroxyethylpiperazine-*N'*-2-ethanesulfonic acid; PMS, *N*-methylphenazonium methosulfate.

* Present address: Department of Botany and Plant Pathology, Michigan State University, East Lansing, Mich. 48823, U.S.A. (mailing address).

** Present address: Laboratory of Biochemistry, B. C. P. Jansen Institute, University of Amsterdam, Plantage Muidergracht 12, Amsterdam, The Netherlands.

*** Present address: Department of Biophysics, School of Physics, Moscow State University, Moscow 117234, U.S.S.R.

those compounds induced a Photosystem II inhibition and uncoupling simultaneously. This seems to have been indeed the case with salicylaldoxime, since Katoh and San Pietro[3] later demonstrated that isolated plastocyanin does not react with salicylaldoxime at any significant rate. They also presented evidence that salicylaldoxime inhibition probably takes place close to Photosystem II. The site of salicylaldoxime inhibition in the electron transport chain has in fact been located before cytochrome *f* (refs 4–6).

It has been shown very recently, however, that under proper conditions KCN does block Photosystem I specifically[7]. Reactions which involve Photosystem I such as the transfer of electrons from water to methylviologen or from diaminodurene to methylviologen, and diaminodurene-mediated cyclic photophosphorylation are almost completely inhibited, while reactions which are assumed to largely by-pass Photosystem I such as the transfer of electrons from water to lipid-soluble oxidants (*e.g.* oxidized phenylenediamines[8]) are scarcely affected. Furthermore, isolated plastocyanin was shown to react with KCN quite rapidly under the conditions required for effective KCN treatment of chloroplasts, thus strongly implicating plastocyanin as the site of inhibition[7].

This paper deals primarily with location of the site of KCN inhibition in the electron transport chain. We conclude that KCN interferes with electron transfer between cytochrome *f* and P700, that is the reaction step which is believed by most workers to involve plastocyanin.

MATERIALS AND METHODS

Preparation and KCN treatment of chloroplasts

Chloroplasts (unfragmented, naked lamellae) were prepared from commercial spinach (*Spinacia oleracea* L.) as described before[8] and finally suspended in a medium containing 0.1 M sucrose, 10 mM *N*-2-hydroxyethylpiperazine-*N'*-2-ethanesulfonic acid (HEPES)–NaOH buffer (pH 7.4) and 2 mM $MgCl_2$ (chlorophyll, approx. 2 mg/ml). KCN treatment of chloroplasts was carried out as follows: 3 ml of the above chloroplast suspension were transferred to an ice-chilled test tube containing a mixture of 1 ml each of 0.15 M KCN and 0.3 M Tricine (acid) and 25 μl of 10 mM potassium ferricyanide. The final pH of the mixture was 7.8–7.9. The trace of ferricyanide included was not an essential ingredient but it accelerated the development of KCN inhibition. The test tube was sealed and allowed to stand at 0 °C in the dark. After 60–90 min incubation the mixture was exposed to room light, and the treatment was terminated by diluting and lowering the pH of the mixture with 10 ml of a medium containing 0.1 M sucrose, 30 mM HEPES–NaOH buffer (pH 7.2) and 2 mM $MgCl_2$. This procedure was effective in preventing the development of a secondary effect of KCN (Photosystem II inhibition) which would otherwise become appreciable after 90 min incubation. At no stage was it necessary to add fresh KCN to compensate for dilution since the KCN inhibition is essentially irreversible.

Measurements

Oxidation–reduction of cytochrome *f* (cytochrome c_{554}) and P700 was observed with a Hitachi–Perkin Elmer dual-wavelength spectrophotometer (Model 356). Reactions were run in a standard 1-cm cuvette thermostated at 20 °C. The actinic light

was provided by a pair of 100-W quartz–iodine lamps. Monochromatic red light (660 nm; half-band width 10 nm) and far-red light (714 nm; half-band width, 10 nm) were obtained by means of interference filters. The oxidation–reduction of cytochrome *f* was followed by observing the absorbance change of the α-band at 554 nm (reference wavelength, 540 or 565 nm). The oxidation–reduction of P700 was observed at 701 nm (reference 730 nm). The P700 changes were also observed by following the EPR signal (signal I; $g=2.0025$)[9,10] with a Varian E4 EPR spectrometer routinely operated at a microwave power of 5 mW. The peak-to-peak modulation amplitude used was 4 G for field scans and 8 G for kinetic experiments. In the latter experiments, changes in the height of the low-field derivative peak were followed with a time constant of 0.5 to 0.03 s. The deflections recorded were 1/5 to 1/4 of the full scale.

RESULTS

The effect of KCN on oxidation–reduction of cytochrome f

The responses of cytochrome *f* to red (660 nm) and far-red (714 nm) light in KCN-treated chloroplasts were compared with those in 3-(3,4-dichlorophenyl)-1,1-dimethylurea (DCMU)-poisoned chloroplasts (Fig. 1). The electron acceptor used was methylviologen. In these chloroplasts the Hill reaction activity with methylviologen was inhibited by more than 90%. The top trace of Fig. 1A represents the familiar pattern of cytochrome *f* oxidation–reduction in untreated (control) chloroplasts which has been documented in detail by Avron and Chance[11]. The middle trace of Fig. 1A clearly shows that KCN severely inhibited the oxidation of cytochrome *f* by 714-nm light. However, once the cytochrome was photooxidized at a diminished rate, it could be readily reduced by 660-nm light, suggesting that the pathway of electrons from water to cytochrome *f* was not blocked. In sharp contrast, DCMU stimulated the oxidation of cytochrome *f* by 714-nm light, as one would expect from blocking of the flow of electrons from Photosystem II (which is weakly activated by 714-nm light). Similarly, 660-nm light, now largely acting as Photosystem I light, oxidized cytochrome *f* instead of reducing it (Fig. 1A, bottom trace). An impeded oxidation of cytochrome *f* in KCN-treated chloroplasts was also clearly observed in a series of experiments given in Fig. 1B in which the effect of 714-nm light was examined in the presence of a weak 660-nm background light. Fig. 1C shows light-*minus*-dark difference spectra obtained under the conditions of Fig. 1A. There was no evidence that any chloroplast component other than cytochrome *f* was contributing to the spectra, except for the tail end of the 518-nm shift or/and the "570-nm shift"[12,13].

Experiments were also conducted using chloroplasts in which the Hill reaction activity with methylviologen was completely inhibited by a prolonged KCN treatment (2 h). In these experiments the reference wavelength was chosen at 565 nm to minimize the influence of the 518-nm shift. The mild reductant ascorbate (5 mM) was included in the reaction mixture so as to ensure the reduced state of cytochrome *f* before illumination, and DCMU to block Photosystem II and provide the optimal condition for observing the photooxidation of cytochrome *f*. The effectiveness of ascorbate was evident from the experiments with untreated chloroplasts shown by the top row traces of Fig. 2. The traces depict that the very slow reduction process (due to exhaustion of electron pools) of cytochrome *f* after oxidation by 714-nm light was markedly accelerated by the presence of ascorbate. Clearly, however, the donation of

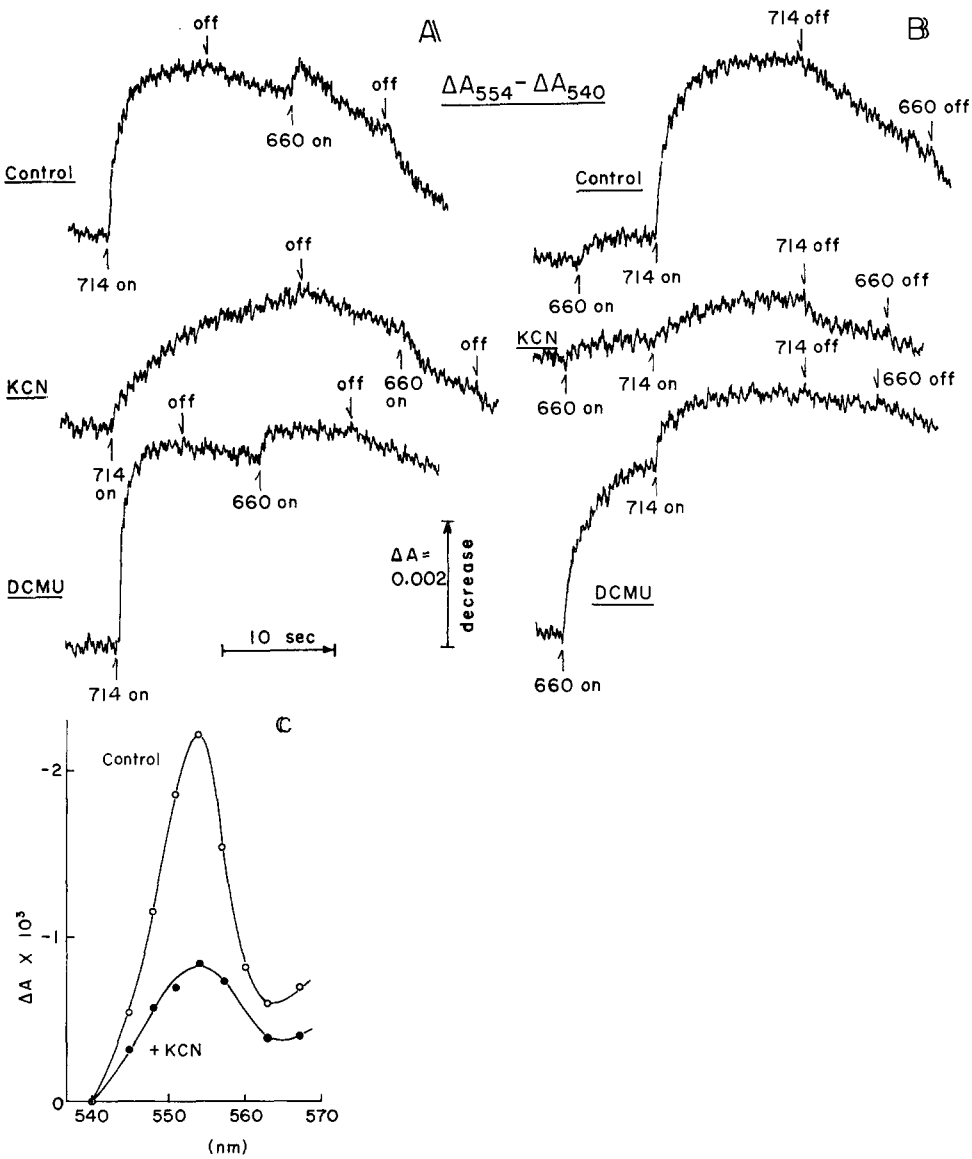

Fig. 1. Inhibition of cytochrome *f* oxidation by KCN treatment as contrasted with the inhibition of cytochrome *f* reduction by DCMU. The reaction mixtures (2 ml) contained 0.1 M sucrose, 40 mM Tricine–NaOH buffer (pH 7.8), 2 mM $MgCl_2$, 10 μM methylviologen (MV) and, if used, 1 μM DCMU. The concentration of chlorophyll was 62 μg/ml in the experiments of Fig. 1A or 75 μg/ml in Fig. 1B. The intensities of actinic light in kergs·s^{-1}·cm^{-2} were: (A) 12 (660 nm) and 8 (714 nm); (B) 2 (660 nm) and 8 (714 nm). The light-*minus*-dark spectra of C were obtained under the conditions of A. For KCN treatment of chloroplasts, see Methods.

electrons from ascorbate was still far too slow to counterbalance the withdrawal of electrons from cytochrome *f* by the 714-nm light. In KCN-treated chloroplasts, no trace of cytochrome *f* photooxidation was observed regardless of the presence or

absence of ascorbate and DCMU (Fig. 2, middle row traces). Yet in the same chloroplasts the photoreduction of cytochrome *f* was clearly observed when the cytochrome had been partially oxidized beforehand chemically with the lipid-soluble oxidant duroquinonediimide (oxidized diaminodurene), indicating that the pathway of electrons from water to cytochrome *f* was still open (Fig. 2, bottom traces). A slight photoreduction of cytochrome *f* was also detected in the presence of ferricyanide (0.4 mM) but only 3–4 min after the addition of ferricyanide. Apparently this hydrophilic oxidant does not react with cytochrome *f in situ* as readily as does oxidized diaminodurene.

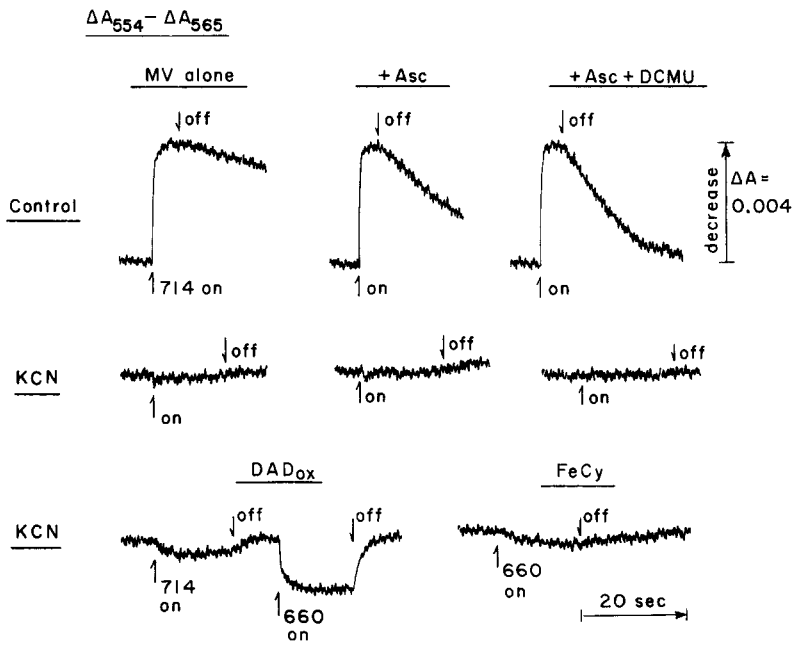

Fig. 2. Complete inhibition of cytochrome *f* oxidation by prolonged (2 h) KCN treatment of chloroplasts. The basic composition of reaction mixtures was as in Fig. 1. Oxidised diaminodurene (duroquinonediimide; final 0.4 mM) was prepared immediately before the reaction by mixing 0.8 μmole of diaminodurene and excess potassium ferricyanide (2.4 μmoles) in the buffered reaction mixture (2 ml). When ferricyanide was used alone, the concentration was 0.4 mM. The chlorophyll concentration was 80 μg/ml. The intensities of actinic light (red and far-red) were as in Fig. 1A. The light-*minus*-dark difference spectra of these changes in the 540–570-nm region confirmed that they were primarily due to cytochrome *f* changes. MV, methylviologen; Ass, ascorbate; DAD_{ox}, oxidised diaminodurene.

The effect of KCN on oxidation–reduction of P700

The effect of KCN treatment of chloroplasts on P700 was first examined spectrophotometrically by observing the absorbance changes at 701 nm (reference 730 nm) after flashes of 660-nm light (Fig. 3A). In control chloroplasts, no P700 shift remained when the fluorescence caused by the flashes had disappeared (top trace), indicating that photooxidized P700 was re-reduced as soon as the light was shut off or, more likely, it stayed reduced during the 660-nm flashes which strongly activate Photosystem II as well as Photosystem I (see also Fig. 4). In KCN-treated chloroplasts,

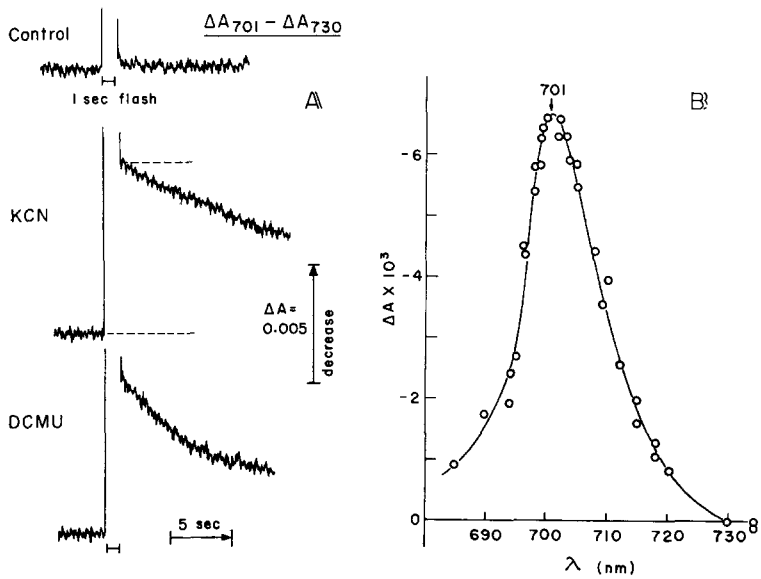

Fig. 3. Inhibition of P700 reduction by KCN treatment and by DCMU as observed spectrophotometrically by the dark decay of P700 after flashes. The basic composition of reaction mixtures was as in Fig. 1A. The chlorophyll concentration was 52 μg/ml. The intensity of actinic light (660 nm) was 24 kergs·sec^{-1}·cm^{-2}. The photomultiplier was guarded with a Corning CS2-64 filter and Kodak Wratten filters No. 36 and No. 70. The large signals observed during flashes were due to chlorophyll fluorescence.

however, a slow process of dark reduction of P700 was clearly observed after the flashes (Fig. 3A, middle trace). The decay kinetics were indeed so slow that there was practically no need for extrapolating the trace to estimate the oxidation level of P700 achieved in the light. (A typical light-*minus*-dark difference spectrum thus obtained is given in Fig. 3B.) Very similar results were obtained with DCMU-poisoned chloroplasts (Fig. 3A, bottom trace). Thus, viewing from P700, there is no clear distinction between the effects of KCN and DCMU: both inhibitors block the pathway of electrons from Photosystem II to P700.

The inhibition of P700 reduction by KCN was also confirmed by following the light-induced EPR signal (Signal I)[9,10] which originates from the oxidized form of P700 (Fig. 4). The "push–pull" effect of red and far-red light on P700 was very clearly observed in control chloroplasts (Fig. 4A, top row traces). This two-light effect, which is very similar to that on cytochrome *f*, was first demonstrated by Kok and Beinert[14] and was confirmed recently by Bochman *et al.*[15]. Both KCN and DCMU abolished this effect. The red light was no longer able to reduce P700; instead, it acted simply as Photosystem I light, always causing an oxidation of P700. Again a slowed-down process of reduction of P700 was evident (Fig. 4A, middle and bottom traces).

Thus, comparing the effects of KCN and DCMU on cytochrome *f* with their effects on P700, an unambiguous picture emerges: DCMU blocks electron transport at a point that precedes both cytochrome *f* and P700 (as is well-known), whereas KCN interferes with the transfer of electrons from cytochrome *f* to P700.

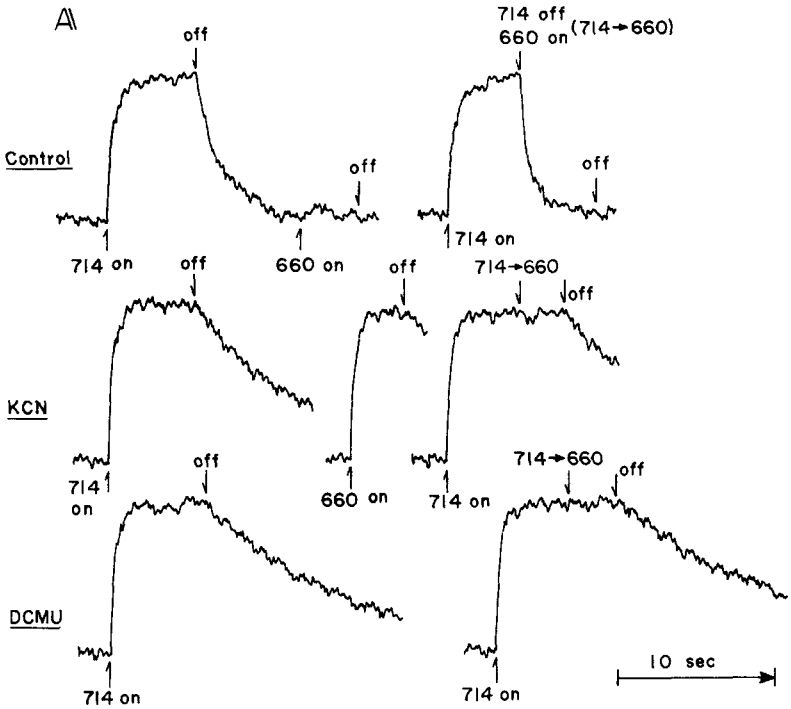
A
Control
KCN
DCMU
off
714 off
660 on (714→660)
714 on
660 on
714→660
10 sec

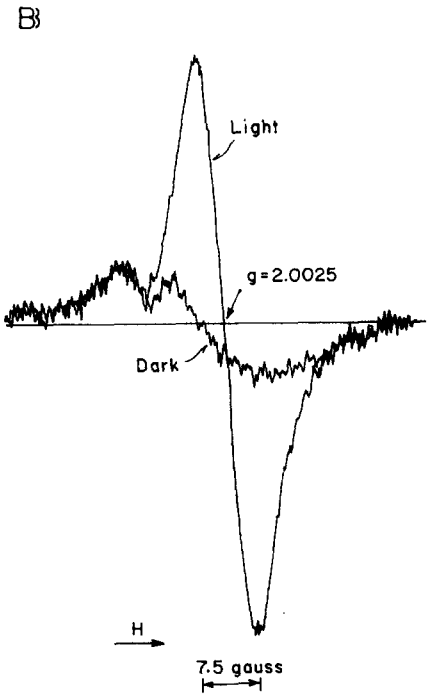
B
Light
g=2.0025
Dark
H
7.5 gauss

Accessibility of P700 to artificial electron donors in KCN-treated chloroplasts

In order to further differentiate the site of KCN inhibition from the known site of DCMU inhibition, the behavior of P700 (as EPR signal) in KCN-treated chloroplasts was compared with that in DCMU-blocked chloroplasts in the presence of various artificial electron donors. It should be noted here that in these "inhibited" chloroplasts Photosystem II is functionally disconnected from Photosystem I, and therefore the effect of light on P700 is always in the direction of oxidation.

Fig. 5A represents experiments with relatively weak far-red light. When DCMU blocked the electron transport chain near Photosystem II, P700 was still easily accessible, through the rest of the chain, to diaminodurene, reduced 2,6-dichlorophenolindophenol (DCIP) and reduced *N*-methylphenazonium methosulfate (PMS) (high or low concentrations). This is suggested by the fact that in the presence of any of these reductants the actinic light failed to oxidize P700. In sharp contrast, when KCN blocked the chain near Photosystem I, only high concentrations of PMS (0.2 mM; partly reduced with 0.1 mM ascorbate) were able to keep P700 completely reduced in the light. Qualitatively, these observations are quite consistent with the fact that DCMU inhibits none of the reactions supported by these reductants, while KCN inhibits all of the reactions except the cyclic photophosphorylation supported by high concentrations of PMS[7] (see also inhibition data cited in Fig. 5A). Ascorbate, when given alone (5 mM) had virtually no access to P700 when the electron transport chain was blocked by either of these inhibitors.

Fig. 5B depicts an independent series of experiments with a different batch of chloroplasts, in which a much higher light intensity and a faster instrumental time constant (resolution, approx. 0.1s) were employed. It can be seen in DCMU experiments that the donation of electrons from reduced DCIP was no longer able to keep pace with an increased rate of P700 photooxidation. This is clearly a reflection of the fact that reduced DCIP is a much poorer donor compared with diaminodurene and (reduced) PMS. In KCN-treated chloroplasts a full photooxidation of P700 was now achieved even in the presence of diaminodurene or reduced DCIP. Only high concentrations of partially reduced PMS continued to prevent the photooxidation of P700. However, the kinetics of the dark reduction of P700 by reduced DCIP (dark decay) in KCN-treated chloroplasts were relatively fast ($t_{1/2} \leqslant 0.1$ s), in line with the fact that the transfer of electrons from reduced DCIP to methyviologen contains an appreciable portion which is insensitive to KCN[2,7]. (In the chloroplast preparations utilized in these studies the control and KCN-inhibited rates of the reduced DCIP $\rightarrow$methylviologen reaction were typically 400 and 150 μequiv $\cdot h^{-1} \cdot mg^{-1}$ chlorophyll, respectively.)

Fig. 4. (A) Effects of KCN treatment and DCMU on the light-induced oxidation–reduction of P700 as observed by the EPR signal (Signal I). The height of the low-field peak of the first derivative EPR spectrum of oxidized P700 (Fig. 4B) was followed with a time constant of 0.5 s. The upward deflections (appearance of signal) indicate the oxidation of P700 and the downward deflections (disappearance of signal) indicate reduction. The peak-to-peak modulation amplitude used was 8 G for kinetics or 4 G for spectrum. The microwave power was 5 mW. The reaction mixture (0.5 ml) in a flat quartz sample cell (thickness 0.25 mm) contained 0.1 M sucrose, 50 mM HEPES–NaOH buffer (pH 7.6), 2 mM $MgCl_2$, 10 μM methylviologen and, if used, 2 μM DCMU. The chlorophyll concentration was 500 μg/ml. The intensities of red (660-nm) and far-red (714-nm) light were 26 and 12 kergs $\cdot s^{-1} \cdot cm^{-2}$, respectively. MV, methylviologen.

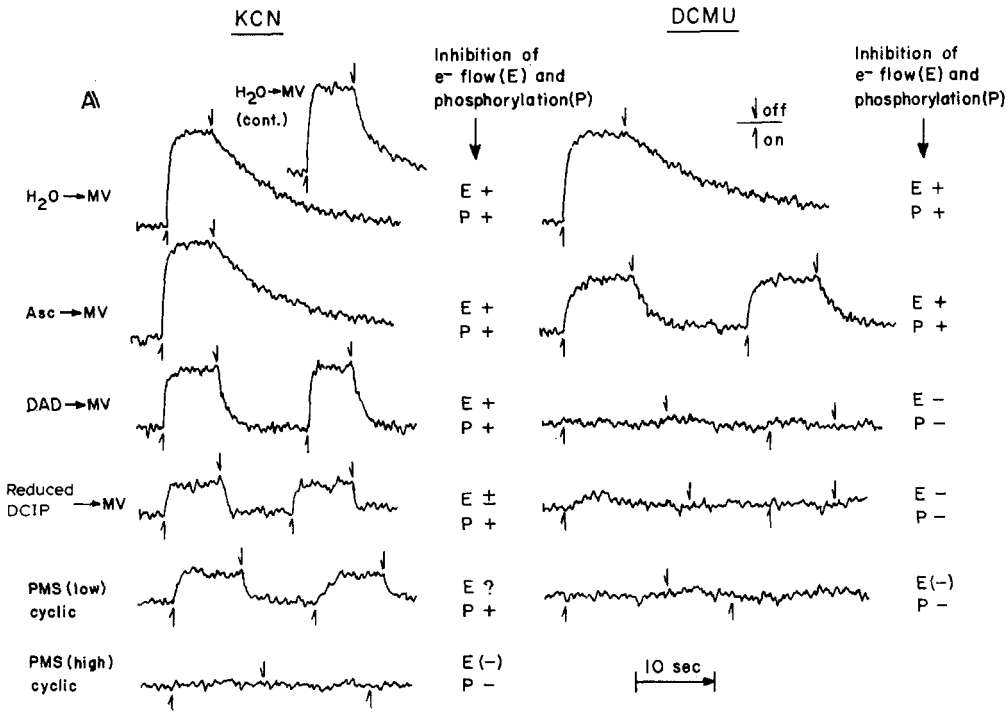
KCN
DCMU
A
Inhibition of e⁻ flow (E) and phosphorylation (P)
Inhibition of e⁻ flow (E) and phosphorylation (P)
H2O→MV (cont.)
off
on
H2O→MV
Asc→MV
DAD→MV
Reduced DCIP →MV
PMS (low) cyclic
PMS (high) cyclic
E + P +
E + P +
E + P +
E ± P +
E ? P +
E (−) P −
E + P +
E + P +
E − P −
E − P −
E(−) P −
10 sec

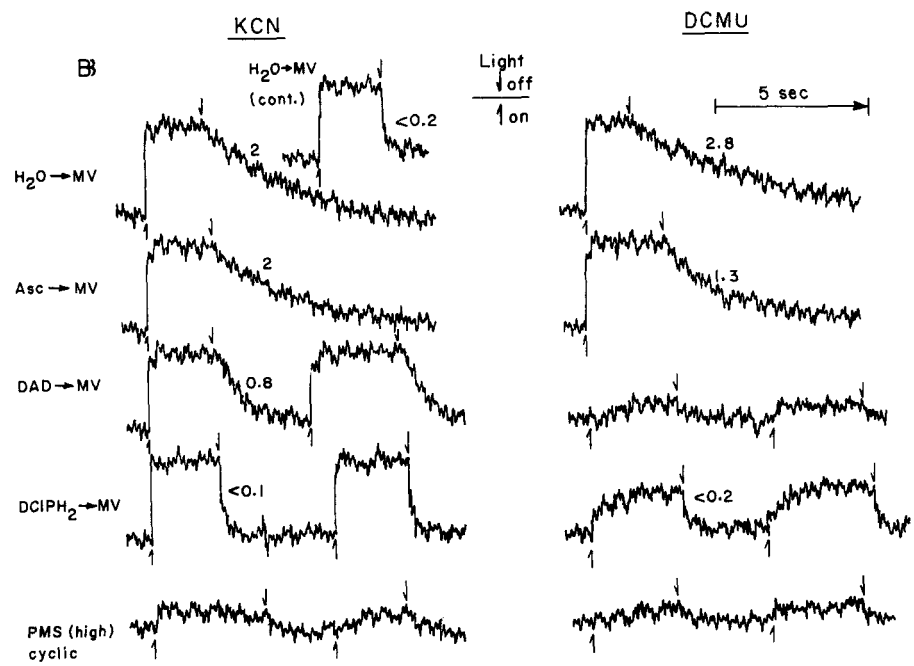
KCN
DCMU
B
H2O→MV (cont.)
Light
off
on
5 sec
H2O→MV
Asc→MV
DAD→MV
DCIPH2→MV
PMS (high) cyclic
2
<0.2
2
0.8
<0.1
2.8
1.3
<0.2

DISCUSSION

Plastocyanin as the site of KCN inhibition

In this paper we have presented spectroscopic evidence that KCN blocks the transfer of electrons from cytochrome *f* to P700. This location of the KCN inhibition site is in harmony with the inhibition data previously obtained for various partial reactions[7]. The fact that KCN inhibition occurs closer to P700 than does DCMU inhibition has also been confirmed by the experiments with artificial electron donors described in the preceding section. As for the identity of the target for the KCN inhibition, isolated plastocyanin has already been shown to react with KCN quite rapidly under the conditions required for electron transport inhibition[7]. Katoh's dialysis experiment suggests that KCN may remove copper from plastocyanin[16]. No reaction between isolated cytochrome *f* and KCN has been detected[7]. These observations, taken together with the various lines of evidence which indicate the involvement of plastocyanin in electron transfer between cytochrome *f* and P700 (refs 17–21), lead us to the following conclusion. The KCN inhibition of chloroplast electron transport arises primarily from a blocking of electron transfer between cytochrome *f* and P700, and this blocking is due to an inactivation of plastocyanin involved therein. Conversely, it could be said that our observations speak strongly in favor of the view which places plastocyanin between cytochrome *f* and P700, rather than the view advanced by Knaff and Arnon[22] which places plastocyanin before cytochrome *f*.

The inhibitors of chloroplast reactions which have so far been established to block the entry of electrons to Photosystem I are very few: an antibody to plastocyanin[23], polycations[24,25] and the cyanide dealt with here. All of these agents appear to react specifically or primarily with plastocyanin *in situ* but all under limited conditions: in extensively sonicated chloroplasts (antibody), in the absence of salts (polycations), or after 60 min preincubation (KCN). For studying reactions that involve phosphorylation or require membrane integrity, KCN seems to have advantage over the other two in that it is applicable to well coupled chloroplasts without frag-

---

Fig. 5. Effects of KCN treatment and DCMU on the oxidation–reduction of P700 in the presence of various artificial electron donors (EPR experiments). The upward deflections (appearance of signal) indicate the oxidation of P700 and the downward deflections (disappearance) indicate reduction. The basic composition of reaction mixtures was the same as in Fig. 4 except for the presence of various reductants. The concentration of reductants were: ascorbate (in the ascorbate →methylviologen system) 5 mM; diaminodurene, 0.2 mM (with 5 mM ascorbate); reduced DCIP, 0.24 mM (with 5 mM ascorbate), low PMS, 10 μM (with 10 μM ascorbate) and high PMS, 0.2 mM (with 0.1 mM ascorbate). In A the inhibition data for electron transport (E) and phosphorylation (P) are from ref. 7 except for the ascorbate→methylviologen system which are from unpublished data of one of the authors (S.I.). The + sign indicates strong inhibition; −, no or little effect; ±, partial inhibition. The signs in parentheses for electron transport are deductions from phosphorylation data. In Fig. 5A the chlorophyll concentration was 520 μg/ml. The actinic light used was 714-nm light (12 kergs·s^{-1}·cm^{-2}). Other assay conditions were as in Fig. 4. B represents a series of experiments conducted separately from those of A using a different batch of chloroplast preparation. The compositions of reaction mixtures were as in A except for the chlorophyll concentration which was 500 μg/ml. The actinic light used was relatively strong broad-band red light (640–700 nm; 180 kergs·s^{-1}·cm^{-2}). In these experiments the changes in signal height were followed with a time constant of 30 ms. The figures, 0.2, 2, 2.8, *etc.*, represent approximate half-times (s) of dark decay (P700 reduction). In both A and B the top trace labelled "cont." is for control (uninhibited) chloroplasts. MV, methylviologen; Asc, ascorbate; DAD, diaminodurene.

menting or exposing them to unfavorable ionic environment. There has been no indication of KCN affecting the mechanism of phosphorylation in any way. In fact, KCN inhibition has already been successfully applied in attempts to resolve phosphorylation sites[7], and also in a membrane-probe study designed to assess the relative energy output from various segments of the electron transport chain[26].

Interpretation of KCN-resistant Photosystem I reactions

The phosphorylation reaction associated with the transfer of electrons from reduced DCIP to methylviologen is abolished by KCN, but the electron transport itself is only partially inhibited[7]. The EPR experiments of Figs 5A and 5B revealed that KCN in fact does not completely block the pathway of electrons from reduced DCIP to P700, suggesting that a part of electron donation from reduced DCIP takes place directly at P700. The implication seems clear: the electrons entering the transport chain at P700 do not support phosphorylation. Only that portion of electrons which enters the chain at a point that precedes the KCN-sensitive site (plastocyanin) supports phosphorylation, presumably because this point also precedes a site of phosphorylation associated with the main pathway of electron transport (*cf.* refs 12 and 27). This interpretation also offers an explanation to the well-known but poorly understood fact that the phosphorylation associated with reduced DCIP reactions often appears to be totally unrelated to the observed electron flux[28].

Cyclic photophosphorylation catalyzed by PMS represents a unique case. It is almost as sensitive to KCN as is the diaminodurene-mediated system when catalyzed by 10 μM PMS, but becomes highly insensitive when the PMS concentration is raised to 0.2 mM (ref. 7). The EPR experiments of Figs 5A and 5B suggest that P700 may be easily accessible to the electrons from high concentrations of reduced PMS even when the electron transfer between cytochrome *f* and P700 is blocked by KCN. This finding is reminiscent of the observations of several workers[29–31] that at least in some chloroplast preparations (long-aged chloroplasts or detergent-prepared particles) P700 can accept electrons from reduced PMS (>30 μM) directly and very rapidly. These facts may seem to suggest that in the PMS cyclic system the phosphorylation reaction can be supported by the electrons entering the transport chain at P700. However, Fork and Murata[32] clearly showed that in chloroplast fragments the dark reduction of P700 by reduced PMS was much more efficient when the native state of the linkage between P700 and cytochrome *f* was partially preserved than when it was disrupted by detergents. Thus, in unfragmented chloroplasts, quite possibly a large portion of electrons from (photo-)reduced PMS may enter the main transport chain well before the plastocyanin–P700 region, and it may be this cyclic electron flow that supports phosphorylation. There might not be any important difference between this PMS cycle and the cycle mediated by diaminodurene. The fact that high concentrations of PMS relieve KCN inhibition of cyclic photophosphorylation could be explained if one considers the possibility that PMS, besides mediating cyclic electron transport, tends to create a by-pass in the plastocyanin region. The reported ability of PMS to complex with P700 (ref. 31) seems to suggest such a possibility. Some variable portions of the electrons from reduced PMS may well enter the chain at P700 simultaneously, and form a second cycle which, however, is probably nonphosphorylating as in the case of reduced DCIP. This may explain why the quantum efficiency of PMS-mediated

Travel funds for E.K.R. were granted through Mutual Exchange Program between

the Ministry of Higher Education (U.S.S.R.) and the International Research Exchanges Board (U.S.A.). The authors would like to thank Dr Britton Chance for his interest in this study and for valuable suggestions.

ACKNOWLEDGEMENTS

This work was supported by grants from the National Institute of Health (71-2444, GM-12202), partly by grants from the National Science Foundation (GB-22657 to S.I. and GB-27600 to D.D.) and also by a grant from the Netherlands Organization for the Advancement of Pure Research (Z.W.O.) and a U.S. Public Health Service International Postdoctoral Fellowship (1-F05-TW-1821-01) to R.K. Travel funds for E.K.R. were granted through Mutual Exchange Program between the Ministry of Higher Education (U.S.S.R.) and the International Research Exchanges Board (U.S.A.). The authors would like to thank Dr Britton Chance for his interest in this study and for valuable suggestions.

REFERENCES

1 Bishop, N. I. and Spikes, J. D. (1955) *Nature* 176, 307–308
2 Trebst, A (1963) *Z. Naturforsch.* 13b, 317–321
3 Katoh, S. and San Pietro, A (1966) *Biochem. Biophys. Res. Commun.* 24, 903–908
4 Fork, D. C. and Urbach, W. (1965) *Proc. Natl. Acad. Sci. U.S.* 53, 1307–1315
5 Chance, B., Devault, D., Hildreth, W. W., Parson, W. W. and Nishimura, M. (1966) *Brookhaven Symp. Biol.* 19, 115–131
6 Hildreth, W. W. (1968) *Plant Physiol.* 43, 303–312
7 Ouitrakul, R. and Izawa, S. (1973) *Biochim. Biophys. Acta* (in the press)
8 Saha, S., Ouitrakul, R., Izawa, S. and Good, N. E. (1971) *J. Biol. Chem.* 246, 3204–3209
9 Beinert, H., Kok, B. and Hoch, G. (1962) *Biochem. Biophys. Res. Commun.* 7, 209–212
10 Weaver, E. C. (1968) *Annu. Rev. Plant Physiol.* 19, 283–294
11 Avron, M. and Chance, B. (1966) *Brookhaven Symp. Biol.* 19, 149–160
12 Larkum, A. and Bonner, W. D. (1972) *Biochim. Biophys. Acta* 267, 149–159
13 Larkum, A. and Bonner, W. D. (1972) *Arch. Biochem. Biophys.* 153, 249–257
14 Kok, B. and Beinert, H. (1962) *Biochem. Biophys. Res. Commun.* 9, 349–354
15 Bochman, R., Blumenfeld, L. A., Kukushkin, A. K. and Ruuge, E. K. (1971) *Dokl. Acad. Nauk S.S.S.R.* 201, 1138–1139
16 Katoh, S. (1960) *Nature* 186, 533–534
17 Wessels, J. S. C. (1966) *Biochim. Biophys. Acta* 126, 581–583
18 Hind, G. (1968) *Biochim. Biophys. Acta* 153, 235–240
19 Avron, M. and Shneyour, A. (1971) *Biochim. Biophys. Acta* 226, 498–550
20 Gorman, D. S. and Levine, R. P. (1965) *Proc. Natl. Acad. Sci. U.S.* 54, 1665–1669
21 Nelson, N. and Racker, E. (1972) *J. Biol. Chem.* 247, 3848–3853
22 Knaff, D. B. and Arnon, D. I. (1970) *Biochim. Biophys. Acta* 223, 201–204
23 Hauska, G. A., McCarty, R. E., Berzborn, R. J. and Racker, E. (1971) *J. Biol. Chem.* 246, 3524–3531
24 Brand, J., Baszynski, T., Crane, F. L. and Krogmann, D. W. (1972) *Biochem. Biophys. Res. Commun.* 45, 538–543
25 Brand, J., San Pietro, A. and Mayne, B. (1972) *Arch. Biochem. Biophys.* 152, 426–428
26 Kraayenhof, R., Izawa, S. and Chance, B. (1972) *Plant Physiol.* 50, 713–718
27 Neumann, J., Arntzen, C. J. and Dilley, R. A. (1971) *Biochemistry* 10, 866–873
28 Avron, M. and Neumann, J. (1968) *Annu. Rev. Plant Physiol.* 19, 137–166
29 Rumberg, B. and Witt, H. T. (1964) *Z. Naturforsch.* 19b, 693–707
30 Ke, B. (1964) *Biochim. Biophys. Acta* 88, 297–303
31 Vernon, L. P., Ke, B. and Shaw, R. (1967) *Biochemistry* 7, 2210–2220
32 Fork, D. C. and Murata, N. (1971) *Photochem. Photobiol.* 13, 33–44
33 Black, C. C., Fewson, C. A., Gibbs, M. and Gordon, S. A. (1963) *J. Biol. Chem.* 238, 3802–3805
34 Schwartz, M. (1967) *Biochim. Biophys. Acta* 131, 548–558

Biochimica et Biophysica Acta, 314 (1973) 340–353

BBA 46597

ROLE OF THE SUPEROXIDE FREE RADICAL ION IN PHOTOSYNTHETIC ASCORBATE OXIDATION AND ASCORBATE-MEDIATED PHOTOPHOSPHORYLATION

E. F. ELSTNER and R. KRAMER

Lehrstuhl für Biochemie der Pflanzen, Ruhr-Universität Bochum, D-463 Bochum-Querenburg (Germany)

(Received March 22nd, 1973)

SUMMARY

The mechanism of ascorbate photooxidation in isolated chloroplasts has been studied. The enzyme superoxide dismutase has been used as a tool to show that ascorbate is oxidized by the superoxide free radical ion, which is formed during the autooxidation of a low-potential electron acceptor.

In the absence of an artificial, low-potential electron acceptor, addition of ascorbate stimulates photophosphorylation in isolated chloroplasts. This effect of ascorbate is abolished by superoxide dismutase, indicating that both the superoxide free radical ion and ascorbate are responsible for the stimulation of photophosphorylation. In this case, the superoxide free radical ion seems to be formed during the autooxidation of an endogenous electron acceptor.

In the presence of ferredoxin and $NADP^+$, photophosphorylation in isolated chloroplasts stops as soon as the available $NADP^+$ is fully reduced. If ascorbate is present in this system, however, a linear rate of photophosphorylation is maintained in spite of the fact, that $NADP^+$ is fully reduced. This ascorbate-mediated photophosphorylation again is abolished by superoxide dismutase.

During the catalysis of this oxygen-dependent photophosphorylation, ascorbate consumption is not observed. These findings support the idea, that in chloroplasts ascorbate together with the superoxide free radical ion may function in providing additional ATP by an oxygen-dependent photophosphorylation.

INTRODUCTION

The photooxidation of ascorbate by isolated chloroplasts has been investigated by many authors (*cf.* ref. 1), and the effects of ascorbate on numerous photosynthetic chloroplast reactions have been described. These observations might be ordered in three groups: (1) Stimulation of endogenous photophosphorylation[2–4]. (2) Stimulation of coupled ATP formation in the $NADP^+$ reduction[5,6]. (3) Quinone-stimulated photooxidation[7].

Abbreviations: DCMU, 3-(3,4-dichlorophenyl)-1,1-dimethylurea; AQ, anthraquinone-2-sulfonic acid.

The following reasons for the observed effects have been offered: (a) Poising of the redox state of an endogenous system and/or acting as a protective agent. (b) Cycling of the three redox states of ascorbate. (c) Stoichiometric consumption of ascorbate in photooxidations. It is difficult to be absolutely certain which of the above three explanations (a, b or c) best account for stimulations of the individual photosynthetic reactions. For example, (a) or (b) could be responsible for the stimulation of endogenous photophosphorylation or of coupled noncyclic ATP formation in photosynthetic $NADP^+$ reduction. (b) or (c) could be the cause of the stimulation of oxygen uptake in pseudocyclic electron transport (Mehler reaction). Furthermore two possible mechanisms for ascorbate photooxidation are conceivable. Ascorbate could be the electron donor for the electron transport chain before Photosystem II[1,7] or ascorbate is oxidized by a peroxide formed by Photosystem I[8,9].

The present paper tries to find a common cause for the effects of ascorbate. Our approach has been to pinpoint the conditions under which ascorbate is an electron donor for the photosynthetic electron transport chain and those in which it is oxidized by a peroxide radical, formed by Photosystem I. For this purpose, the effect of superoxide dismutase on photosynthetic reactions has been studied. This enzyme catalyzes the dismutation of the superoxide free radical ion into O_2 and H_2O_2 and, therefore, inhibits those reactions, in which a superoxide free radical anion participates[10,11].

MATERIALS AND METHODS

Superoxide dismutase was isolated from dry peas. The purification of the enzyme from a crude extract by $(NH_4)_2\,SO_4$ and acetone precipitation was carried out using a procedure modified from Sawada *et al.*[12]. The protein fraction of the second $(NH_4)_2SO_4$ precipitation was taken up in 2.5 mM potassium phosphate buffer, pH 7.8, and heated in portions of 2 ml for 2 min at 60 °C, since superoxide dismutase proved to be rather heat stable. After centrifugation, the supernatant was chromatographed on a Whatman DE 52 column (13 cm × 5 cm). The enzyme, visible as one blue-green zone, was eluted with a linear gradient from 0 to 0.1 M NaCl in 2.5 mM potassium phosphate buffer, pH 7.8. All 10-ml fractions, in which 0.1 ml at a dilution of 1:400 showed an inhibition of the cytochrome *c* reduction by the xanthine oxidase reaction[10] of more than 50%, were concentrated by $(NH_4)_2SO_4$ precipitation, adsorbed on another column of Whatman DE 52 (1 cm × 8 cm) and eluted with 0.2 M NaCl in 2.5 mM potassium phosphate buffer, pH 7.8. The number of activity units was determined by means of the inhibition of either the cytochrome *c* reduction or epinephrine oxidation[10,13], with xanthine oxidase as the generator of the superoxide radical ion. The overall purification was 150-fold, compared with a crude extract from dried, green peas. The average preparation had about 1000 enzyme units per mg protein. The purified preparation contained 1.14 μg Cu/mg protein (0.18 gatom Cu/10 mg protein). The molecular weight of green pea superoxide dismutase was estimated to be 31000, containing 2 gatoms Cu and 2 gatoms Zn per mole enzyme protein[12]. From the protein and copper determinations we calculated (assuming that no other copper-containing protein was present) that our preparation was about 30% pure. About 50 enzyme units ($6.2 \cdot 10^{-5}$ μmole) of superoxide dismutase were used in the experiments, where indicated. This is 5-fold the amount, which gave a

90% inhibition in the cytochrome *c* reduction test. In addition to superoxide dismutase, about 8000 units of catalase were present in most of the experiments as indicated in the tables and figures.

The photosynthetic assays were carried out at 15 °C in Warburg vessels. Oxygen uptake or evolution was measured manometrically.

Broken chloroplasts were prepared from spinach leaves as described by Nelson *et al.*[14]. Heated chloroplasts were prepared and ascorbate was determined as described by Böhme and Trebst[1]. The NADPH present in the supernatant was determined at 340 or 366 nm after centrifugation of the samples at 15000 × *g*. Absorbances were measured and adsorption spectra were recorded in either a Zeiss PMQ II or a Cary 15 spectrophotometer. Protein was determined according to the method of Murphy and Kies[15]. Copper was determined with a Zeiss PMQ spectrophotometer fitted to a FA 2 atomic absorption unit with a hollow cathode lamp (λ = 324.7 nm). Ferredoxin and a ferredoxin–$NADP^+$ reductase-containing fraction were isolated from spinach leaves as described by Tagawa and Arnon[16] and Shin *et al.*[17], respectively. ATP was determined as [^{32}P]ATP[18]. Cytochrome *c*, catalase, xanthine oxidase, xanthine, glucose 6-phosphate and glucose-6-phosphate dehydrogenase were obtained from Boehringer, Mannheim. Epinephrine was obtained from Merck, Darmstadt.

RESULTS

(*1*) *The photooxidation of ascorbate*

The stoichiometry of the photooxidation of ascorbate during the pseudocyclic photophosphorylation was studied in detail by Trebst *et al.*[7] and by Böhme and Trebst[1]. These authors could show, that in isolated chloroplasts with an autooxidizable electron acceptor, the photooxidation of ascorbate was stoichiometric to photophosphorylation, O_2 uptake and H_2O_2 formation. From the inhibition of these reactions by 3-(3,4-dichlorophenyl)-1,1-dimethylurea (DCMU) it was concluded, that ascorbate might act as an electron donor for Photosystem II. Studying the oxidation of hydroxylamine and ascorbate in digitonin-fragmented chloroplasts and with artificial

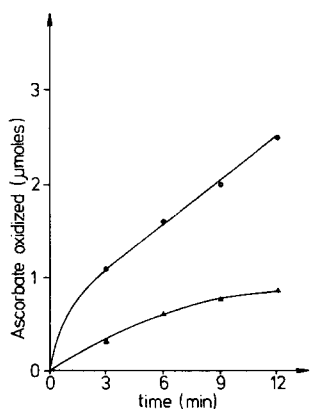

Fig. 1. Kinetics of ascorbate photooxidation. For experimental conditions see Table I. ●—●, without superoxide dismutase; ▲—▲, *plus* superoxide dismutase.

enzymatic systems, Elstner *et al.*[8] proposed an alternative mechanism for the oxidation of ascorbate, in which a peroxide other than H_2O_2 (formed during the autooxidation of the reduced electron acceptor) is the oxidant.

Fig. 1 shows the kinetics of the ascorbate photooxidation by isolated chloroplasts with a low-potential electron acceptor. Superoxide dismutase inhibits the reaction to about 65%. After the light reaction proceeds for 10–12 min, the oxidation in the vessel which contains superoxide dismutase comes to a virtual halt, while the one without superoxide dismutase still proceeds linearly. An almost complete inhibition of ascorbate photooxidation can be achieved by the addition of both superoxide dismutase and catalase. Catalase alone has no or very little effect on the ascorbate photooxidation (Table I).

TABLE I

INHIBITION OF ASCORBATE PHOTOOXIDATION IN ISOLATED CHLOROPLASTS WITH METHYL VIOLOGEN AS ELECTRON ACCEPTOR BY SUPEROXIDE DISMUTASE AND CATALASE

The reaction medium contained in 3 ml: broken chloroplasts with 0.1 mg chlorophyll, 80 μmoles Tris–HCl, pH 8.0, 0.2 μmoles methyl viologen, 10 μmoles ascorbate, 5 μmoles NH_4Cl, 5 μmoles $MgCl_2$; the reaction was allowed to proceed for 15 min at 25000 lux and 15 °C in air.

Additions	*μmoles ascorbate oxidized/mg chlorophyll per h*	*μmoles O_2 taken up/mg chlorophyll per h*
None	112	88
plus catalase	100	52
plus superoxide dismutase	28	28
plus superoxide dismutase *plus* catalase	4	12

The kinetics of oxygen uptake during the ascorbate oxidation with anthraquinone as electron acceptor are shown in Fig. 2. No or little oxygen uptake is observed when only anthraquinone is present; after a lag phase (probably due to the reduction of AQ, *cf.* ref. 1), an oxygen uptake is measured, if in addition to AQ, 10^{-3} M KCN is present. Addition of ascorbate causes a rapid oxygen uptake, which can be inhibited by superoxide dismutase. The vessel with both AQ and ascorbate continues taking up oxygen in the dark after switching off the light for at least 5 min. Addition of 10^{-3} M KCN stimulates the rate of oxygen uptake in the dark, due to the inhibition of an endogenous catalase activity, which simultanously splits the H_2O_2 accumulated during the light reaction. A similar observation was made by Good and Hill[19] with ascorbate in quinone-treated chloroplasts.

Oxygen uptake varied with different chloroplast preparations in the absence of KCN, probably because of different endogenous catalase activities (*cf.* refs 7 and 20). The values for oxygen uptake are omitted in the following tables since KCN cannot be added to our test system, because it also inhibits the superoxide dismutase[21] (*cf.* Table II).

Ascorbate oxidation by an enzymatic system which mimics the "pseudocyclic" conditions was reported by Elstner *et al.*[8] and was confirmed by Epel and Neumann[9].

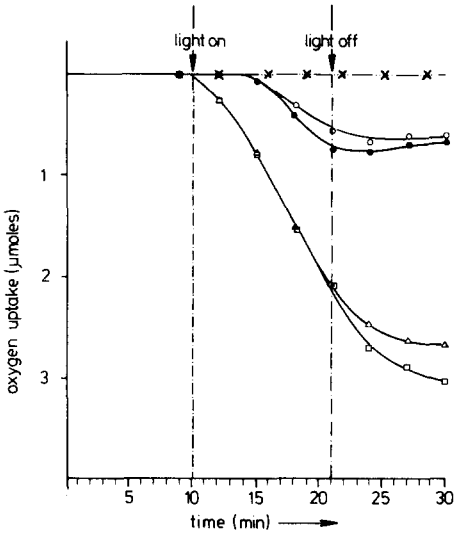

Fig. 2. Kinetics of oxygen uptake by isolated chloroplasts with 0.6 μmole anthraquinone-2-sulfonic acid (AQ) as electron acceptor. For experimental conditions see Table I. × · · —· · × , *plus* AQ; ○—○, *plus* AQ *plus* 10^{-3} M KCN; ●—●, *plus* AQ *plus* 10 μmoles ascorbate *plus* superoxide dismutase *plus* catalase; △—△, *plus* AQ *plus* 10 μmoles ascorbate; □—□, *plus* AQ *plus* 10 μmoles ascorbate *plus* 10^{-3} M KCN.

TABLE II

THE CO-OXIDATION OF ASCORBATE DURING THE DIAPHORASE-CATALYZED OXIDATION OF NADPH WITH ANTHRAQUINONE AND ITS INHIBITION BY SUPEROXIDE DISMUTASE AND CATALASE

The reaction mixture contained in 3 ml: 10 μmoles glucose 6-phosphate, 10 μg glucose-6-phosphate dehydrogenase, 1 μmole $NADP^+$, an $NADP^+$–ferredoxin reductase fraction containing 2 mg protein, 0.2 μmole AQ; 15-min dark reaction in air at 15 °C.

Additions	*μmoles ascorbate oxidized/15 min*
Complete	1.9
plus 10^{-3} M KCN	2.7
plus superoxide dismutase *plus* catalase	0.3
plus superoxide dismutase *plus* catalase *plus* 10^{-3} M KCN	2.5
minus glucose 6-phosphate	0
minus AQ	0.1
minus $NADP^+$–ferredoxin reductase	0

This system with AQ ($E_0 = -200$ mV), reduced by NADPH in a diaphorase-catalyzed reaction, in the dark oxidizes ascorbate apparently *via* superoxide free radical ion. KCN stimulates the oxidation of ascorbate in this system as previously reported[8]. In the presence of 10^{-3} M KCN the ascorbate oxidation is no longer inhibited by superoxide dismutase and catalase (Table II).

As shown in Table III, the addition of both superoxide dismutase and catalase has no influence on the ATP formation in pseudocyclic photophosphorylation regardless whether ascorbate is present or not, while the photooxidation of ascorbate is inhibited to about 90%.

(2) The stimulation of the endogenous photophosphorylation by ascorbate

The photophosphorylation in isolated chloroplasts without an artificial electron acceptor ("endogenous" photophosphorylation, *cf.* ref. 4) is stimulated by ascorbate as already reported by other groups[2–4]. This stimulatory effect of ascorbate can be inhibited by the addition of both superoxide dismutase and catalase or by DCMU (Table IV).

As shown in Table IV, ascorbate brings about a 4-fold stimulation of the "endo-

TABLE III

THE LACK OF INFLUENCE OF SUPEROXIDE DISMUTASE ON THE PSEUDOCYCLIC PHOTOPHOSPHORYLATION IN THE PRESENCE AND ABSENCE OF ASCORBATE

Experimental conditions, see Table I. Changes: *minus* NH_4Cl, *plus* 10 μmoles phosphate, *plus* 10 μmoles ADP.

Additions	*μmoles ATP formed /mg chlorophyll per h*	*μmoles ascorbate oxidized /mg chlorophyll per h*
None	50	—
plus 10 μmoles ascorbate	52	88
plus superoxide dismutase *plus* catalase	50	—
plus 10 μmoles ascorbate *plus* xsuperoxide dismutase *plus* catalase	54	10

TABLE IV

THE EFFECT OF ASCORBATE ON THE "ENDOGENOUS" PHOTOPHOSPHORYLATION IN ISOLATED CHLOROPLASTS AND ITS INHIBITION BY SUPEROXIDE DISMUTASE AND CATALASE

Experimental conditions, see Table III. Change: *minus* methyl viologen.

Additions	*μmoles ATP formed /mg chlorophyll per h*	*μmoles ascorbate oxidized/mg chlorophyll per h*
None	6.0	—
plus $2 \cdot 10^{-5}$ M DCMU	1.0	—
plus 10 μmoles ascorbate	25	0
plus 10 μmoles ascorbate *plus* $2 \cdot 10^{-5}$ M DCMU	1.5	0
plus 10 μmoles ascorbate *plus* superoxide dismutase *plus* catalase	7.5	0

genous" photophosphorylation, but no consumption of ascorbate is observed. In the presence of superoxide dismutase and catalase, the stimulatory effect of ascorbate disappears, and the rate of photophosphorylation is reduced to the endogenous rate. $2 \cdot 10^{-5}$ M DCMU inhibits both the endogenous and the ascorbate-mediated photophosphorylation.

Similar results are obtained with heat-treated chloroplasts (Table V). The important difference in this case, compared to the experiment described in Table IV, is the neglegible rate of endogenous phosphorylation, which is not further inhibited by DCMU. However, as in the experiment shown in Table IV no oxidation of ascorbate can be observed. This result is in agreement with the findings of Forti and Jagendorf[4]. The stimulatory effect of ascorbate can be inhibited again by the addition of both superoxide dismutase and catalase and by DCMU.

TABLE V

THE EFFECT OF ASCORBATE ON THE PHOTOPHOSPHORYLATION IN HEAT-TREATED CHLOROPLASTS AND ITS INHIBITION BY SUPEROXIDE DISMUTASE AND CATALASE

Experimental conditions, see Table III. Changes: heat-treated chloroplasts were used, in the absence of methyl viologen.

Additions	*μmoles ATP formed/mg chlorophyll per h*
None	1.6
plus $2 \cdot 10^{-5}$ M DCMU	1.0
plus 10 μmoles ascorbate	10
plus 10 μmoles ascorbate *plus* $2 \cdot 10^{-5}$ M DCMU	1.2
plus 10 μmoles ascorbate *plus* superoxide dismutase *plus* catalase	3.5

(3) Stimulation of the ATP formation in a $NADP^+$-reducing system

Jacobi[6] showed that, with $NADP^+$ as the acceptor in the presence of ascorbate and air, photophosphorylation can still proceed in spite of the fact that all of the added $NADP^+$ was reduced. The rate of this photophosphorylation seemed to be independent of anaerobic photophosphorylation, which is coupled to the $NADP^+$ reduction and was thus interpreted as an extra ATP site.

By following the kinetics of the $NADP^+$ reduction and ATP formation with limiting amounts of added $NADP^+$ (in the presence or absence of ascorbate) (Fig. 3), we found a stoichiometry of about 1:1 between ATP formation and $NADP^+$ reduction after 8–10 min of light. At all shorter times more NADPH than ATP is formed. After 10 min, some NADPH is reoxidized and reaches a steady state at about 15 min. Around 75% of the added $NADP^+$ is found reduced at all times after 15 min. At about 15 min, the amount of ATP formed in experiments without added ascorbate reaches a plateau which is equivalent to the amount of $NADP^+$ added (2 μmoles). In the presence of ascorbate, however, photophosphorylation proceeds even after NADPH formation has reached a steady state. The rate of this ATP formation is

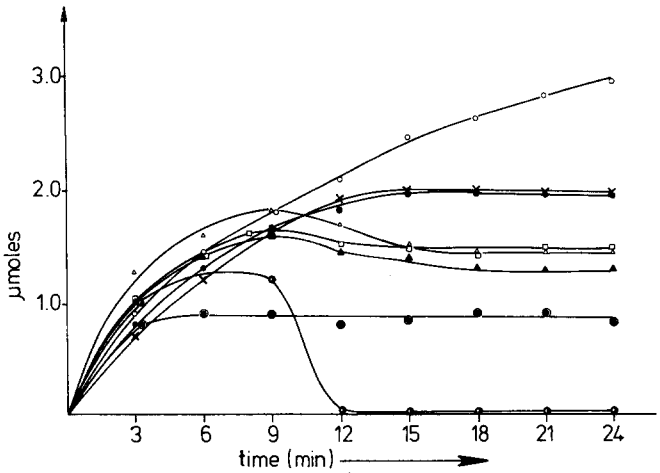

Fig. 3. Kinetics of photophosphorylation and $NADP^+$ reduction in the presence or absence of ascorbate and with or without superoxide dismutase *plus* catalase. Experimental conditions: chloroplast fragments with 0.2 mg chlorophyll, 10 nmoles ferredoxin, 2 μmoles $NADP^+$, 10 μmoles phosphate, 10 μmoles ADP, light reaction in air, 25000 lux, 15 °C. ○—○, ATP in the presence of 10 μmoles ascorbate; ×—×, ATP in the presence of 10 μmoles ascorbate *plus* superoxide dismutase *plus* catalase; ●—●, ATP; △—△, NADPH; ▲—▲, NADPH in the presence of 10 μmoles ascorbate; □—□, NADPH in the presence of 10 μmoles ascorbate *plus* superoxide dismutase *plus* catalase; ⊙—⊙, ascorbate oxidized; ◑—◑, ascorbate oxidized in the presence of superoxide dismutase *plus* catalase.

about half of the initial rate. Another unexpected result is that the oxidation of ascorbate reaches a plateau at about 8% oxidized after only 3–5 min of light.

The effect of superoxide dismutase and catalase on photophosphorylation under conditions of limiting amounts of $NADP^+$in the presence of ascorbate is the following. The amounts of reduced $NADP^+$ and formed ATP at all times are identical with those in the absence of ascorbate. The amount of initially oxidized ascorbate disappears quantitatively. After 15 min of light (the time at which the systems without ascorbate reach their plateau or steady state) we observe the stoichiometries shown in Table VI.

TABLE VI

STOICHIOMETRY OF PHOTOSYNTHETIC PARAMETERS OBSERVED AT THE BEGINNING OF THE NADPH STEADY STATE

For the experimental conditions, see Fig. 3.

Additions	*μmoles $NADP^+$ formed*	*Δ*	*μmoles ATP formed*	*Δ*	*μmoles ascorbate oxidized*	*Δ*
None	1.5		1.9		—	
10 μmoles ascorbate	1.4	0.1	2.3	0.4	0.8	
10 μmoles ascorbate *plus* superoxide dismutase *plus* catalase	1.5	0.1	1.9	0.4	0	0.8

The same stoichiometric relationships were found in several independent experiments. As shown in Table VI, at the endpoint of photophosphorylation in the absence of ascorbate, the difference between photophosphorylation *plus* ascorbate and photophosphorylation *minus* ascorbate is about 0.4 μmole; exactly the same difference can be obtained if we subtract the ATP values, which are found with ascorbate in the presence of superoxide dismutase and catalase from those in the absence of superoxide dismutase and catalase. This difference we should like to refer to as "ascorbate-mediated photophosphorylation". In the presence of superoxide dismutase and catalase no ascorbate oxidation can be observed, starting from the point of the apparent end of the $NADP^+$-coupled photophosphorylation. At this point we find a stoichiometry of 0.4 μmole ATP formed by the ascorbate-mediated photophosphorylation for 0.8 μmole of ascorbate oxidized. One might conclude from the stoichiometry at this point, that the oxidation of 2 equiv of ascorbate can mediate the formation of 1 equiv of ATP. The question arises, however, why this stoichiometry is only observed at a certain point and why the ratio of ascorbate reduced to ascorbate oxidized is constant during the $NADP^+$/NADPH steady state. After the light reaction has proceeded for 21 min, for example, 0.8 μmole of ATP are formed by the ascorbate-mediated photophosphorylation. According to the above mentioned stoichiometry, we should observe the oxidation of 1.6 μmoles of ascorbate. As a possible explanation for this discrepancy, the possibility of the rereduction of the oxidized ascorbate by NADPH as pointed out by Marrè and co-workers[22,23] was tested. By measuring the oxidation of NADPH in the presence of ascorbate, an enzyme fraction from spinach which contains $NADP^+$–ferredoxin reductase, and in the presence of xanthine *plus* xanthine oxidase as the generator couple for superoxide free radical ion (which can oxidize ascorbate), we made the observation, that the fastest oxidation of NADPH occurs in the presence of all components: xanthine oxidase, xanthine, and the enzyme fraction from spinach and ascorbate. The observed rates under the described conditions (0.3 μmole NADPH oxidized/h), however, are too small, to count as the sole mechanism for the reduction of oxidized ascorbate. The finding, that in isolated chloroplasts without an added electron acceptor, ascorbate can stimulate the photophosphorylation without being oxidized[4] (Table IV) suggests, that another or additional mechanisms than the one described by Marrè and co-workers[22,23] are responsible. We, therefore, tested the influence of dehydroascorbate on photophosphorylation in isolated chloroplasts without any other electron acceptor and found a marked stimulation of the endogenous rate of ATP synthesis (Table VII).

As shown in Table VII, the stimulation of the photophosphorylation by dehydroascorbate is inhibited by DCMU and proceeds independently from (essentially superimposed on) the photophosphorylation, which is mediated by ascorbate. This result can be explained by the assumption, that dehydroascorbate is acting as a Hill reagent.

Another observation supports this assumption. In heat-treated chloroplasts, ascorbate can mediate a photophosphorylation as already shown in Table V, whereas dehydroascorbate has no effect on the photophosphorylation in this system. Dehydroascorbate is apparently only a weak electron acceptor in systems where an electron donor is present. A reduction of dehydroascorbate by isolated chloroplasts in the light has been observed by other workers[24–26].

TABLE VII

EFFECT OF DEHYDROASCORBATE ON PHOTOPHOSPHORYLATION IN ISOLATED CHLOROPLASTS

Experimental conditions, see Table IV.

Additions	*μmoles ATP formed/mg chlorophyll per h*
None	5.5
10 μmoles dehydroascorbate	11.0
10 μmoles ascorbate	21
10 μmoles ascorbate *plus* 10 μmoles dehydroascorbate	30
10 μmoles dehydroascorbate *plus* $2 \cdot 10^{-5}$ M DCMU	1.2
10 μmoles dehydroascorbate *plus* 10 μmoles ascorbate *plus* $2 \cdot 10^{-5}$ M DCMU	1.6

DISCUSSION

The stimulation of oxygen uptake by isolated chloroplasts with a low-potential electron acceptor and the concomitant oxidation of ascorbate[7] on one hand and the stimulation of photophosphorylation under certain conditions[2–6] on the other hand, were the focus of investigations, concerning the function of ascorbate in photosynthetic reactions. We have attempted to find a common mechanism for the effects of ascorbate on the photosynthetic reactions in isolated chloroplasts. Our results can be summarized as follows:

(a) Ascorbate photooxidation, mediated by an autooxidizable acceptor of Photosystem I, like methyl viologen, is inhibited by superoxide dismutase. This inhibition is independent of whether the acceptor is reduced by light or by NADPH.

(b) ATP formation coupled to pseudocyclic electron transport is not influenced by superoxide dismutase, regardless of whether ascorbate is oxidized concomitantly.

(c) The stimulation of endogenous photophosphorylation by ascorbate (*i.e.* without any other addition) is abolished by superoxide dismutase.

(d) The endogenous photophosphorylation is also stimulated by dehydroascorbate, but ascorbate and dehydroascorbate together are even more effective.

(e) The stimulation of ATP formation coupled to photosynthetic $NADP^+$ reduction by ascorbate, when followed kinetically, becomes apparent only when 75% of the added $NADP^+$ has been reduced. ATP formation proceeds in the presence of ascorbate, after $NADP^+$ reduction has levelled off. This additional ATP formation is abolished by superoxide dismutase.

(f) NADPH oxidation by the superoxide radical ion (regenerated by xanthine oxidase) is stimulated by the addition of ascorbate.

These results suggest that a superoxide radical ion participates in the reactions described and is oxidizing ascorbate to monodehydroascorbate. The superoxide radical ion is formed by the reaction of oxygen with the reduced form of an electron acceptor like methyl viologen or AQ, which might either be reduced by light or by NADPH *via* the $NADP^+$-ferredoxin reductase.

The autooxidation of a reduced low-potential acceptor results in the formation of superoxide radical ion. According to Musso and Döpp[27], the events of the reoxidation of a reduced quinone-type electron acceptor can be written as follows (Reactions a and b; Acc, electron acceptor).

$$\begin{array}{l} |O| \\ \| \\ Acc + 2e \rightarrow \\ \| \\ |O| \end{array} \qquad \begin{array}{l} |\overline{O}|^{(-)} \\ | \\ Acc \\ | \\ |\underline{O}|_{(-)} \end{array} \tag{a}$$

$$\begin{array}{l} |\overline{O}|^{(-)} \\ | \\ Acc + O_2 \rightarrow \\ | \\ |\underline{O}|_{(-)} \end{array} \qquad \begin{array}{l} |\dot{O}| \\ | \\ Acc + O_2^{\cdot -} \\ | \\ |\underline{O}|_{(-)} \end{array} \tag{b}$$

The superoxide radical ion thus formed can be further reduced to hydrogen superoxide by ascorbate ($AscH_2$), forming the monodehydroascorbate radical AscH·, (Reaction c).

$$O_2^{\cdot -} + AscH_2 \rightarrow AscH\cdot + HOO^- \tag{c}$$

The fact that the oxidation of ascorbate in this reaction is accompanied by an increased oxygen uptake might be explained by the following assumption, though nothing is known about the thermodynamic equilibrium. Monodehydroascorbate radical can reduce the acceptor anion radical $\begin{pmatrix} O\cdot \\ Acc \\ O^- \end{pmatrix}$ to the dianion (Reaction d), which in turn can take up a second molecule of oxygen during its reoxidation (Reactions b and e). Reaction b is probably the rate-limiting step.

$$\begin{array}{l} \quad |O| \\ \quad | \\ AscH\cdot + Acc \rightarrow \\ \quad | \\ \quad |\underline{O}|_{(-)} \end{array} \qquad \begin{array}{l} |\overline{O}|^{(-)} \\ | \\ + Acc + H^+ + Asc_{ox} \\ | \\ |\underline{O}|_{(-)} \end{array} \tag{d}$$

$$\begin{array}{l} |\overline{O}|^{(-)} \\ | \\ Acc + O_2 \rightarrow \\ | \\ |\underline{O}|_{(-)} \end{array} \qquad \begin{array}{l} |O| \\ | \\ Acc + O_2^{\cdot -} \\ | \\ |\underline{O}|_{(-)} \end{array} \tag{e}$$

The acceptor anion radical $\begin{pmatrix} O\cdot \\ Acc \\ O^- \end{pmatrix}$ on the other hand can dismutate into the oxidized and reduced form. The reduced acceptor can autooxidize again, so that per mole of ascorbate oxidized the number of moles oxygen taken up may become more than 1, depending on the pH of the reaction medium and on the autooxidability of the acceptor[27]. A 2–4-fold stimulation of oxygen uptake by ascorbate, which has been observed by many groups[1,4,7,9] can be explained by the sequence of the Reactions b–e as the induction of a chain reaction (c, d, e,→c, d, e,...), which is independent of light as soon as a certain amount of the reduced low-potential acceptor is formed. A light-dependent production of a catalyst for oxidation of ascorbate in quinone-treated chard chloroplasts has been shown by Good and Hill[19]. These authors observed, that the oxidation of ascorbate and the oxygen uptake by isolated chloroplasts could carry on in the dark after an illumination period in the presence of a quinone. The above mechanism is in good agreement with these results (Fig. 2). The simultaneous dismutation of the acceptor anion radical, however, leads to a slow termination of this chain reaction. If superoxide dismutase is present in the reaction mixture, the concentration of $O_2^{\cdot -}$ is decreased drastically, since the rate constant of the superoxide dismutase reaction has been found to be about $1 \cdot 10^9$ to $2 \cdot 10^9$ at 25 °C[21,28]. The reaction sequence a to e, may be a feasible explanation for our results, especially as far as the oxygen uptake in the dark after an illumination period is concerned, if quinone-type electron acceptors like AQ are used. In the case of methyl viologen as autooxidizable electron acceptor, however, it seems rather unlikely, that the increased oxygen uptake in the presence of ascorbate can be explained by a reduction of the autooxidized dye by monodehydroascorbate radical, because of the very negative redox potential of methyl viologen. The increased oxygen uptake in this case might simply be explained by the fact, that ascorbate can reduce the superoxide radical ion to H_2O_2, avoiding the dismutation[9]. Since methyl viologen or AQ are the better electron acceptors for Photosystem I compared with monodehydroascorbate radical or dehydroascorbate, a net oxidation of ascorbate is observed. The observed stimulation of photophosphorylation in the absence of a low-potential electron acceptor by ascorbate is abolished by superoxide dismutase. Since ascorbate is not consumed in these reactions, we would like to propose a mechanism for these photophosphorylations, which includes the participation of the three redox states of ascorbate in a cyclic process as well as the superoxide radical ion.

We assume, that a compound (y), which acts as electron donor for Photosystem II, is oxidized; an electron acceptor (Acc–Fe(III)) is reduced by Photosystem I:

$$2y + ADP + P_i \xrightarrow{\text{Photosystems}} 2y^+ + 2e + ATP \qquad (I)$$

$$2e + 2\ \text{Acc–Fe(III)} \rightarrow 2\ \text{Acc–Fe(II)} \qquad (II)$$

The reduced acceptor is autooxidizable and can reduce oxygen:

$$2\ \text{Acc–Fe(II)} + 2\ O_2 \rightarrow 2\ \text{Acc–Fe(III)} + 2\ O_2^{\cdot -} \qquad (III)$$

The formed superoxide radical ion is reduced by ascorbate, forming a stoichiometric amount of peroxide:

$$2\,AscH_2 + 2\,O_2^{\cdot -} \rightarrow 2\,AscH\cdot + 2\,HOO^- \qquad (IV)$$

The monodehydroascorbate radical, in turn can donate one electron to the photooxidized y^+:

$$2\,AscH\cdot + 2y^+ \rightarrow 2y + 2\,Asc_{ox} + 2\,H^+ \qquad (V)$$

This sequence of reactions can be inhibited by $2 \cdot 10^{-5}$ M DCMU at Reaction I and by superoxide dismutase at Reaction IV. In the system with $NADP^+$ as electron acceptor, Acc–Fe(II, III) is probably ferredoxin, which was added to the reaction mixture and which has been shown to reduce oxygen during its autooxidation[29].

According to this mechanism, the superoxide radical anion formed by the reaction of an unidentified acceptor for Photosystem I with oxygen (possibly bound ferredoxin[30–33]) oxidizes ascorbate and leads to the formation of monodehydroascorbate. The latter is an electron donor for Photosystem, II (at least in heat-treated chloroplasts, Table V, *cf.* ref. 1), or eventually (in the absence of a low-potential electron acceptor) an electron acceptor for Photosystem I in isolated chloroplasts with an intact water-splitting system. In both cases, a stimulation of electron transport is achieved, and it is measured as an increase in photophosphorylation. The above statements are summarized in Scheme 1.

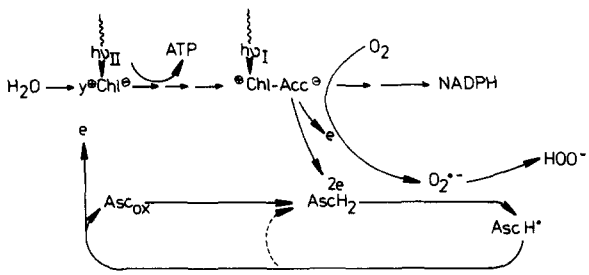

Our results are not consistent with the proposal, that ascorbate acts only as a protective agent[34,35] in respect to photophosphorylation. We wish to support the idea, that ascorbate together with oxygen is able to maintain photophosphorylation under conditions, where the $NADP^+$-coupled photophosphorylation is bound to stagnate. As demonstrated by Champigny and Gibbs[36] the CO_2 fixation in isolated chloroplasts is stimulated several-fold by the addition of ascorbate. It has been shown, that about 40% of the total content of ascorbate in plant cells is located in the chloroplasts[37]. If the assumption is correct, that the rate of CO_2 fixation is governed by the availability of ATP, ascorbate may play a physiological role in the energy balance of the chloroplasts.

REFERENCES

1 Böhme, H. and Trebst, A (1969) *Biochim. Biophys, Acta* 180, 137–148
2 Arnon, D. I., Whatley, F. R. and Allen, M. B. (1955) *Biochim. Biophys. Acta* 16, 605–608
3 Wessels, J. S. C. (1958) *Biochim. Biophys. Acta* 29, 113–123
4 Forti, G. and Jagendorf, A. (1961) *Biochim. Biophys. Acta* 54, 322–330
5 Jacobi, G. (1963) *Z. Naturforsch.* 18b, 711–717

6 Jacobi, G. (1964) *Z. Naturforsch.* 19b, 470–480
7 Trebst, A., Eck, H. and Wagner, S. (1963) in *Photosynthetic Mechanisms of Green Plants* (Kok, B. and Jagendorf, A., eds), *Natl. Acad. Sci. — Natl. Res. Council Publ.* 1145, 174–194
8 Elstner, E. F., Heupel, A. and Vaklinova, S. (1970) *Z. Pflanzenphysiol.* 62, 184–200
9 Epel, B. L. and Neumann, J. (1972) in *6th Int. Congr. Photobiol., Bochum, 1972* (Schenk, G. O., ed.), Abstract No. 237
10 McCord, J. M. and Fridovich, I. (1969) *J. Biol. Chem.* 244, 6049–6055
11 McCord, J. M. and Fridovich, I. (1970) *J. Biol. Chem.* 245, 1374–1377
12 Sawada, Y., Ohyama, T. and Yamazaki, I. (1972) *Biochim. Biophys. Acta* 268, 305–312
13 Aust, S. D., Roerig, D. L. and Pederson, T. C. (1972) *Biochem. Biophys. Res. Commun.* 47, 1133–1137
14 Nelson, N., Drechsler, Z. and Neumann, J. (1970) *J. Biol. Chem.* 245, 143–151
15 Murphy, J. B. and Kies, M. W. (1960) *Biochim. Biophys. Acta* 45, 382–384
16 Tagawa, K. and Arnon, D. I. (1962) *Nature* 195, 537–543
17 Shin, M. K., Tagawa, K. and Arnon, D. I. (1963) *Biochem. Z.* 338, 84
18 Sugino, Y. and Miyoshi, Y. (1964) *J. Biol. Chem.* 239, 2360–2364
19 Good, N. and Hill, R. (1955) *Arch. Biochem. Biophys*, 57, 355–366
20 Ikeda, S. (1959) *Mem. Res. Inst. Food Sci. Kyoto Univ.* 18, 57–64
21 Rotilio, G. (1972) *Biochem. Soc. Transactions, Metalloenzymes Conf., Oxford, 1972*, pp. 24–26
22 Marrè, E. and Arrigoni, O. (1958) *Biochim. Biophys. Acta* 30, 453–457
23 Marrè, E., Arrigoni, O. and Rossi, G. (1959) *Biochim. Biophys. Acta* 36, 56–64
24 Mehler, A. (1951) *Arch. Biochem. Biophys.* 34, 339–351
25 Luger, H. (1954) *Protoplasma* 44, 212–238
26 Marrè, E. and Laudi, G. (1955) *Rend. Acc. Naz. Lincei* 18, 402–409
27 Musso, H. and Döpp, H. (1967) *Chem. Ber.* 100, 3627–3643
28 Fridovich, I. (1972) *Biochem. Soc. Transactions, Metalloenzymes Conf., Oxford, 1972*, pp. 22–24
29 Telfer, A., Cammack, R. and Evans, M. C. W. (1970) *FEBS Lett.* 10, 21–24
30 Malkin, R. and Bearden, A. J. (1971) *Proc. Natl. Acad. Sci. U.S.* 68, 16–19
31 Yang, C. S. and Blumberg, W. E. (1972) *Biochem. Biophys. Res. Commun.* 46, 422–428
32 Leigh Jr, J. S. and Dutton, P. L. (1972) *Biochem. Biophys. Res. Commun.* 46, 414–421
33 Evans, M. C. W., Telfer, A. and Lord, A. V. (1972) *Biochim. Biophys. Acta* 267, 530–537
34 Arnon, D. I., Whatley, F. R. and Allen, M. B. (1957) *Nature* 180, 182–185
35 Avron, M. (1960) *Biochim. Biophys. Acta* 40, 257–272
36 Champigny, M. L. and Gibbs, M. (1969) in *Progress in Photosynthesis Research* (Metzner, H., ed.), Vol. III, pp. 1534–1537, Laupp, Tübingen
37 Gerhard, B. (1964) *Planta* 61, 101–129

Biochimica et Biophysica Acta, 314 (1973) 354–359

BBA 46595

THE MEASUREMENT OF CYCLIC PHOTOPHOSPHORYLATION IN ISOLATED CHLOROPLASTS BY DETERMINATION OF HYDROGEN ION CONSUMPTION.
AN EVALUATION OF THE METHOD USING TITRATION AT CONSTANT pH

R. McC. LILLEY and D. A. WALKER

Department of Botany, The University, Sheffield S10 2TN (Great Britain)

(Received April 2nd, 1973)

SUMMARY

1. An improved method for the continuous measurement of phosphorylation is reported.

2. This method, in which the consumption of H^+ during the reaction is followed by titration at constant pH using commercially available apparatus, has been evaluated for photophosphorylation by isolated chloroplasts.

3. By use of an independent assay for ATP it is shown that the method gives a valid and precise measurement of photophosphorylation.

INTRODUCTION

The measurement of phosphorylation from the uptake of H^+ during ATP formation was first investigated by Nishimura *et al.*[1]. These workers measured the pH change associated with phosphorylation by suspensions of mitochondria and chromatophores. The method has subsequently been widely used for the measurement of photophosphorylation by isolated chloroplasts[2–4], and it therefore seemed desirable to check its validity by an independent assay of the ATP formed.

A reaction that consumes protons may be followed either by measuring the pH change or by titration of acid at constant pH. The necessity to calibrate pH changes by subsequent back titration, which should be done in the same conditions of illumination[5], is avoided by pH-stat titration. A further advantage of measuring photophosphorylation at a constant pH value is that both the rate of ATP formation and the ratio of H^+ consumed to ATP formed vary with pH[1].

This paper reports an evaluation of the pH-stat method for the continuous measurement of cyclic photophosphorylation in isolated chloroplasts, using commercially available apparatus.

MATERIALS AND METHODS

Chloroplasts preparation

Envelope-free spinach chloroplasts were prepared in sorbitol–phosphate

medium by the method of Emmett and Walker[6]. Chlorophyll was determined by the method of Arnon[7].

Titration at constant pH

The twin reaction vessels and apparatus for illumination were similar to those described previously[8] for photosynthetic oxygen evolution measurements. Each reaction mixture was contained in a cylindrical glass vessel (15-mm diameter) surrounded by a water jacket through which water at 15 °C was circulated from a Haake model FJ thermostat. The reaction mixture was vigorously stirred by a magnetic stirrer. The reaction vessel was illuminated by the 150-W quartz–iodine lamp of a slide projector. The beam was passed through a 150-mm-diameter spherical water-filled flask, a red filter (I.C.I. Perspex No. 400) transmitting 80–90% of light at wavelengths above 625 nm, and an infrared filter (Balzer interference filter, Calflex-C, Tempax).

The pH of the reaction mixture was measured by miniature glass and reference electrodes (Radiometer type G222C and K4112 respectively), connected to a Radiometer PM 26 pH meter. The output of the meter was recorded on one channel of a Rikadenki B 24 recorder. The pH of the reaction mixture was controlled by a Radiometer titration assembly consisting of a TT 11 titration control, ABU 12 autoburette, and SBR 2 recorder. The titrant was standardised 10 mM HCl, delivered to the reaction vessel by polythene tubing with a finely drawn out tip. The entire apparatus described was duplicated to allow two experiments to be run simultaneously.

The reaction mixture contained, in a total volume of 2.0 ml 0.33 M glucose, 10 mM KCl, 2 mM $MgCl_2$, 1.25 mM sodium phosphate, 1.25 mM potassium phosphate, 30 μM pyocyanine and chloroplasts equivalent to 100 μg chlorophyll. The pH was adjusted with 0.1 M HCl or NaOH to 0.05 unit over the pH-stat value set on the titration apparatus. The reaction mixture was then illuminated and the titration assembly switched on. After titration to the selected pH-stat value, phosphorylation was initiated by addition of approximately 0.6 μmole ADP.

ATP analysis

Firefly luciferin and luciferase were extracted from desiccated *Photinus pyralis* tails (Sigma) and partially purified by the methods of Nielsen and Rasmussen[9]. Light emission by assay mixtures was measured in a Nuclear-Chicago Unilux 2 scintillation counter by the method of Stanley and Williams[10]. Each series of assays was calibrated with freshly prepared ATP standard solutions and a linear relation was observed between count rate and amount of ATP within the range 1–10 pmoles ATP for assay. Assay specificity checks showed that the count rate per pmole ADP was less than 2% of that for ATP.

ATP was extracted from reaction mixtures as follows: 10 μl of chloroplast suspension was injected into 1.0 ml of ice-cold ethanol–5 mM EDTA (4:1, v/v). This was placed in a boiling water bath until the volume reduced to 0.1 ml (approx. 5 min), removed and placed on ice, and the volume made up to 1.0 ml with water. After centrifugation at $1000 \times g$ for 2 min, and 0.2 ml sample was taken and mixed with 50 μl 20 mM $MgCl_2$, 0.1 M potassium phosphate (pH 7.3). The ATP concentration of this solution was determined as described. Each series of assay was accom-

panied by triplicated control extractions from chloroplast suspensions containing a known amount of ATP standard. For all experiments reported the mean recovery of ATP in the control experiments was ±5% of the ATP added to the chloroplast suspensions.

Preparation of ATP and ADP solutions

ATP and ADP (sodium salts) were of the highest grade obtainable from the Sigma Chemical Co. The concentration of standard solutions was checked by absorbance measurements, and the solutions stored at −15 °C. The pH of ADP solutions was adjusted with 0.1 M NaOH to the same value as that to be maintained during the pH-stat titration. Standard ADP solutions were prepared immediately on receipt of ADP from the manufacturer, and were used within a few days.

RESULTS AND DISCUSSION

Simultaneous recorder traces of the pH of the reaction mixture and of the volume of titrant acid added are shown in Fig. 1. The pH of the reaction mixture during photophosphorylation is controlled by the apparatus to within 0.01 unit, apart from the initial transient excursion of pH on the addition of ADP. The rate of titration of acid remained linear until the reaction was about 90% complete, suggesting that the addition of titrant to the chloroplast suspension was without

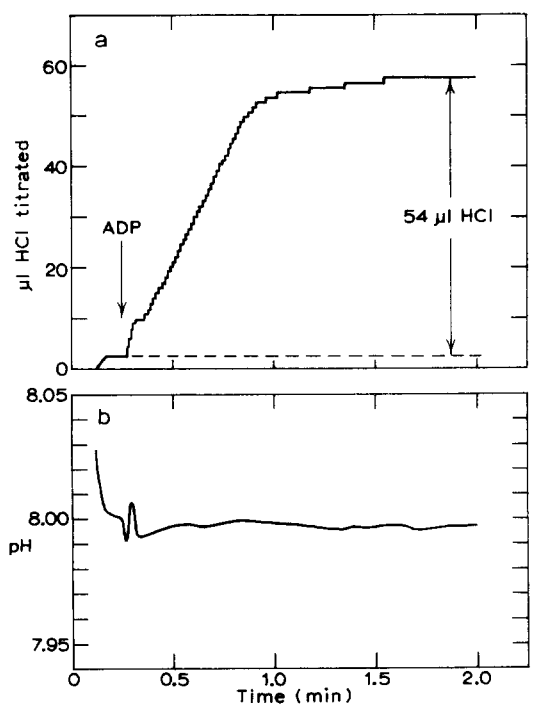

Fig. 1. Simultaneous recorder traces of (a) the volume of 0.0107 M HCl titrated and (b) the pH of the chloroplast suspension during photophosphorylation of 0.6 µmole ADP. Reaction conditions as described in Methods.

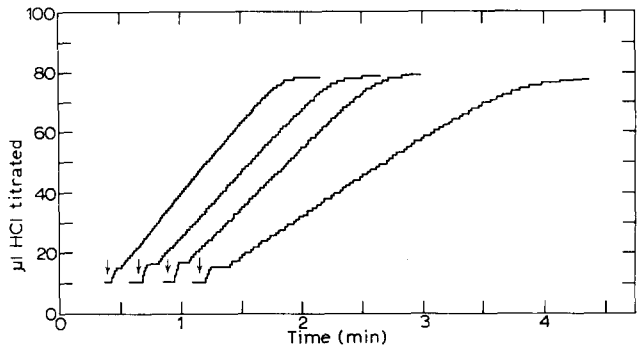

Fig. 2. Consecutive recorder traces of the volume of acid titrated showing the effects of chloroplast preparation ageing on the rate of H^+ consumption during photophosphorylation of equal amounts of ADP. The time interval between each measurement was 30 min, and the amount of ADP added, indicated by the vertical arrow, was approx. 0.8 μmole. Other conditions as described in Methods.

effect on the reaction (total dilution of reaction mixture $<5\%$). The rate of H^+ consumption was determined from the linear section of the titrant volume recording.

The consecutive traces in Fig. 2 have been chosen to illustrate the behaviour of a preparation of chloroplasts showing unusually marked ageing effects. Although the rate of H^+ consumption during photophosphorylation decreased as the chloroplasts aged, the total amount of H^+ consumed during phosphorylation of equal amounts of ADP was not affected. The decrease in rate with time was normally rather less than that exhibited by the particular chloroplast suspension used for this experiment. Ageing effects were compensated for in routine measurements by conducting control and test experiments simultaneously on the duplicated apparatus.

In Fig. 3, the relation between the rate of H^+ consumption during photophosphorylation and the amount of chloroplasts in the reaction mixture is shown. The rate of H^+ consumption during photophosphorylation measured by the appara-

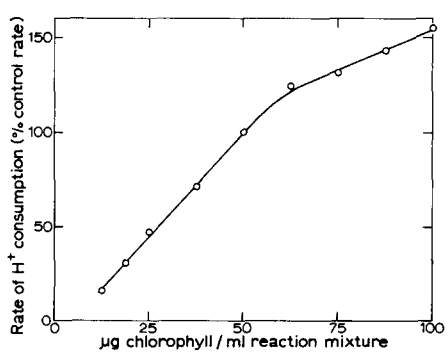

Fig. 3. The relation between the amount of chlorophyll present and the rate of H^+ consumption during photophosphorylation by spinach chloroplasts. Conditions, other than variation of chlorophyll content, as described in Methods. The control reaction mixture contained 50 μg chlorophyll/ml. Average control rate of H^+ consumption, 547 μmoles $H^+ \cdot mg^{-1}$ chlorophyll $\cdot h^{-1}$.

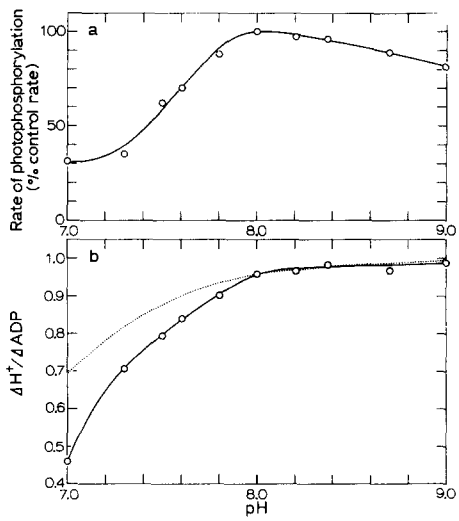

Fig. 4. Effect of pH on the rate of photophosphorylation and $\Delta H^+/\Delta ADP$. Conditions other than pH as described in Methods. (a) Rate of photophosphorylation determined from the rate of H^+ consumption and the $\Delta H^+/\Delta ADP$ value shown in (b). Average control rate, 332 μmoles ADP·mg^{-1} chlorophyll·h^{-1} at pH 8.00±0.01. (b) Effect of pH on $\Delta H^+/\Delta ADP$ determined from the total HCl titrated during photophosphorylation of 0.612 μmole ADP. The dotted line represents a theoretical curve calculated[1] for the magnesium salts of ATP, ADP and P_i.

tus was linearly related to the amount of chloroplasts in the suspension up to a chlorophyll concentration of 60 μg/ml. The slight departure from direct proportionality with decreasing chlorophyll concentrations is typical for photophosphorylation[11] and other chloroplast reactions[12], while the departure from linearity at high concentrations is caused by light limitation. Photophosphorylation with pyocyanine as cofactor requires extremely high light intensities for saturation[13]. The theoretical maximum rate of addition of titrant by the apparatus is 5 times greater than the highest rates observed here, and there was never any indication from the pH recordings of inadequate pH control.

Fig. 4 shows the effect of pH on the $\Delta H^+/\Delta ADP$ ratio and on the rate of photophosphorylation. The maximum rate was observed at pH 8.0. The measured values of $\Delta H^+/\Delta ADP$ were close to those calculated from the pK_a' values for the magnesium salts of ATP, ADP and P_i by Nishimura *et al.*[1] at pH values of 8.0 and above. However, at lower pH a progressive departure was observed. The values measured here are also lower than the $\Delta H^+/\Delta P_i$ ratio of 0.882±0.048 at pH 7.4 determined by these authors from the pH change during photophosphorylation by *Rhodospirillum rubrum* chromatophores. The reason for this disparity is not known, although a possible cause might be the influence of divalent cations other than magnesium in the chloroplasts on the pK_a' values for ATP, ADP and P_i. For practical purposes it is obviously desirable to determine the $\Delta H^+/\Delta ADP$ ratio for individual conditions.

The validity of pH-stat titration as a measure of photophosphorylation was tested by comparing the $\Delta H^+/\Delta ADP$ ratio measured during phosphorylation of a standard amount of ADP with $\Delta H^+/\Delta ATP$ ratios determined from the direct assay for ATP by firefly luciferase, and the results are shown in Table I. The $\Delta H^+/\Delta ATP$

TABLE I

STOICHIOMETRY OF H^+ CONSUMPTION DURING PHOTOPHOSPHORYLATION

pH 8.00 ± 0.01, reaction conditions described in Methods. Values are expressed as means ± S.E. (number of determinations).

$\Delta H^+/\Delta ATP$ (phosphorylation of approx. 50% added ADP)	0.967 ± 0.022 (8)
$\Delta H^+/\Delta ATP$ (phosphorylation to completion)	0.976 ± 0.020 (8)
$\Delta H^+/\Delta ADP$ (phosphorylation to completion)	0.959 ± 0.004 (14)

ratios were calculated from the amount of acid titrated after addition of approx. 0.8 μmole ADP to the illuminated chloroplasts, and the amount of ATP formed as determined by the firefly luciferase assay procedure. The reaction was terminated either by switching off the light after phosphorylation of about 50% of the added ADP in the first set of experiments, or by allowing the reaction to continue in the light until titration of acid ceased due to phosphorylation of all the ADP, as in the second set of experiments. The $\Delta H^+/\Delta ADP$ ratio was determined from the total amount of acid titrated during photophosphorylation of a standard amount of ADP. Similar mean values for $\Delta H^+/\Delta ATP$ were obtained whether phosphorylation was allowed to proceed to completion in the light, or terminated at 50% completion. The volume of acid titrated by the apparatus should not be affected by any net H^+ efflux from the chloroplast thylakoids on darkening, if phosphorylation in the dark is negligible. The $\Delta H^+/\Delta ATP$ values were not significantly different from the mean $\Delta H^+/\Delta ADP$ ratio. This gives considerable confidence that under these conditions of cyclic photophosphorylation, the reaction mixture is free from any variable side reactions involving hydrogen ions, and from any other reactions involving ADP or ATP.

It may be concluded from these results that the continuous recording of H^+ consumption by titration at constant pH in the apparatus described can be used as a convenient and precise method for the continuous measurement of photophosphorylation.

ACKNOWLEDGEMENTS

We wish to thank Mrs K. Holborow and Mrs C. Case for their technical assistance. This work was supported by a grant from the S.R.C. (U.K.).

REFERENCES

1 Nishimura, M., Itoh, T. and Chance, B. (1962) *Biochim. Biophys. Acta* 59, 177–182
2 Walz, D., Schuldiner, S. and Avron, M. (1971) *Eur. J. Biochem.* 22, 439–444
3 Gross, E. (1971) *Arch. Biochem. Biophys.* 147, 77–84
4 Shavit, N., Degani, H. and San Pietro, A. (1970) *Biochim. Biophys. Acta* 216, 208–219
5 Polya, G. M. and Jagendorf, A. T. (1969) *Biochem. Biophys. Res. Commun.* 36, 696–703
6 Emmet, J. M. and Walker, D. A. (1973) *Arch. Biochem. Biophys.* 157, 106–113
7 Arnon, D. I. (1949) *Plant Physiol.* 24, 1–10
8 Delieu, T. and Walker, D. A. (1971) *New Phytol.* 71, 201–225
9 Nielsen, R. and Rasmussen, H. (1968) *Acta. Chem. Scand.* 22, 1757–1762
10 Stanley, P. E. and Williams, S. G. (1969) *Anal. Biochem.* 29, 381–392
11 Allen, M. B., Whatley, F. R. and Arnon, D. I. (1958) *Biochim. Biophys. Acta* 27, 16–23
12 Walker, D. A., Kosciukiewicz, K. and Case, C. (1973) *New Phytol.* 72, 237–247
13 Avron, M. and Neumann, J. (1968) *Annu. Rev. Plant Physiol.* 19, 137–166

Biochimica et Biophysica Acta, 314 (1973) 360–371

BBA 46593

MONOMOLECULAR FILMS OF BACTERIOCHLOROPHYLL AND DERIVATIVES AT AN AIR–WATER INTERFACE: SURFACE AND SPECTRAL PROPERTIES*

P. REINACH, B. B. AUBREY and S. S. BRODY

Department of Biology, New York University, Washington Square, New York, N. Y. 10003 (U.S.A.)

(Received March 19th, 1973)

SUMMARY

Monomolecular films of bacteriochlorophyll, bacteriopheophytin and 2-desvinyl-2-acetyl chlorophyll *a* were prepared and studied on aqueous subphases containing pH 7.8 buffer and $4 \cdot 10^{-4}$ M ascorbate. These monolayers are mechanically stable in the dark and light at 15 °C. At surface pressures below about 18 dynes/cm the slope of the surface isotherm of bacteriochlorophyll is steeper than at pressures greater than 18 dynes/cm. The surface dipole moments of bacteriochlorophyll are less than half that reported for chlorophyll *a*. Compression of bacteriochlorophyll or bacteriopheophytin monolayers result in changes of their absorption spectra.

Compression of bacteriochlorophyll monolayers to 18 dynes/cm results in a shift of the pigment's red peak from 787 to 749 nm as well as the appearance of a new absorption maximum at 896 nm. Continued compression to 24 dynes/cm results in a slight decrease in peak height of the 794-nm maximum and further increase in the absorbance of the 896-nm maximum. With bacteriopheophytin the red maximum at 760 nm starts to shift when the film is compressed to a surface pressure of only 2 dynes/cm; further compression yields a new absorption maximum at 846 nm. Compression of a film of 2-desvinyl-2-acetyl chlorophyll *a* results in only a 10-nm shift of the absorption maximum at 690 nm.

An orientation of bacteriochlorophyll at an air–water interface is proposed that is different from that for chlorophyll *a*. Like chlorophyll *a* bacteriochlorophyll monolayers are closely packed, but different in that bacteriochlorophyll allows greater interaction between pigment molecules. In compressed monolayers bacteriochlorophyll appears to aggregate differently than in other model systems.

INTRODUCTION

The infrared absorption maxima of bacteriochlorophyll *a*, bacteriochlorophyll, was shown to occur at considerably longer wavelengths in chromatophores than in organic solvents[1]. The specialized environment giving rise to the red shift of bacterio-

* This paper is based upon a dissertation submitted by Peter Reinach in partial fulfillment of the requirements for the Ph. D. degree of New York University, New York, N.Y., U.S.A.

chlorophyll in the condensed *in vivo* state has been attributed to interaction of bacteriochlorophyll with other bacteriochlorophyll molecules, proteins, and lipids[2,3]. In bacteriochlorophyll–protein complexes it has been shown that interaction of at least five bacteriochlorophyll molecules are responsible for both the dichroic properties and the observable exciton splitting[4]. Since bacteriochlorophyll contains both hydrophobic and hydrophillic groups, it has been suggested that most of the molecules are arranged at interfaces between proteins and lipids or between a lipid double layer[5].

A well defined model system that lends itself to quantitative interpretation an reproduces, in part, the *in vivo* structure is a bacteriochlorophyll monolayer at an air–water interface. In such a system the pigment packing appears to approximate the *in vivo* situation better than other model systems. Heretofore, the lability of bacteriochlorophyll monolayers has precluded their systematic study. Recently it has been demonstrated that by the addition of sodium ascorbate to the aqueous subphase, monomolecular films of bacteriochlorophyll can be stabilized[6].

The physical, spectral, and chemical properties of bacteriochlorophyll and several of its derivatives in monomolecular films at an air–water interface are presented in this paper. The spectral properties of bacteriochlorophyll monolayers are found to resemble those of photosynthetic bacteria. The spectral transformations observed with compressed bacteriochlorophyll monolayers are sufficient to be indicative of strong exciton interactions. These spectral transformations appear to be related to characteristic changes in the surface isotherm and surface potential of monomolecular films of bacteriochlorophyll.

METHODS AND MATERIALS

Monolayer and spectral studies were carried out using the apparatus described previously[7–9]. *Rhodospirillum rubrum* was grown under conditions described by Eimhjellen[10]. Bacteriochlorophyll, oxidized bacteriochlorophyll and bacteriochlorophyll pheophytin were prepared by methods described by Smith and Calvin[11]. All monolayer studies were carried out at 15 °C.

The subphase contained $2 \cdot 10^{-2}$ M phosphate buffer (pH 7.8) and $4 \cdot 10^{-4}$ M sodium ascorbate. Bacteriochlorophyll was spread onto the aqueous surface using benzene as a spreading solvent. The exact concentration of the spreading solution was determined spectrometrically (Cary 14R). The concentration of pigment in benzene was calculated from the absorbance using the molar extinction coefficients which were determined to be $75 \cdot 10^3$ $M^{-1} \cdot cm^{-1}$ for bacteriochlorophyll (at 780 nm), $60 \cdot 10^3$ $M^{-1} \cdot cm^{-1}$ for oxidized bacteriochlorophyll (at 682 nm). The surface of the subphase was cleaned and then about 300 μl of solution was delivered slowly over the surface from a Hamilton microliter syringe. The environmental chamber housing the surface balance was evacuated with a vacuum pump and then flushed several times with nitrogen.

Three parameters were used to characterize bacteriochlorophyll monolayers: (π–A) surface isotherms, surface potentials, ΔV, and absorption spectra. The area per molecule extrapolated to zero surface pressure ($\pi = 0$) is referred to as A_0. A has dimensions of Å^2/molecule. The surface pressure, π, at which bacteriochlorophyll monolayers collapse is referred to as π_c. ΔV is the difference in surface potential between a clean water surface, V_{H_2O}, and film on the water surface, V (*i.e.* $\Delta V = V - V_{H_2O}$).

The perpendicular component of the molecular surface dipole moment $\mu_\perp$ can be calculated from the data using the relationship

$$\Delta V = 12\,\pi\,\mu_\perp/A + V_w \qquad (1)$$

where $1/A$ is pigment concentration on the surface. From the slope of the line determined by Eqn 1, $\mu_\perp$ can be calculated in millidebyes, mD. V_w, the surface potential of water under the bacteriochlorophyll film, is equal to the y intercept of Eqn 1.

The spectral behavior of bacteriochlorophyll in monlayers was studied by measuring the absorbances of the pigments' absorption maxima as a function of $1/A$. The absorption maxima are given as $A\,\lambda$ (*e.g.* A 896) where λ is the wavelength (in nm) of the absorption maxima. In cases where the wavelength of absorption maxima are obtained from the deconvolution of the absorption spectra the bands are designated as $B\,\lambda$ (*e.g.* B 870). The absorption bands were deconvoluted using the program RESOLV[12].

Potassium phosphate salts were purchased from Fisher Chemical, sodium ascorbate from Fluka, A. G. (Bucks, S. G.), benzene spectral grade from Mallinckrodt, oleyl alcohol and lecithin from Applied Science Laboratories (State College Park, Pa.).

RESULTS

Bacteriochlorophyll in benzene solution

The characteristic spectra of bacteriochlorophyll, bacteriopheophytin, and oxidized bacteriochlorophyll in benzene are shown in Fig. 1. Spectral data for the above pigments are summarized in Table I.

Bacteriochlorophyll in benzene decomposes rapidly when exposed to air and light. In air and darkness the pigment undergoes a slow oxidation to 2-desvinyl-2-acetyl chlorophyll a[11]. Under a nitrogen atmosphere and in darkness bacteriochlorophyll can be stored in wet benzene without signs of decomposition; no change in the red/blue ratio is observed after storage for 24 h.

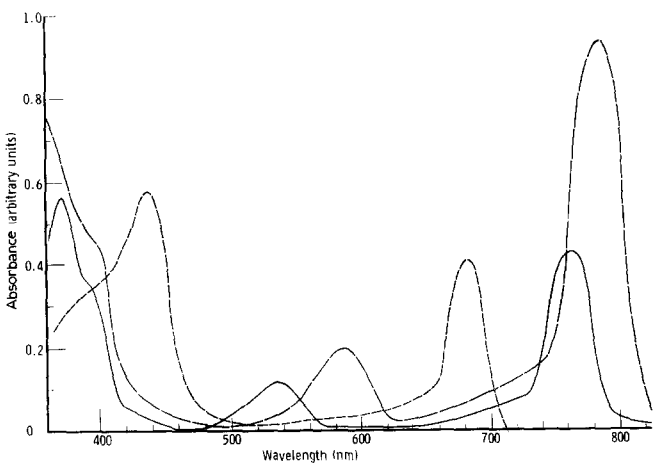

Fig. 1. Absorption spectra of benzene solutions of bacteriochlorophyll is shown by long dashes (— — —), bacteriopheophytin by a solid line (———), and 2-desvinyl-2-acetyl chlorophyll *a* by short dashes (- - - - -).

TABLE I

SPECTRAL PROPERTIES OF BACTERIOCHLOROPHYLLOUS PIGMENTS IN BENZENE SOLUTION

	Wavelengths of maxima (nm)	*Extinction coefficient of red band* ($M^{-1} \cdot cm^{-1}$)	*Red/blue ratio*
Bacteriochlorophyll	357, 396, 578, 780	$75 \cdot 10^3$	1.30 (780/357)
Bacteriopheophytin	364, 390, 530, 749	$60 \cdot 10^3$	0.65 (749/364)
Oxidized bacteriochlorophyll	436, 682	$68 \cdot 10^3$	0.71 (682/436)

Bacteriochlorophyll isotherms

A monolayer of bacteriochlorophyll on a subphase containing only $2 \cdot 10^{-2}$ M phosphate buffer (pH 7.8) is not stable. Isotherms of bacteriochlorophyll show a time-dependent increase in the value for A_0 even if the environmental chamber is kept in a nitrogen atmosphere and darkness. In Fig. 2 are shown two isotherms measured 20 and 90 min after the bacteriochlorophyll monolayer is formed. A_0 is seen to increase 15Å^2/molecule during this time. However, with $4 \cdot 10^{-4}$ M sodium ascorbate added to the subphase A_0 is invariant. In the presence of ascorbate bacteriochlorophyll monolayers are chemically stable for at least 6 h in either air or nitrogen. Furthermore, the films are stable in light.

One of the techniques used to examine the spectral stability of bacteriochlorophyll monolayers is to collect the film and measure their absorption spectra in a benzene solution. A criterion of bacteriochlorophyll purity is the value of the peak ratio 780/357 nm; pure bacteriochlorophyll in benzene has a peak ratio of 1.30. The rate of formation of oxidized bacteriochlorophyll (*i.e.* decrease in the peak ratio of 780/357

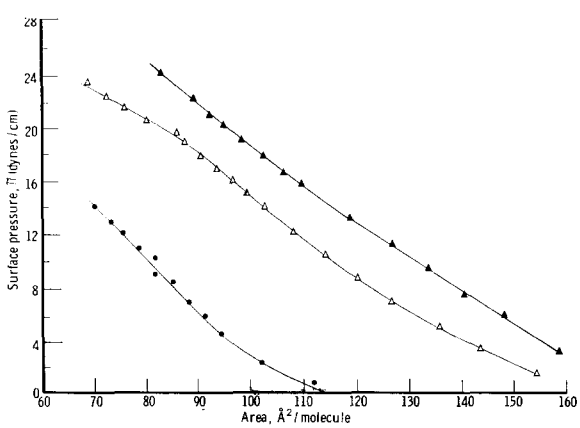

Fig. 2. Surface pressure (π, dynes/cm) as a function of area per molecule (Å^2) in a N_2 atmosphere and darkness. Initial bacteriochlorophyll isotherm is shown by △—△; isotherm after film has been on the surface for 1.5 h with no ascorbate in subphase is shown by ▲—▲. The subphase contains 0.02 M phosphate buffer (pH 7.8) at 15 °C. The surface isotherm of bacteriopheophytin measured with a subphase containing $2 \cdot 10^{-2}$ M sodium acetate buffer (pH 3.7) and no ascorbate is shown by ●—●.

nm) can be correlated with the time-dependent increases in A_0. Only when the subphase contains $4 \cdot 10^{-4}$ M sodium ascorbate is the value of the ratio 780/357 nm of the recovered bacteriochlorophyll in agreement with that for pure bacteriochlorophyll. In all the subsequent monolayer studies the subphase contains $2 \cdot 10^{-2}$ M phosphate buffer (pH 7.8) and $4 \cdot 10^{-4}$ M sodium ascorbate.

Isoterms of bacteriochlorophyll monolayers have an A_0 of 147 Å^2/molecule. When these monolayers are slowly compressed at the rate of 0.5–25 Å^2/molecule per min they collapse at a π_c between 24 and 25.5 dynes/cm. Between 18 dynes/cm and π_c the isotherm appears to have a shallower slope than between 0 and 18 dynes/cm (Fig. 2).

When the pH of the subphase is < 4 monolayers of bacteriochlorophyll are rapidly converted into bacteriopheophytin. Monolayers of bacteriopheophytin collapse at a π_c of 16 dynes/cm. Pheophytinization of bacteriochlorophyll on subphases more alkaline than pH 4 results in bacteriopheophytin monolayers that a only compressible to between 8 and 12 dynes/cm. In Fig. 2 is shown the isotherm of bacteriopheophytin on a subphase of pH 3.7; the A_0 is 105 Å^2/molecule.

Surface potential measurements of bacteriochlorophyll monolayers

The surface potential, ΔV, of bacteriochlorophyll monolayers increases gradually upon compression. In Fig. 3b ΔV increases for concentrations between $6.5 \cdot 10^{13}$ and $9 \cdot 10^{13}$ molecules/cm^2 and also between $10 \cdot 10^{13}$ molecules/cm^2 and π_c; ΔV appears to remain constant between $9 \cdot 10^{13}$ and $10 \cdot 10^{13}$ molecules/cm^2. Within the precision of the experiments (*i.e.* $\pm$ 10 mD) the values of $\mu_\perp$ between $6.5 \cdot 10^{13}$ and $9 \cdot 10^{13}$ molecules/cm^2 and between $10 \cdot 10^{13}$ molecules/cm^2 and π_c are 310 and 283 mD, respectively.

The surface potential measured for water in the absence of a bacteriochlorophyll monolayer, V_{H_2O}, (*i.e.* -30 mV) does not agree with V_w (*i.e.* 180 mV) which is obtained from Eqn 1 and the data in Fig. 3b. (The value of V_{H_2O} is a little high; values of -80 mV or less are more common.)

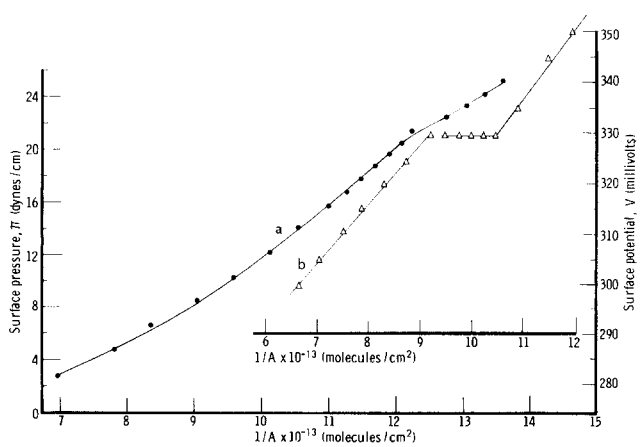

Fig. 3. Surface potential (Curve b) and surface pressure (Curve a) for a film of bacteriochlorophyll as a function of pigment concentration, $1/A$. The subphase contained 0.02 M phosphate buffer (pH 7.8) and $4 \cdot 10^{-4}$ M ascorbate at 15 °C.

Absorption spectra of bacteriochlorophyll monolayers

The absorption spectrum of bacteriochlorophyll monolayers at surface pressures of 1.5, 22.3 and 26.5 dynes/cm are shown in Fig. 4, respectively. At 1.5 dynes/cm absorption maxima are at 584 and 787 nm. Compressing the film to π = 18 dynes/cm results in broadening of the absorption band and a red shift of the 584 and 787 nm maxima to 592 and 794 nm, respectively. From the difference in the absorption spectrum between expanded and slightly compressed bacteriochlorophyll monolayers it is found that a pigment species is formed having an absorption maximum around 825 nm (see Fig. 9). At π = 20 dynes/cm a new band with an absorption maximum at about 882 nm is clearly resolved. With further compression this latter band appears to shift toward longer wavelengths reaching a limiting value of 896 nm at π = 22 dynes/cm. The absorbance of A_{896nm} continues to increase even after the film is compressed beyond its collapse point.

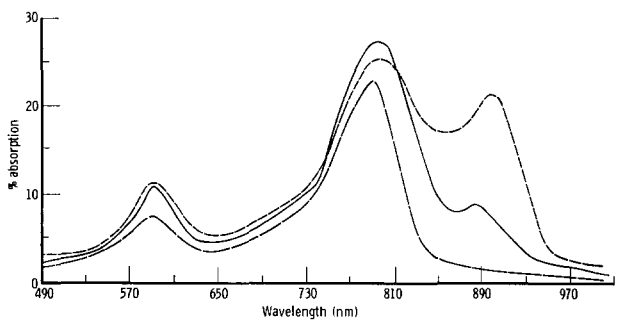

Fig. 4. Absorption spectra of a monolayer of bacteriochlorophyll at different surface pressures, π; the subphase is the same as in Fig. 3. The spectrum at π = 1.5 dynes/cm is shown by (– – –); the spectrum at π = 22.3 dynes/cm is shown by (———); the spectrum at π = 26.5 dynes/cm is shown by (– – – – –). Percent absorption is for light passing through the film 18 times.

In Fig. 5 are shown the absorbances at 592, 794, and 896 nm as a function of molecules/cm^2, $1/A$. Compression of bacteriochlorophyll monolayers results in complex changes of the absorbances of these absorption bands. Both A 592 and A 794 increase rather linearly to about 18 dynes/cm ($1/A = 10.5 \cdot 10^{13}$ molecules/cm^2, *i.e.* 100 Å^2/molecule). In the region between $10.5 \cdot 10^{13}$ and $13.7 \cdot 10^{13}$ molecules/cm^2 the values of A 592 and A 794 are found to decrease slightly. At still higher concentrations the absorbance of these bands increase again. A 896 first appears at 20 dynes/cm, its absorbance continues to increase with compression even beyond π_c.

Absorption spectra of mixed monolayers

Mixed monolayers of bacteriochlorophyll with lecithin and bacteriochlorophyll with oleyl alcohol were studied to determine whether these diluants prevent the pigment interactions which lead to the appearance of A 896. A 592 and A 794 for mixed films of bacteriochlorophyll and oleyl alcohol or lecithin as a function of bacteriochlorophyll concentration in the film, $1/A_m$, are shown in Fig. 5. The absorbances for a mixed monolayer of bacteriochlorophyll and oleyl alcohol (pigment mole fraction 0.24) or lecithin (pigment mole fraction 0.42) are slightly greater than the extrapolated values for pure bacteriochlorophyll monolayers. With either diluent compressed

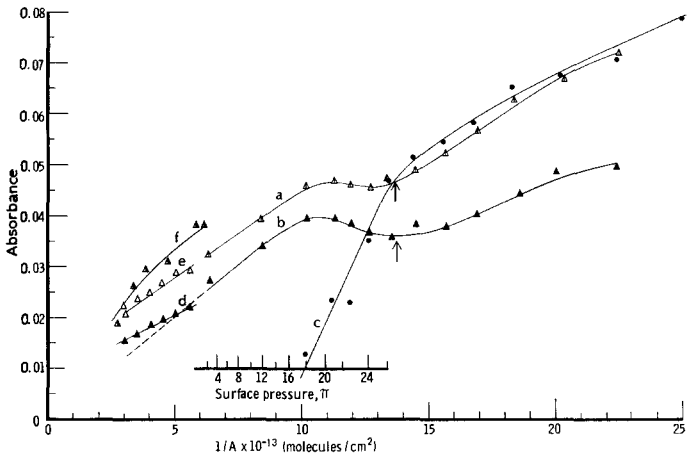

Fig. 5. Absorbance at 592 nm (a), 794 nm (b) and 896 nm (c) for a film of bacteriochlorophyll as a function of pigment concentration, $1/A$. The absorbance axis must be multiplied by 2 for the 896-nm band an by 4 for the 794-nm band. For a mixed film of bacteriochlorophyll and oleyl alcohol the absorbance at 592 nm is shown by Curve f; the mole fraction of bacteriochlorophyll is 0.24. For a mixed film of bacteriochlorophyll and lecithin the absorbance at 592 nm and 794 nm are shown by Curves e and d, respectively; mole fraction of bacteriochlorophyll is 0.42. The collapse pressure is indicated by an arrow, ↗. The surface pressure corresponding to $1/A$ for a bacteriochlorophyll isotherm is indicated by the horizontal axis inserted in the figure. The absorbance is for light passing through the film 18 times. The subphase is the same as in Fig. 3.

films do not show the characteristic long wavelength band at 896 nm found in compressed monolayers of bacteriochlorophyll.

Absorption spectra of bacteriopheophytin monolayers

A film of bacteriopheophytin is found to have absorption maxima at 530, 762 and 846 nm. In Fig. 6 is shown the spectra at π equal to 2, 6, and 10 dynes/cm. At π = 10 dynes/cm, films of bacteriopheophytin collapse.

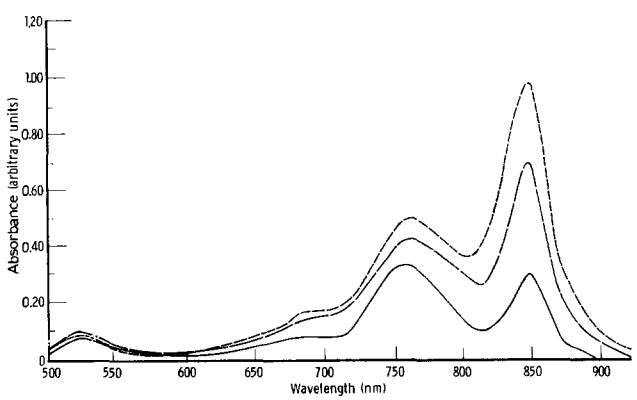

Fig. 6. Absorption spectra of a film of bacteriopheophytin, at surface pressure of 2 (———), 6 (– – –) and 10 (– – – – –) dynes /cm. The absorbance is for light passing through a film 18 times. The subphase is the same as in Fig. 3.

Deconvolution of absorption spectra of bacteriochlorophyll monolayers

Absorption spectra may be deconvoluted by fitting Gaussian and mixed Gaussian and Lorentian curves to the spectra[12]. In Fig. 7 is shown the result of one curve fitting carried out by French on an absorption spectrum of a compressed film of bacteriochlorophyll. This analysis showed that the spectra of bacteriochlorophyll

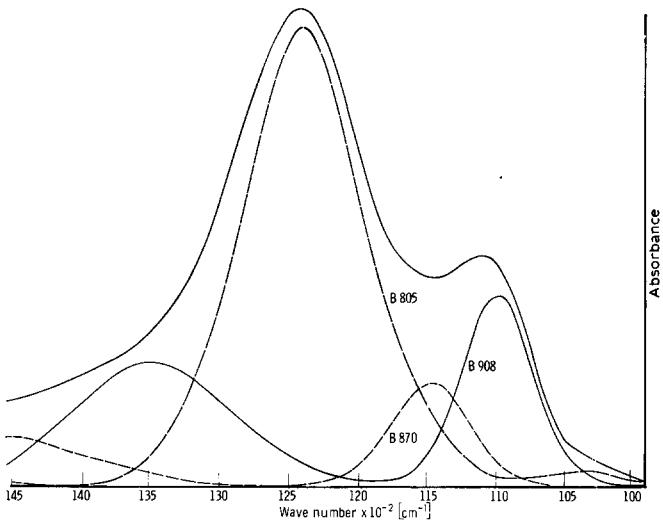

Fig. 7. Deconvolution of the absorption spectrum of the bacteriochlorophyll monolayer shown in Fig. 4 at π = 26.5 dynes/cm (courtesy of C.S. French). Absorbance is plotted as a function of wave number.

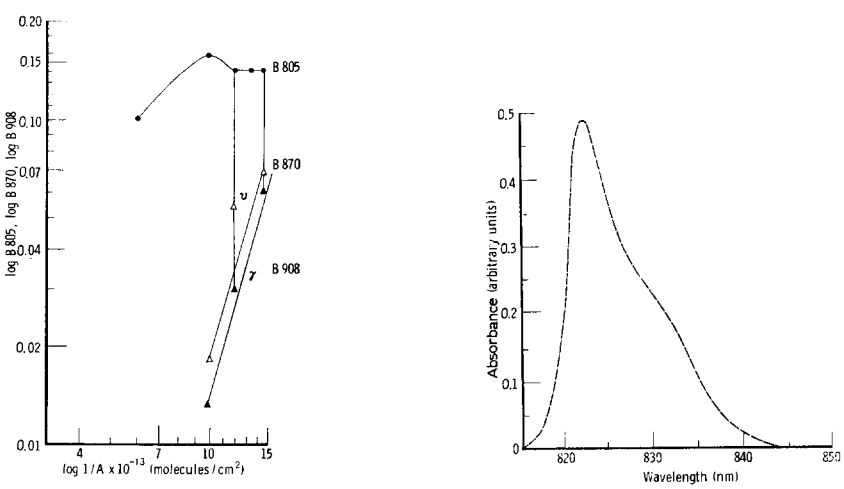

Fig. 8. Log–log plot of *B* 805, *B* 870 and *B* 908 as a function of surface concentration $1/A$. Absorbances are obtained from deconvolution of the absorption spectra shown in Fig. 4. The absorbance is for light passing through a film 18 times. The subphase is the same as in Fig. 3.

Fig. 9. Difference in absorption spectra of a bacteriochlorophyll monolayer at two different surface concentrations, *i.e.* $1/A$ is equal to $6 \cdot 10^{13}$ and $8 \cdot 10^{13}$ molecules/cm^2. The subphase is the same as in Fig. 3.

film (Fig. 4) can be deconvoluted into three absorption maxima in the 800–910-nm region. These maxima are designated *B* 805, *B* 870, and *B* 908 where the numerics indicate the peak position of the red absorption maximum. In Fig. 8 is shown a log–log plot of *B* 805, *B* 870, and *B* 908 as a function of $1/A$. The slopes of *B* 870 and *B* 908 are the same and the ration of *B* 908/*B* 870 is constant. This indicates that *B* 870 and *B* 908 are probably characteristic of a single absorbing species. At higher values of $1/A$ there is indication of still another absorbing species *B* 950

DISCUSSION

It is of interest to compare the properties of bacteriochlorophyll monolayers with those reported for chlorophyll monolayers (Bellamy *et al.*[13]). The A_0 for bacteriochlorophyll is 147 Å^2/molecule while for chlorophyll it is 122 Å^2/molecule[13]. Unlike the uniform slope of the chlorophyll isotherm the slope of the bacteriochlorophyll isotherm changes in value at around 18 dynes/cm. This change in slope of bacteriochlorophyll isotherms may reflect a reorientation of the pigment on the surface. A shallower slope indicates a decrease in intermolecular repulsive forces. A change in the orientation of the porphyrin planes with respect to the water surface or change in points of attachment may account for the increase in compressibility.

The surface dipole moments of bacteriochlorophyll and chlorophyll are very different. Bellamy *et al.*[13] obtained a single value of about 700 mD for chlorophyll. In the case of bacteriochlorophyll the $\mu_\perp$ appears to vary with $1/A$. The values of $\mu_\perp$ for bacteriochlorophyll are about 400 mD smaller than for chlorophyll. From Fig. 3b it was calculated that $\mu_\perp$ has values of 210 and 283 mD. In Fig. 3a where π is also plotted as a function of $1/A$ it can be seen that the transition region in the behavior of ΔV lies between 10 and 16 dynes/cm. That the above change in ΔV (or $\mu_\perp$) occurs at a lower value of $1/A$ than the change in slope of the surface isotherm (18 dynes/cm) might indicate that ΔV is a more sensitive parameter for detecting changes in molecular orientation. The smaller values of $\mu_\perp$ for bacteriochlorophyll compared to chlorophyll could, in part, be accounted for by bacteriochlorophyll lying flatter on the surface and having a larger A_0 than chlorophyll.

Bellamy *et al.*[13] have suggested that the chlorophyll porphyrin rings are anchored to the water surface by the ester linkages on Rings IV and V. It appears that Ring I of bacteriochlorophyll might be closer to the aqueous surface than is the case for chlorophyll's Ring I. This suggestion stems, in part, from the fact that the measured potential for water, V_{H_2O}, does not agree with V_w, the surface potential of water under the bacteriochlorophyll film. Similar suggestions of reorientation of subphase molecules have been made for other surface active materials[14,15]. An orientation for bacteriochlorophyll which could account for the difference between V_w and V_{H_2O} is one where the acetyl group of Ring I as well as the ester linkages of the molecule serve as anchorage points for bacteriochlorophyll to the aqueous surface. The strong electronegative charge of oxygen in the acetyl group of Ring I might induce a reorientation of the water molecules at the interface. The fact that V_w is about +180 mV might indicate that the more electropositive hydrogens are closer to the surface than would be the case in the absence of a bacteriochlorophyll film (where V_{H_2O} is −30 mV).

This suggestion of an orientation for bacteriochlorophyll different from that

of chlorophyll is consistent with a suggestion made previously on the basis of the oxidative properties of bacteriochlorophyll monolayers[16]. Since addition of an oxidant to the subphase resulted in a dehydrogenation of Ring II (to form 2-desvinyl-2-acetyl chlorophyll *a*, oxidized) bacteriochlorophyll it was suggested that Ring II of bacteriochlorophyll lies close to the aqueous surface. The proximity of Ring II to the aqueous surface may result from an additional anchorage point for bacteriochlorophyll at Ring I.

Jacobs *et al.*[17] described the spectral transformations of chlorophyll from a solution to a crystalline phase. With methyl bacteriochlorophyllide they observed a progressive shift of the red band from 770 to about 850 nm. The band with absorption maximum at 850 nm had a long wavelength shoulder extending to nearly 950 nm. They calculated the interaction energy $\Delta E/hc$ for the formation of this spectral shift to be 1800 cm^{-1}. They interpreted their observed spectral shifts as resulting from interaction between molecules in a monolayer.

Bacteriochlorophyll dissolved in benzene has a red peak at 780 nm while in an expanded monolayer a maximum at 787 nm is observed. This red shift is a result of solvent and pigment interaction with the aqueous subphase. Upon compression of bacteriochlorophyll monolayers to 18 dynes/cm an additional red shift from 787 to 794 nm (and band broadening) results from weak interaction between pigment molecules. Interaction energies, $\Delta E/hc$ are qual to $(1/\lambda_1 - 1/\lambda_2)$, where λ_1 is the red absorption maximum in a gaseous state, λ_2 is the red absorption maximum in a monolayer. For bacteriochlorophyll at low compression $\lambda_2 = 794$ nm; according to Rabinowitch[18] $\lambda_1 = 740$ nm. In this case $\Delta E/hc$ is weak only about 10 cm^{-1}. This value for $\Delta E/hc$ is close to that obtained for chlorophyll monolayers compressed to 15 dynes/cm[13]. The spectroscopic properties of compressed chlorophyll monolayers were interpreted as resulting from weak chromophore interaction[19], which are not sigificant enough to modify the pigment's singlet states.

At $\pi > 18$ dynes/cm, the absorbance of A 592 and A 794 decreases even though $1/A$ continues to increase. This complex behavior of A 592 and A 794 is not fully explained simply by assuming that the absorption dipoles change orientation so that they are more parallel to the direction of the incident light. The absorption transition dipoles for A 592 and A 794 are perpendicular to each other and both are in the porphyrin plane[20]. Depending upon the points of attachment of bacteriochlorophyll to the aqueous surface the projections of the absorption dipoles normal to the incident light could decrease as the porphyrin plane is compressed into a vertical orientation. Furthermore, it is to be expected that the increasing intermolecular interaction upon compression could modify the intensity of the absorption transitions.

At $\pi > 18$ dynes/cm the spectra are characteristic of a strong type of pigment interaction. The interaction energy in compressed bacteriochlorophyll monolayers is 2500 cm^{-1}; this is greater than that observed in condensed phases of methyl bacteriochlorophyllide. Such strong interaction energy is characteristic of an exciton mechanism where the interaction between absorption dipoles is large enough to affect the energy levels of bacteriochlorophyll. The strong interaction in bacteriochlorophyll monolayer probably results form pigment aggregation. The intermolecular forces resulting in the spectral changes of bacteriochlorophyll are probably weak, since the spectral transformation are completely reversible, even if the film is compressed beyond π_c and then re-expanded.

The spectral behavior may result from weak long range dipole interactions at low values of π while in more compressed states stronger short range dipole interaction prevails. These weak and strong interactions may be associated with different types of pigment aggregates or orientations. Formation of aggregates could readily result in orientation changes of bacteriochlorophyll at the surface, as well as alterations of energy levels and absorption transition probabilities. Further data is required to develop a detailed model correlating spectral transformations with the changes in orientation and aggregation accompanying compression of bacteriochlorophyll monolayers.

The appearance of an absorption maximum at 846 nm in monolayers bacteriopheophytin of upon compression to only 2 dynes/cm indicates a stronger type of pigment interaction than that found in bacteriochlorophyll monolayers. Removal of Mg from the porphyrin nucleus apparently permits strong interaction even when $1/A$ is comparatively small.

The spectral transformations observed upon compression of oxidized bacteriochlorophyll monolayers are similar to those found with chlorophyll monolayers. These changes include a slight increase of the half-band width of the red band and a linear increase in absorbance of the red band with pigment concentration. The spectral changes indicate a weak type of pigment interaction (*i.e.* $\Delta E/hc < 10\ cm^{-1}$). Unlike the change in slope of the surface isotherm and potential observed with bacteriochlorophyll, uniform behavior of both parameters are obtained with oxidized bacteriochlorophyll.

The fact that in monolayers bacteriochlorophyll and its pheophytin show stronger pigment interaction than chlorophyll and oxidized seems to result from differences in chemical structure and possibly also pigment orientation. The removal of two hydrogens from bacteriochlorophylls tetrahydroporphyrin nucleus to form the dihydroporphyrin derivative, oxidized bacteriochlorophyll, eliminates the possibility of strong interaction. In oxidized bacteriochlorophyll a double bond substistitutes for the two hydrogens on Ring II of bacteriochlorophyll. Perhaps this double bond is important for shielding the dipoles of contiguous chromophores from one another so that only weak interactions result.

The absorption spectrum of a compressed film of bacteriochlorophyll is similar to the spectra of *Chromatium* and *Rhodopseudomonas palustris* in that the absorption band of *A* 896 is less than *A* 794. In some species of photosynthetic bacteria the major absorption band is around 880 nm (*Rhodospirillum rubrum*) or 850 nm (*Rhodopseudomonas spheroides*). The similarity of the absorption spectra of bacteriochlorophyll monolayer with *in vivo* spectra makes the bacteriochlorophyll monolayers attractive as a model for *in vivo* phenomena. The preceeding supports the finding that pigment–pigment interactions in a membrane account to a large extent for the spectral properties observed *in vivo*[21].

REFERENCES

1 Clayton, R. K. (1963) in *Bacterial Photosynthesis* (Gest, A., San Pietro, A. and Vernon, L. P. eds), pp. 495–500, Antioch Press, Yellow Springs, Ohio

2 Olson, J. M. and Stanton, E. K. (1966) in *The Chlorophylls* (Vernon, L. P. and Seeley, G. R., eds), pp. 381–382, Academic Press, New York, N.Y.

3 Clayton, R. K. (1965) *Molecular Physics in Photosynthesis*, p. 150, Blaisdell Publishing Co., New York, N.Y.
4 Phillipson, K. and Sauer, K. (1972) *Biochemistry* 11, 1880–1885
5 Oelze, N. and Drews, G. (1972) *Biochim. Biophys. Acta* 265, 209–241
6 Reinach, P. (1972) Ph. D. Thesis, New York University, New York, N.Y.
7 Aghion, J., Broyde, S. and Brody, S. S. (1969) *Biochemistry* 8, 3120–3126
8 Brody, S. S. (1971) *Z. Naturforsch.* 26b, 134–139
9 Brody, S. S. (1971) *Z. Naturforsch.* 26b, 922–929
10 Eimhjellen, K. E., Aasmundrud, O. and Jensen, A. (1963) *Biochem. Biophys. Res. Commun.* 10, 232–236
11 Smith, J. R. L. and Calvin, M. (1966) *J. Am. Chem. Soc.* 88, 4500–4506
12 Tunnicliff, D. D. (1970) *Shell Development*, Oakland, Calif. and French, C. S., Stanford University, Palo Alto, Calif., private communication
13 Bellamy, W. D., Gaines, G. L. and Tweet, A. G. (1963) *J. Chem. Phys.* 39, 2528–2538
14 Gaines, G. L. (1966) *Insoluble Monolayers at Liquid–Gas Interfaces*, pp. 191–192, J. Wiley–Interscience, New York, N.Y.
15 Ghosh, S. and Bull, H. B. (1963) *Biochemistry* 2, 411–415
16 Reinach, P. and Brody, S. S. (1972) *Biochemistry* 11, 92–96
17 Jacobs, E. E., Holt, A. S., Kromhout, R. and Rabinowitch, E. (1957) *Arch. Biochem. Biophys.* 72, 495–511
18 Rabinowitch, E. (1956) *Photosynthesis and Related Processes*, p. 1823, Interscience, New York, N.Y.
19 Gaines, G. L., Tweet, A. G. and Bellamy, W. D. (1965) *J. Chem. Phys.* 42, 2193–2199
20 Goedheer, J. C. (1957) Ph. D. Thesis, Univ. Utrecht, Utrecht
21 Olson, J. M. and Stanton, E. K. (1966) in *The Chlorophylls* (Vernon, L. P. and Seeley, G. R., eds), p. 387, Academic Press, New York, N.Y.

Biochimica et Biophysica Acta, 314 (1973) 372–381

BBA 46604

BIPYRIDYLIUM QUATERNARY SALTS AND RELATED COMPOUNDS. V. PULSE RADIOLYSIS STUDIES OF THE REACTION OF PARAQUAT RADICAL WITH OXYGEN. IMPLICATIONS FOR THE MODE OF ACTION OF BIPYRIDYL HERBICIDES*

J. A. FARRINGTON[a], M. EBERT[b], E. J. LAND[b] and K. FLETCHER[c]

[a] *Imperial Chemical Industries Limited, Jealott'sHill Research Station, Bracknell, Berkshire, RG12 6EY*; [b] *Paterson Laboratories, Christie Hospital and Holt Radium Institute, Manchester, M20 9BX*; [c] *Imperial Chemical Industries Limited, Alderley Park, Macclesfield, Cheshire (Great Britain)*

(Received March 14th, 1973)
(Revised manuscript received June 27th, 1973)

SUMMARY

1. Rate constants for reduction of paraquat ion (1,1′-dimethyl-4,4′-bipyridylium, PQ^{2+}) to paraquat radical ($PQ^{+\cdot}$) by e^-_{aq} and $CO_2^{-\cdot}$ have been measured by pulse radiolysis. Reduction by e^-_{aq} is diffusion controlled ($k = 8.4 \cdot 10^{10}$ $M^{-1} \cdot s^{-1}$) and reduction by $CO_2^{-\cdot}$ is also very fast ($k = 1.5 \cdot 10^{10}$ $M^{-1} \cdot s^{-1}$).

2. The reaction of paraquat radical with oxygen has been analysed to give rate constants of $7.7 \cdot 10^8$ $M^{-1} \cdot s^{-1}$ and $6.5 \cdot 10^8$ $M^{-1} \cdot s^{-1}$ for the reactions of paraquat radical with O_2 and $O_2^{-\cdot}$, respectively. The similarity in these rate constants is in marked contrast to the difference in redox potentials of O_2 and $O_2^{-\cdot}$ (— 0.59 V and + 1.12 V, respectively).

3. These rate constants, together with that for the self-reaction of $O_2^{-\cdot}$, have been used to calculate the steady-state concentration of $O_2^{-\cdot}$ under conditions thought to apply at the site of reduction of paraquat in the plant cell. On the basis of these calculations the decay of $O_2^{-\cdot}$ appears to be governed almost entirely by its self-reaction, and the concentration 5 μm away from the thylakoid is still 90% of that at the thylakoid itself. Thus, $O_2^{-\cdot}$ persists long enough to diffuse as far as the chloroplast envelope and tonoplast, which are the first structures to be damaged by paraquat treatment. $O_2^{-\cdot}$ is therefore sufficiently long-lived to be a candidate for the phytotoxic product formed by paraquat in plants.

INTRODUCTION

The reaction between oxygen and paraquat radical [$PQ^{+\cdot}$, the stable 1-electron reduction product of the herbicide paraquat**, 1,1′-dimethyl-4,4′-bipyridylium, PQ^{2+}] is of interest in that it is a product of this reaction which is thought to be the true phytotoxic species which gives paraquat dichloride and other bipyridylium salts their biological activity[1]. Conventional techniques have shown[1] that hydrogen perox-

* Part IV: *J. Chem. Soc. Perkin Trans.* 1 (1972) 138–142.

** B.S.I. registered name.

ide is a stable intermediate in the reduction of oxygen to water by paraquat radical, and no intermediate radical, *e.g.* $O_2^{\cdot-}$, between oxygen and hydrogen peroxide has been detected. Such a radical is, however, a possibility for the phytotoxic species, provided it can survive long enough to diffuse to the cell membranes, which is where damage is first observed[2] in plants treated with paraquat. The lifetime of this radical will be determined by its rate of formation from paraquat radical and oxygen relative to its rate of destruction by reaction with further paraquat radical, with cell constituents, or with itself. Pulse radiolysis appeared to offer a method for measuring these rate constants, from which the status of the intermediate radical as the phytotoxic species could be assessed.

METHODS AND RESULTS

The pulse radiolysis equipment and its method of use were essentially as indicated by Land and Swallow[3]. Revised parameters used in calculating radiation doses were, for the hydrated electron, $G = 2{\cdot}80$ (ref. 4), ε (700 nm) = 17400 (ref. 5).

Irradiation of 10^{-4} M aqueous paraquat dichloride with a shorter than 0.1-μs, 600-rad pulse gave almost pure paraquat radical, as judged by comparison of the spectrum of the product formed 10 μs after pulsing with that of authentic paraquat radical solution produced by chemical reduction with zinc. The slight discrepancy between the spectra was probably due to the presence of a product formed from HO· and paraquat (see below). After irradiating a 10^{-5} M solution of paraquat dichloride, the decay curve for e^-_{aq} at 700 nm and the appearance curve for paraquat radical at 395 nm were both first order, with half-reaction times of 1.19 ± 0.01 μs and 1.22 ± 0.02 μs, respectively, giving a second-order rate constant for reaction of e^-_{aq} with paraquat of $8.4 \cdot 10^{10}$ $M^{-1} \cdot s^{-1}$.

After saturating the 10^{-4} M aqueous paraquat dichloride with nitrous oxide, irradiation gave a product with a considerably broader spectrum than paraquat radical. The absorbance at 395 nm was less than 8% of the absorbance in the absence of N_2O, and the rate of formation of the product was much slower ($t_{\frac{1}{2}} = 10$ μs). In the presence of N_2O, the hydrated electron is rapidly converted to HO· (ref. 6) which therefore becomes the major reactive species. This evidently reacts with paraquat, but not to give paraquat radical.

In order to remove this complicating side reaction, all subsequent irradiations were carried out in 0.1 M sodium formate solution. Formate reacts rapidly with HO· and H· to give $CO_2^{\cdot-}$ and either H_2O or H_2 (ref. 7). Hence, both the radicals produced in formate, *viz.* e^-_{aq} and CO_2^-, are reducing species. When 10^{-4} M paraquat dichloride in 0.1 M sodium formate solution was irradiated (200-rad pulses), the spectrum of the product was virtually identical with that of authentic paraquat radical (Fig. 1), and the yield of radical was approximately double that obtained in water alone. Based on an extinction coefficient of $1.33 \cdot 10^4$ at 605 nm for paraquat radical, determined by reducing aqueous paraquat dichloride with zinc in a stepwise manner until maximum absorption was obtained, the G value for paraquat radical formation in aqueous formate was 5.9 (*cf.* $G(e^-_{aq}) + G(HO\cdot) + G(H\cdot)^4 = 5.8 \pm 0.4$).

Irradiation of $2.5 \cdot 10^{-5}$ M paraquat dichloride in formate with pulses of increasing size (up to 9100 rad) showed that paraquat radical was not stable to large pulses. A plot of the yield of paraquat radical against pulse size gave a curve in which the initial gradient decreased with increasing dose and eventually became negative, im-

plying over-reduction of radical to dihydrobipyridyl. This reaction is known to occur with powerful chemical reducing agents, *e.g.* zinc or sodium dithionite[8]. Because of this instability of paraquat radical to large pulses it was not possible to convert, by irradiation, a solution containing paraquat and oxygen to one containing paraquat radical, $O_2^{\cdot-}$ and no oxygen, to allow the reaction of paraquat radical with $O_2^{\cdot-}$ to be followed. Instead, an indirect method had to be used (see below).

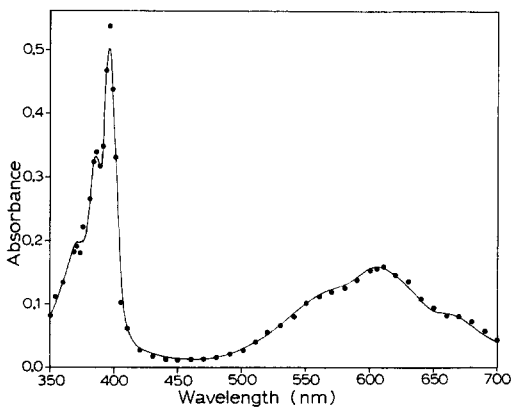

Fig. 1. Optical spectrum of paraquat radical produced by pulse radiolysis of 10^{-4} M paraquat dichloride in 10^{-1} M aqueous sodium formate. Experimental points denoted by ●. The limiting absorbance at each wavelength (10 μs after pulsing) was measured after irradiating with a 0.1-μs pulse and normalised to a constant pulse size. The continuous curve is the spectrum of paraquat radical produced by chemical reduction of paraquat dichloride in water with zinc.

Irradiation of paraquat dichloride in the presence of oxygen

10^{-3} M paraquat dichloride in 0.1 M sodium formate saturated with oxygen was irradiated with a small pulse. The decay of paraquat radical was first order. The products of the reaction were assumed to be paraquat and $O_2^{\cdot-}$ (see Discussion). The second-order rate constant for reaction of paraquat radical with O_2 was calculated (see Table I) assuming the concentration of oxygen had not been altered by the pulse. A closely similar rate constant was obtained when the experiment was repeated after saturating with air rather than oxygen.

In order to find the rate constant for reaction paraquat radical with $O_2^{\cdot-}$, a 10^{-3} M solution of paraquat dichloride in 0.1 M sodium formate saturated with 0.23% oxygen in argon was irradiated with a pulse just sufficient to leave a small residual concentration of paraquat radical after completion of its reaction with O_2 and $O_2^{\cdot-}$. The decay curve for paraquat radical departed significantly from first-order kinetics. It was possible to reproduce it very closely, however, by simulating, on an analogue computer, the differential equations corresponding to the reactions

$$PQ^{\cdot+} + O_2 \rightarrow O_2^{\cdot-} \qquad \text{Rate constant } k_1$$

$$O_2^{\cdot-} + PQ^{\cdot+} \rightarrow \text{products} \qquad \text{Rate constant } k_2$$

Values of k_1 and k_2 and initial concentrations of $PQ^{\cdot+}$ and O_2 were adjusted to produce the best visual fit between the observed and simulated decay curves. The

TABLE I

RATE CONSTANTS FOR REACTION OF PARAQUAT RADICAL WITH OXYGEN (k_1) AND SUPEROXIDE (k_2)

Paraquat radical was generated in the presence of oxygen (see text). Its decay in oxygen- or air-saturated solution was first order and gave k_1 directly. k_1 and k_2 were calculated from the shape of the decay curve in the 0.23% oxygen/argon-saturated solution by the procedure described in the text.

Saturating gas	*pH*	*Wave-length (mn)*	*Pulse (rad)*	*No. of runs*	$t_{\frac{1}{2}}$ (μs)	$k_1(\times 10^8)$ ($M^{-1}\cdot s^{-1}$)	$k_2(\times 10^8)$ ($M^{-1}\cdot s^{-1}$)
Oxygen*	Unbuffered	395	90–2000	5	0.96	5.7	—
Air**	Unbuffered	Various	500	14	4.6	5.9	—
0.23% O_2	6.17	605	1100	1	—	7.5	6.8
0.23% O_2	7.07	605	1100	1	—	7.5	6.9
0.23% O_2	8.09	605	1100	1	—	8.0	6.9
0.23% O_2	Unbuffered	395	430	1	—	7.5	5.8
0.23% O_2	Unbuffered	395	465	1	—	7.5	5.8
0.23% O_2	Unbuffered	395	500	1	—	7.6	6.0
				Preferred values		7.7	6.5

* The concentration of oxygen was assumed to be $1.26\cdot 10^{-3}$ M.
** The concentration of oxygen was assumed to be $2.52\cdot 10^{-4}$ M.

simulations showed that the best conditions for estimating k_2 were when the ratio of initial concentrations of paraquat radical and O_2 was 2:1. They also suggested that an error of 25% in either k_1 or k_2, even when its effect was minimised by optimisation of the other variables, could easily be detected. The preferred values in Table I are probably within 10% of the true values.

DISCUSSION

Excess paraquat radical is known[1] to reduce oxygen to water *via* hydrogen peroxide. We have assumed that this is due to electron transfer and proton uptake, resulting in the successive formation of $O_2^{\cdot-}$ (superoxide ion), hydrogen peroxide and hydroxy radical, *viz.*

$$PQ^{+\cdot} + O_2 \rightarrow PQ^{2+} + O_2^{\cdot-} \qquad \text{Rate constant } k_1 \qquad (1)$$

then

$$O_2^{\cdot-} + PQ^{+\cdot} \rightarrow PQ^{2+} + O_2^{2-} \qquad \text{Rate constant } k_2 \qquad (2)$$

and

$$2O_2^{\cdot-} \rightarrow O_2 + O_2^{2-} \qquad \text{Rate constant } k_3 \qquad (3)$$

followed by

$$2H^+ + O_2^{2-} \rightarrow H_2O_2$$

then

$$H_2O_2 + PQ^{+\cdot} \rightarrow PQ^{2+} + HO\cdot + OH^- \qquad \text{Rate constant } k_4 \qquad (4)$$

and

$$HO\cdot + PQ^{+\cdot} \rightarrow PQ^{2+} + OH^- \qquad \text{Rate constant } k_5 \qquad (5)$$